Fluorinated and Trifluoromethylated Buckybowls

Inaugural-Dissertation towards the academic degree
Doctor rerum naturalium (Dr. rer. nat.)

Submitted to the Department of Biology, Chemistry and Pharmacy,
Freie Universität Berlin

Bernd M. Schmidt, Berlin

December 2012

In Gedenken an meine Großmutter
Waltraut Vogi († 28.08.2011)

The present work was carried out under the supervision of Prof. Dr. Dieter Lentz from October 2009 to December 2012 at the Institute of Chemistry and Biochemistry, at the Freie Universität Berlin.

First Reviewer: Prof. Dr. D. Lentz

Second Reviewer: Prof. Dr. H.-U. Reißig

Date of Defense: 15.02.2013

Publications

Parts of this work have been published prior to submission of this manuscript or are due to be published as described below.

Scientific journals:

B. M. Schmidt, B. Topolinski, S. Higashibayashi, T. Kojima, M. Kawano, D. Lentz, H. Sakurai, The Synthesis of Hexafluorosumanene and its Congeners. *Manuscript in preparation.*

B. M. Schmidt, S. Seki, B. Topolinski, K. Ohkubo, S. Fukuzumi, H. Sakurai, D. Lentz, Electronic Properties of Trifluoromethylated Corannulenes. *Angewandte Chemie International Edition* **2012**, *51,* 11385–11388.

B. M. Schmidt, S. Seki, B. Topolinski, K. Ohkubo, S. Fukuzumi, H. Sakurai, D. Lentz, Elektronische Eigenschaften Trifluormethylierter Corannulene. *Angewandte Chemie* **2012**, *124*, 11548-11551.

B. M. Schmidt, B. Topolinski, P. Roesch, D. Lentz, Electronpoor *N*-substituted Imide-fused Corannulenes. *Chemical Communications* **2012**, *48,* 6520-6522.

B. Topolinski, B. M. Schmidt, M. Kathan, S. I. Troyanov, D. Lentz, Corannulenylferrocenes: Towards a 1D, Non-covalent Metal-organic Nanowire. *Chemical Communications* **2012**, *48*, 6298-6300.

S. Mebs, M. Weber, P. Luger, B. M. Schmidt, H. Sakurai, S. Higashibayashi, S. Onogi, D. Lentz, Experimental Electron Density of Sumanene, a Bowl-shaped Fullerene Fragment; Comparison with the related Corannulene Hydrocarbon. *Organic & Biomolecular Chemistry* **2012**, *10*, 2218-2222.

Conference Lectures:

B. M. Schmidt, H. Sakurai, B. Topolinski, S. Seki, S. Higashibayashi, D. Lentz, 15. Deutscher Fluortag, September 2012, Schmitten (Germany).

B. M. Schmidt, H. Sakurai, B. Topolinski, S. Higashibayashi, D. Lentz, 20th International Symposium on Fluorine Chemistry, July 2012, Kyoto (Japan).

B. M. Schmidt, D. Lentz, at the 15th Meeting of the Graduate School "Fluorine as the Key Element", June 2011, Berlin (Germany.)

Conference Posters:

B. M. Schmidt, B. Topolinski, P. Roesch, H. Sakurai, D. Lentz, at the GDCh-Wissenschaftsforum Chemie, September 2011, Bremen (Germany).

B. M. Schmidt, A. K. Meyer, B. Topolinski, D. Lentz, at the 2nd CSI General Meeting of the Center for Supramolecular Interactions, March 2011, Berlin (Germany).

Acknowledgements

I want to thank *Professor Dr. D. Lentz* for the opportunity to conduct this work in his group and for his constant believe in the success of this thesis. The measurements and computations of countless of difficult X-ray analyses are highly appreciated and were a key to the success of this work.

Professor Dr. H.-U. Reissig reviewed this thesis and provided help with the HPLC separation, which was carried out for one compound in his group.

Professor Dr. H. Sakurai supported me since my undergraduate studies, like my doctoral adviser. I want to thank you not only for countless inspiring discussions, but also for the trust and support you gave to two foreign strangers.

I am grateful for all the help, profound knowledge and willingness to guide and support me, which I received from so many people from so many countries around the world. Especially *Dr. Shuhei Higashibayashi, Dr. Moritz Kühnel, Dr. Qitao Tan, Dr. Katrin Niedermann, Dr. Ryoji Tsuruoka* and *Professor Dr. Shu Seki* are acknowledged.

I am indebted to all the former and present members of the Lentz and Seppelt research group, *Stefanie Fritz, Darina Heinrich, Dr. Thomas Hügle, Juliane Krüger, Annika Meyer, Dr. Matthias Molski*, as well as current and former members of the Sakurai group: *Dr. Nasir Baig, Dr. Raghu Nath Dhital, Setsiri Haesuwannakij, Yuka Ishida, Patcharin Kaewmati, Noriko Kai, Keita Kataoka, Jinyoung Koo, Dr. Yuki Morita, Sachiko Nakano, Yuki Okabe, Satoru Onogi, Professor Dr. Gautam Panda, Dr. Patcharee Preedasuriyachai, Dr. Tsuyuka Sugiishi* and *Dr. Sal Prima Yudha*.

Additionally, I want to thank all research students who joined lab U306, *Alma Jäger, Michael Kathan, Simon Poremski, Kai Redies, Volker Rohde, Philip Roesch, Antti Senf* and *Mihoko Yamada*, for the time we spent discussing inside and outside of the lab and their contributions.

I want to thank *Lena Kaufmann* and *Dominic Gröger* for enjoyable lunch breaks and conversations.

Finally, I am most grateful to my girlfriend Berit and my family & friends for their support and patience.

Contents

1. Introduction

1.1 Discovery of bowlshaped polycyclic aromatic hydrocarbons

During the last 40 years, the chemistry of carbon rich compounds evolved dramatically. The discovery of fullerenes in 1985[1] and the accompanied discovery of the existence of endohedral metallofullerenes,[2] which encapsulate an (metal) atom into its spherical space inside the carbon cage, gave rise to research and the discovery of various types of carbon nanostructures. A related class of three-dimensional carbon surfaces, carbon nanotubes, were prepared in 1991 by using a reactor similar to the one used for the mass production of C_{60}.[3] Single-walled carbon nanotubes (SWNTs) show favourable properties like high thermal conductivity and other fascinating mechanical[4] and electrical properties.[5] Substructures of SWNTs like cycloparaphenylenes inspired various research groups around the world to synthesize cycloparaphenylenes size-selectively and to study their inherent properties and ring-size effects.[6] The latest groundbreaking discovery was made at the beginning of this century, when Andre Geim and Kostya Novoselov succeeded in extracting single-atom-thick crystallites (graphene) from bulk graphite in 2004.[7] Single layers of graphite were previously grown epitaxially on top of other materials but significant charge transfer between the substrate and the graphene notably altered its properties.[8]
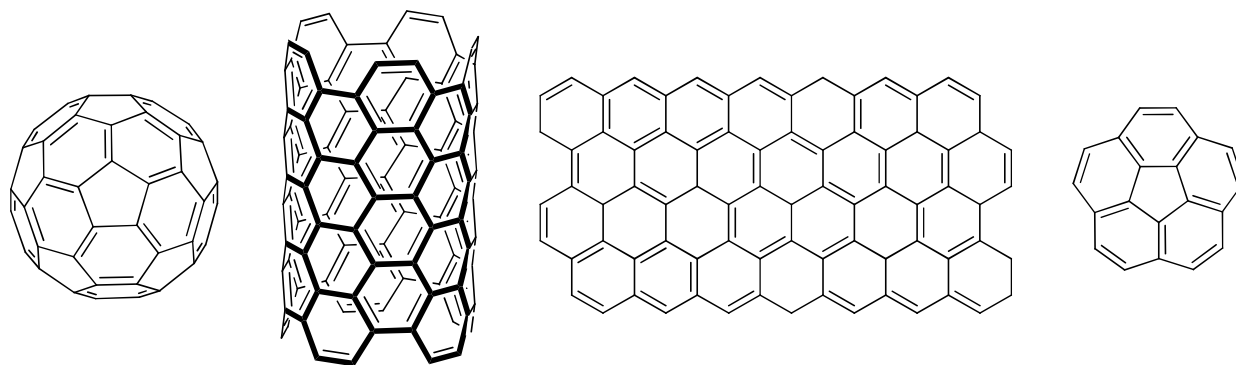
Scheme 1.1. From left to right: Buckminsterfullerene (also called buckyball) C_{60}, an excerpt of a single-wall (5,5) armchair carbon nanotube, a schematic drawing of a graphene sheet, the molecular bowl corannulene ($C_{20}H_{10}$).

Not only in this context, had research on polycyclic aromatic hydrocarbons further emerged together with the organic chemistry.

In 1966 the group of Barth and Lawton synthesized the first bowl-shaped polycyclic aromatic hydrocarbon, [5]circulene, better known as corannulene. The linear synthesis involved 17 steps in total and resulted in less than 1 % overall yield.[9]
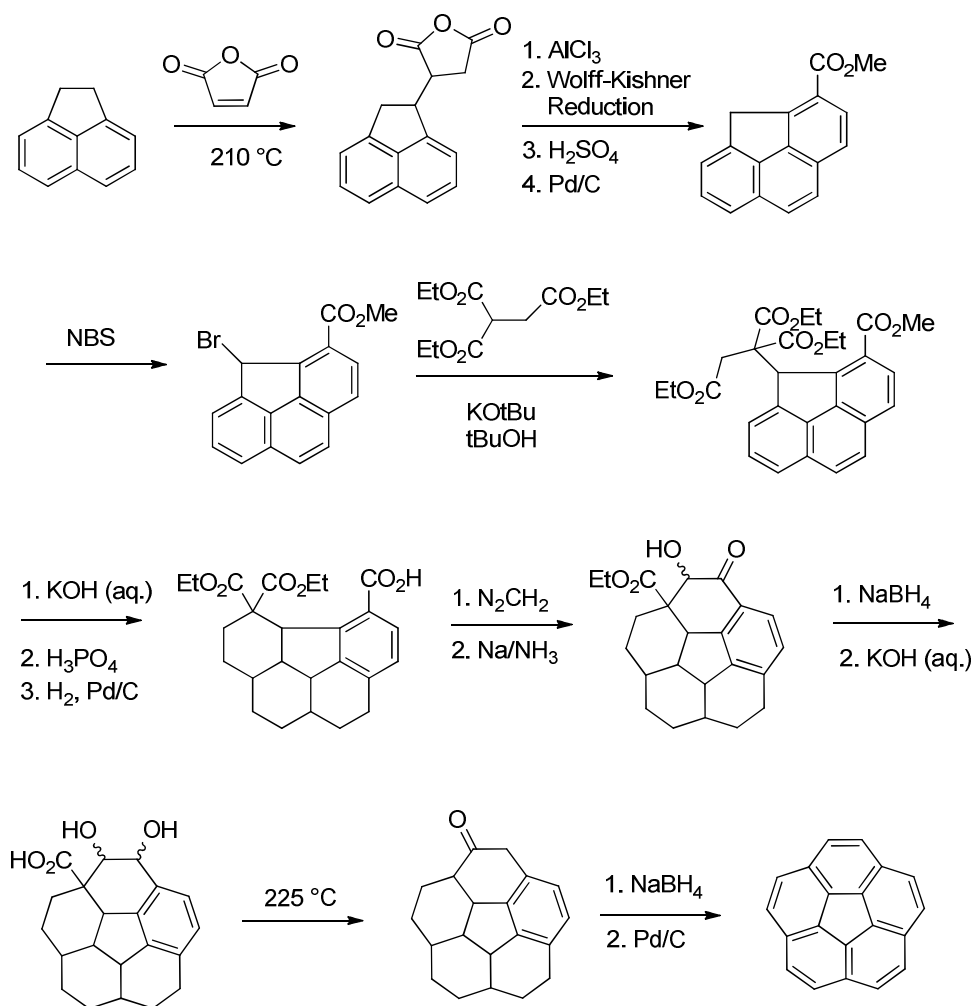
Scheme 1.2. The first synthesis of corannulene.[9]

Research, other than on its crystal structure determination[10] has been prohibited because of its very low availability, but has been revived with the afore-mentioned discovery of fullerenes.[1a] The bowl-shaped C_{20} structure can be considered as a fullerene subunit, which is relevant, not only as model compound for fullerenes, but also because of its own chemical and physical properties, that were investigated when the group of Siegel and Scott started to improve its synthesis during the 1990s.

2
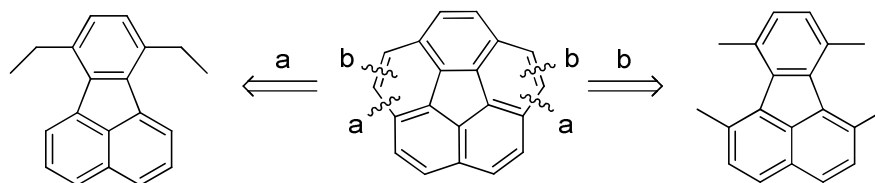
Scheme 1.3. Main retrosynthetic approaches.

The group of Professor Scott designed and executed a short synthesis of corannulene starting with acenaphtenequinone.[11] After further improvement in development and by the use of a simple Diels-Alder reaction, a 7,10-disubstituted fluoranthene was generated and chemically transformed to the precursor molecule 7,10-bis(1-chlorovinyl)fluoranthene. A high-temperature pyrolysis (FVP, flash vacuum pyrolysis) of this precursor generated corannulene in about 30 % yield (200 mg can be obtained from one pyrolysis).[12]
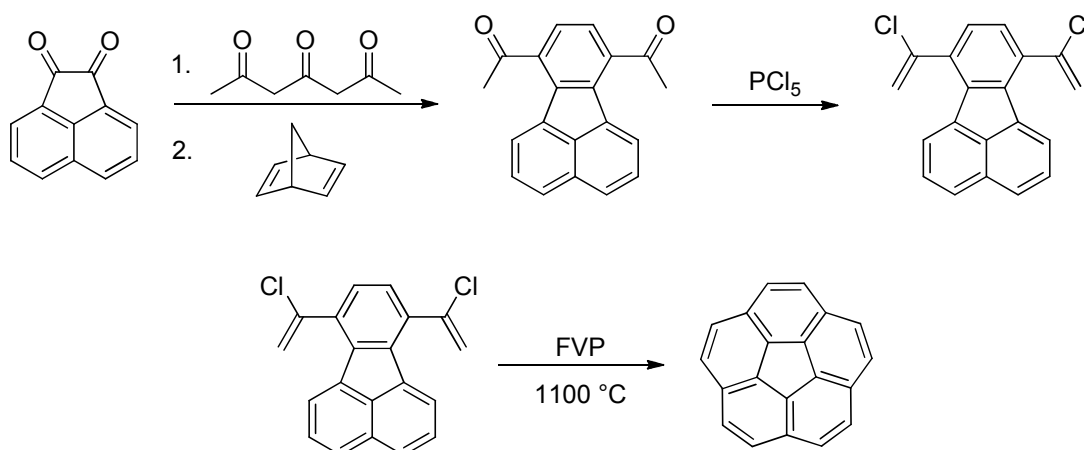
Scheme 1.4. Scott's FVP approach.

The concepts of masked acetylene by the introduction of the 1-chlorovinyl group as a latent ethynyl group in FVP and other mechanisms have been used successfully for the preparation of numerous other new PAHs, related and unrelated to corannulene.[13] This includes the synthesis of [5,5]-fulvalene circulene ($C_{30}H_{12}$),[14] the hemifullerene (triindenotriphenylene, $C_{30}H_{12}$)[14a, 15] and finally the first rational synthesis of Buckminster-fullerene C_{60} in isolable quantities.[16]

Although the preparation of corannulene by FVP includes a small number of synthetic steps, this strategy suffers from several drawbacks. A suitable FVP apparatus, which withstands the high temperatures of more than a 1000 °C has to be used, almost no functional groups are tolerated and

3

scaling up of the reaction is very difficult or impossible. Therefore, a new solution phase synthesis of corannulene became an important target. The first published example of a corannulene derivative made by a solution-phase synthesis, only was reported by Siegel and co-workers a few years later[17] and further improvement on the synthesis followed by the group of Siegel[18] and Rabideau and Sygula.[19] Finally in 2012, the kilogram-scale synthesis of corannulene was again reported by the group of Siegel, providing access to commercial production and engineering applications.[20]
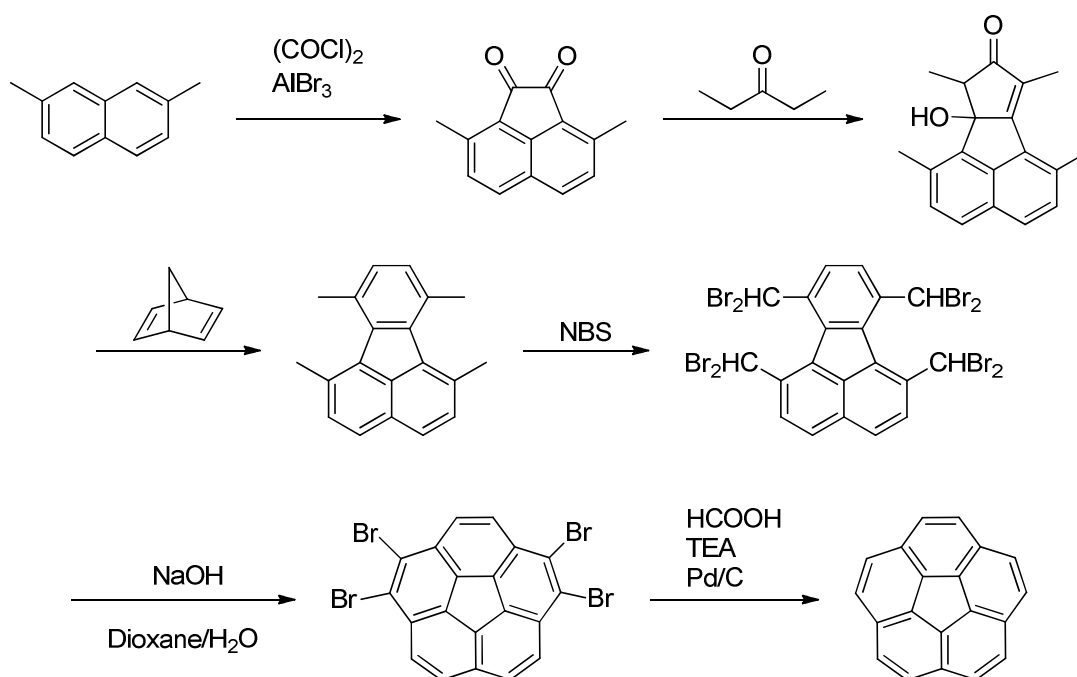
Scheme 1.5. The current benchmark method for the synthesis of corannulene by Siegel's group,[20] including refinements made by Rabideau and Sygula.[19]

The growing availability of corannulene over the course of time increased its popularity and a variety of studies on corannulene and its derivatives appeared.[21] The large π-system undergoes reductions with different alkali metals up to the tetraanion, which was extensively studied by NMR experiments.[22] Condensed and connected corannulene derivatives were also investigated,[23] including their supramolecular oligomerization[24] and heterodimer formation with fullerenes.[25] Hereinafter corannulene anions were studied in the solid state by single-crystal X-ray diffraction,[26] demonstrating selective *endo* and *exo* binding[27] and finally confirming the formation of a sandwich-type supramolecular aggregate for the lithium-coordinated corannulene tetraanion.[28]

η^6-coordination of the curved carbon surface of corannulene was achieved from corresponding ruthenium[29] and osmium[29d] complexes, accompanied by flattening of the corannulene bowl, so that two ruthenium complex ions can be coordinated.[29c] Other metal complexes include η^2-coordination (generating 1D infinite chains)[30] and mono-,[31] di-,[31-32] tetra-,[32] and penta-[32] σ-bonded complexes. These have been obtained from the corresponding halogenated precursors by insertion. Halogenated corannulenes were used to synthesize the whole family of indenocorannulenes by palladium-catalysed cross-coupling reactions[33] and were furthermore studied crystallographically.[34] Wu and Siegel obtained functionalized multiethynylcorannulenes and studied their photophysical properties,[35] in addition to the corannulene conjugates prepared by Sutton.[36]

In 2012 the group of Professor Scott pushed the boundaries of organic synthetic methods. Starting from the symmetrical pentachlorocorannulene,[37] a short [5,5]-SWNT has been synthesized by stepwise chemical methods with a final FVP step.[38]
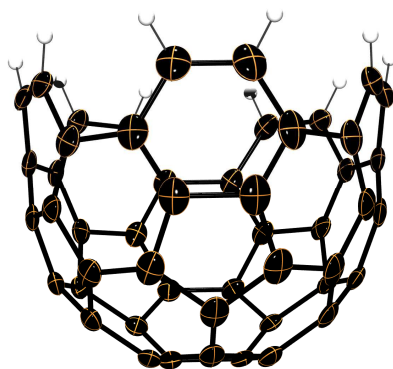
Figure 1.1. Molecular structure of the short carbon nanotube ($C_{50}H_{10}$), as determined by X-ray crystallography in the group of Scott.[38]

The physical properties of pristine corannulene have been investigated thoroughly in the last decades. The solid state structure was investigated and shows a bowl depth of 0.87 Å and no columnar π-stacking or edge-to-face interactions.[10, 39] The bowl however is not rigid, a bowl-to-bowl inversion process *via* a planar transition state occurs.[40] The difference in energy between the curved structure and the transition structure represents the bowl inversion energy $\Delta G^{\ddagger}_{inv}$, which can be measured experimentally by variable-temperature NMR studies of suitable substituted corannulenes. Consequently, the bowl inversion barrier of corannulene was estimated to 11.5 kcal/mol, which

implies that the corannulene system inverts 200,000 times per second at room temperature.[41] Albeit some excerpts,[37, 42] a correlation between rim-substitution, bowl depth and inversion barrier can be established.

In 2003, the group of Sakurai succeeded in synthesizing a missing link,[43] the molecular bowl sumanene ($C_{21}H_{12}$), which can also be considered as a curved subunit of the fullerene C_{60}. The stability of sumanene was predicted several years ago,[44] but attempts to synthesize it, failed.[45] At last, the key to success was to construct a 3D framework mostly based on tetrahedral sp^3 carbons. By oxidative aromatization, the π-conjugated bowl was obtained.
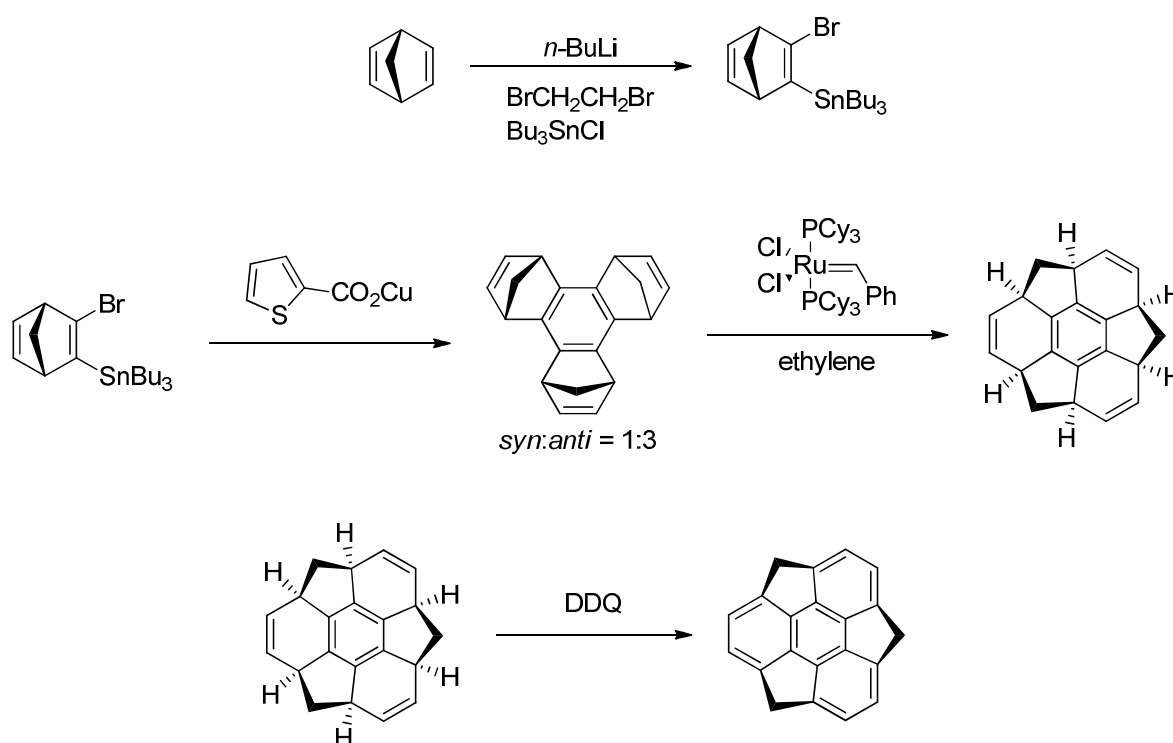
Scheme 1.6. The synthesis of sumanene ($C_{21}H_{12}$).

The bowl inversion energies of sumanene derivatives were experimentally investigated using 2D-EXSY NMR and a value of 20 kcal/mol was obtained,[46] a much slower inversion compared to that of corannulene. In this regard, the experimental bowl depth observed is 1.11 Å,[47] which is deeper than the bowl depth of corannulene (0.87 Å).[10] The curvature already corresponds to 78 % of that of C_{60}.[47a]
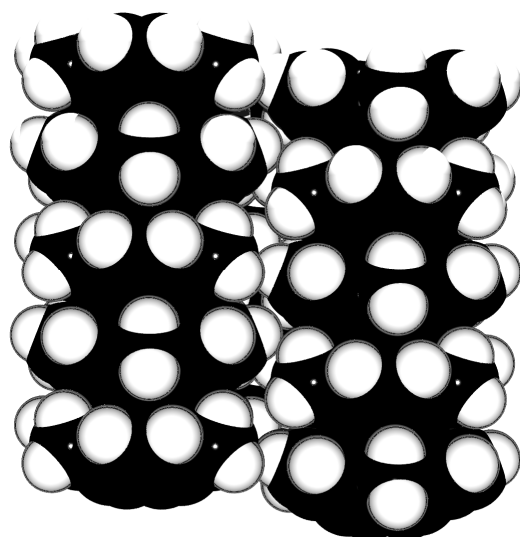
Figure 1.2. Space-filling model of the 1D columnar π-stacking in a concave-convex fashion.[47a]

The group of Seki and Hirao utilized the perfect columnar staggered stacking along the crystallographic *c* axis and could show that sumanene is an organic n-type semiconductor. High electron mobility along the molecular stacking axis was measured by time-resolved microwave conductivity methods (TRMC), with an anisotropic difference of 9.2 times (parallel *versus* perpendicular to the *c* axis) because of the efficient overlap of the molecules.[48]

Further unique features of sumanene are its benzylic positions, which can be used for further functionalization to create new bowl-shaped derivatives, like extended π-bowls[49] and π-extended compounds[50] or which can be oxidized to give sumanenetrione.[51] Other compounds include the C_3 symmetric chiral trimethylsumanene, which was obtained by asymmetric synthesis[52] or the chiral triazasumanenes, opening a complete new field of research of nitrogen-doped buckybowls in 2012.[53]

1.2 Organic compounds and fluorine

Fluoro-organic compounds in general are present in innumerable applications and show many fascinating physical and chemical properties. Fluorinated compounds are encountered by people every day, often without further notice. Examples range from hydrofluorocarbons as refrigerants in air conditioning systems, organic fluorine in pharmaceuticals[54] and radiopharmaceuticals,[54c] water-proof clothes,[55] Teflon non-stick coating pans, to the weatherproof fluorocarbon paint that coats the surface of the N700 Shinkansen, Japans well known high-speed train.[55]

In particular, fluorinated *aromatic* compounds show a manifold, interesting chemistry and are also important for many applications, especially in electronic devices.[56] Perylene bisimides (PBIs) and naphthalene bisimides (NBI) benefit greatly from the introduction of fluorine to the bay positions. The attachment of (partially) fluorinated imide substituents is used to generate tailor made materials with specific physical, optical and electronic properties.[57]
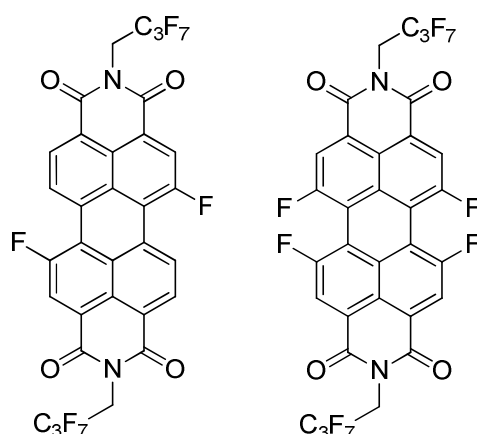
Scheme 1.7. Fluorinated PBI derivatives investigated by Würthner and co-workers.[57]

Rim-substitution and (benz)annulation are common synthetic strategies in molecular engineering to modify perylene bisimides, triphenylenes and coronones for the design of high-performance n-type semiconductors.[58] Especially the introduction of strong electron withdrawing functional groups, e.g. nitrile groups,[59] trifluoromethylgroups,[60] fluorine[57, 61] or chlorine[62] promises to generate molecules with high electron affinity for efficient electron injection. Electron affinities facilitate charge injection and ambient stability, and a strong intermolecular orbital overlap is necessary to achieve high electron mobility.

The introduction of fluorinated alkyl groups also leads to improved air-stability (when the device is operated under air conditions), originating from a shielding effect of the inert fluorocarbons attached.

Fluoro-organic molecules offer a manifold supramolecular chemistry due to the strong electron-withdrawing nature of fluorine and accordingly a significantly polarized C-F bond.[63] The electronic structure of a molecule can be changed drastically and therefore arrangements with a strong interaction between fluorinated and nonfluorinated rings can be designed.[64] The ability of fluorine to participate in C-F⋯H-C interactions makes fluorination a valuable tool in crystal engineering of organic compounds.[65] The most prominent example might be the molecular complex of benzene and hexafluorobenzene which was investigated by Patrick and Prosser more than 50 years ago.[66]
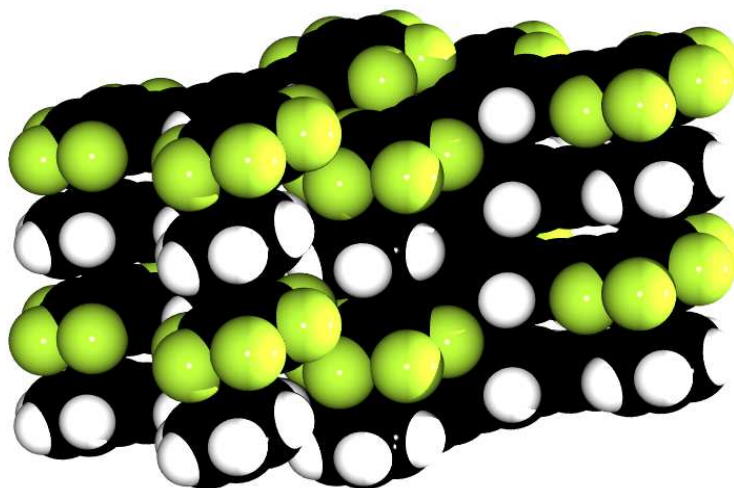
Figure 1.3. Space-filling model of a crystalline, molecular complex of *sym*-tris(perfluoro-phenethynyl)bezene and *sym*-triphenethynylbenzene, showing the anchoring principle of hexafluorobenzene-to-benzene interactions.[67]

In the early stages of this study, fluorinated or perfluoroalkylated bowl-shaped hydrocarbons were not known. The aim of this work was to study, how electron withdrawing substituents can be introduced to buckybowls like corannulene and sumanene and in which way their properties can be influenced, yielding compounds and materials with new and useful properties has yet to be studied.

The solid state structure of corannulene is dominated by C-H⋯π interactions and without a columnar order,[10] but corannulene can be synthesized on a larger scale. It would be interesting to manipulate

the corannulene molecule in some way to achieve a favourable and dense solid state structure like the one of the molecular bowl sumanene.

Sumanene itself is already known to be an organic n-type conductor. The effect of the introduction of electron withdrawing substituents is of great interest to affect its' intrinsic properties. It is challenging to introduce one or more suitable substituents, without inhibiting the columnar order due to sterical or supramolecular interactions.

2. Corannulenes with electron withdrawing substituents

2.1. Synthesis of corannulene

The synthesis of corannulene (**1**) was carried out according to known literature procedures, with some changes made described in previous works.[68-71]

Justifiably, the initial idea was to synthesize the target molecule **1** with late-stage modification through fluorination. According to the retrosynthetic analysis (scheme 1.3) two major approaches are feasible on a reasonable time scale. Professor Scott's "Three-Step Synthesis" was the first choice because it promised fast access to the corannulene molecule (scheme 1.4).[12]

In the first step, heptanetrione (**2**) has to be synthesized. It can be obtained by reacting dehydroacetic acid with aqueous hydrochloric acid to produce **2** in good yields. The labile **2** can be stored at -80 °C for several months. Knoevenagel condensation with acenaphtenquinone (**3**) and subsequent Diels-Alder reaction furnish the diacetylfluoranthene (**4**) in good yields. A transformation to the chlorovinyl species, 7,10-bis(1-chlorovinyl)fluoranthene (**5**), suffered from several by-products, therefore slightly modified conditions were used.[68] The chlorovinyl-precursor **5** can be synthesized on a multi-gram scale and is the direct precursor to corannulene **1**. The most severe disadvantage of this method is the rather complex setup for the pyrolysis apparatus.[13]

Figure 2.1. The pyrolysis apparatus used to prepare corannulene **1**. Left: Nitrogen-inlet, pressure gauge and sample boat. Right: Cold trap immersed in liquid nitrogen and connection to vacuum pump.

To withstand the high temperatures of 1100 °C the hot zone of the FVP apparatus consists of quartz. All parts have to be able to withstand high vacuum. Additionally, a nitrogen inlet needs to be implanted to provide pressure of around 1 mbar of nitrogen during FVP. The precursor molecule placed in a sample boat is continuously moved towards the hot zone of the oven during the FVP (8 hours).

2.2. General remarks regarding nomenclature

Following literature recommendations,[39,72] the C-C bonds in corannulene will be labelled rim, flank, spoke and hub (figure 2.2).
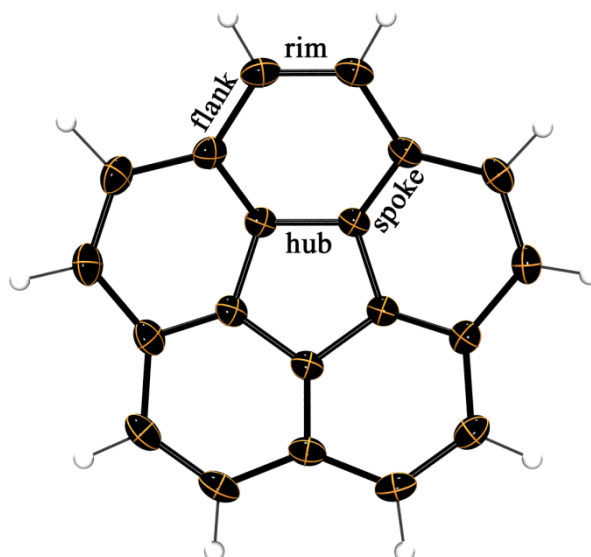
Figure 2.2. C-C bonds in **1**.

The bowl depth is defined as the distance between the planes formed by the central hub atoms and the rim carbon atoms.

Figure 2.3. Bowl depths of corannulenes.

The distance between the planes of two stacking molecules, formed by the central hub atoms, is given as bowl-to-bowl distance for all studied compounds.

2.3. Monohalogenated corannulenes

Introduction of fluorine to **1** can be achieved by a reaction with xenon(II)fluoride. The reaction of corannulene with 1.4 equivalents xenon(II)fluoride in DCM at low temperatures yields a mixture of unreacted **1**, monofluorocorannulene (**6**) and several difluorocorannulenes, as described previously.[68] The mixture cannot be separated by column chromatography and was finally purified by reversed-phase HPLC (Gemini C18, methanol/water: 9/1). After several unsuccessful attempts, the solid-state structure of the needle-like crystals of **6** could be investigated, albeit the quality of the obtained data set was only moderate. As shown in figure 2.4, the structure can be solved in the space group $P2_1/c$, where the fluorine atom is disordered at two positions in the solid state (1,4-position).
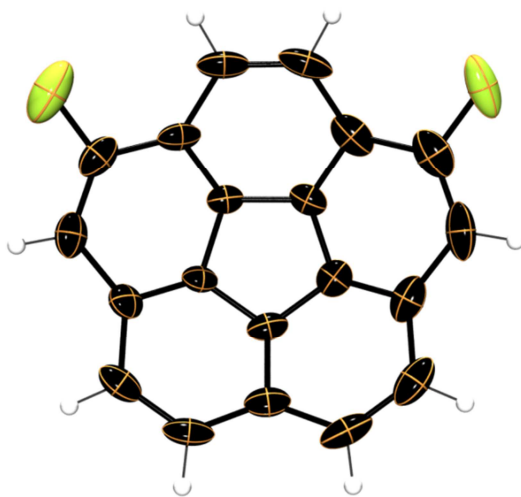
Figure 2.4. Molecular structure of **6**, with a bowl depth of 0.8658(3) Å.

The bowl depth of **6** is slightly shallower (0.87 Å) in comparison to the one of corannulene (0.88 Å).[39] The solid state structure, however, is drastically changed upon the introduction of the strongly electron withdrawing fluorine atom to the corannulene rim. Overall, a slipped stacking motif is present and the molecular bowls are displaced by about 180 °.
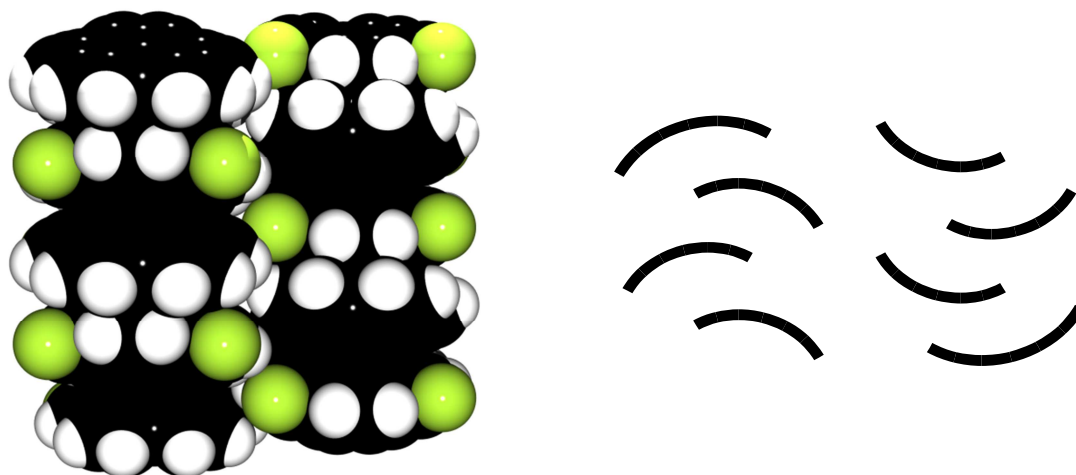
Figure 2.5. Left: The solid-state alignment of **6**, obtained from X-ray analysis. Right: A schematic representation.

A short C-H⋯π interaction[73-75] of 2.86 Å can be observed from one of the C-H rim atoms to the centre of a proximate six-membered ring of corannulenes pointing in the same direction. This occurs within unidirectional columns, whereas the opposing columns participate predominantly by a relevant intermolecular F⋯H-C interaction[64a, 64e] of 2.66 Å yielding the overall solid-state alignment. Affected by the simplicity of the fluorination reaction, several attempts were made to obtain higher fluorinated corannulenes, as from the crude ^{19}F NMR, it can be judged, that difluorinated corannulenes are also present as indicated by a series of doublets between -116 and -119 ppm exhibiting $^3J_{F-H}$ coupling constants of approximately 13 Hz. Efforts to separate the difluorinated corannulenes by using silica gel column chromatography and normal-phase HPLC with a buckyprep column failed. Recycling GPC and separation by reversed-phase HPLC were also unsuccessful. Subsequent fluorination reactions of **6** or starting from **1** suffered from severe decrease of the amount of recovered material, most likely caused by polymerisation of the compounds. The substitution of up to three hydrogen atoms by fluorine can be observed by mass spectrometry, but isolation was not possible.

It should be taken into account that fluorination is supposed to have a weaker effect on the electron acceptor properties than trifluoromethylation and even chlorination, which will be discussed later (chapter 5.1).

Nevertheless, a surprising discovery was made during the purification of **6**, its co-crystallization with pristine corannulene **1**. Mixtures containing variable amounts of **6** and **1** have a needle-like appearance after removal of the solvent, whereas pure corannulene appears as block-like crystals. Satisfactory X-ray data could not be obtained for mixed-crystals due to severe disorders. This finding is in accord with the results of the Scott's group, which could show that several corannulenes undergo complexation reactions with equimolar quantities of perfluoro-*ortho*-phenylenemercury and the corresponding corannulene to yield extended binary stacks in which the molecules alternate.[76] The finding discussed here, should be the first example of co-crystallization between corannulenes.

For comparison, the homologous monochlorocorannulene (**6**) was investigated by X-ray crystallography as well. It is formed as a by-product during the FVP or can be synthesized using gold(III)chloride and *N*-chlorosuccinimide applying the halogenation protocol of Wang.[77]

The solid state structure of a needle-like crystal of **7** shows an almost identical packing structure and disorder of the chlorine atom at the 1- and 4-position. Therefore, it can be concluded that the packing structure is formed mainly because of electrostatic interactions and not due to F···H-C interactions. **7** crystallizes in the orthorhombic space group Pnma with half of a molecule in the asymmetric unit. The short C-H···π interaction of 2.86 Å can again be observed from one of the C-H rim-atoms to the centre of a proximate six-membered ring of corannulenes pointing in the same direction. Intermolecular Cl···H-C interaction are elongated to 2.91 Å in comparison to the studied homologous halogens. The bowl of **7** has a depth of 0.86 Å in the solid state, which might be slightly flattened due to the steric demand of the chlorine atom.
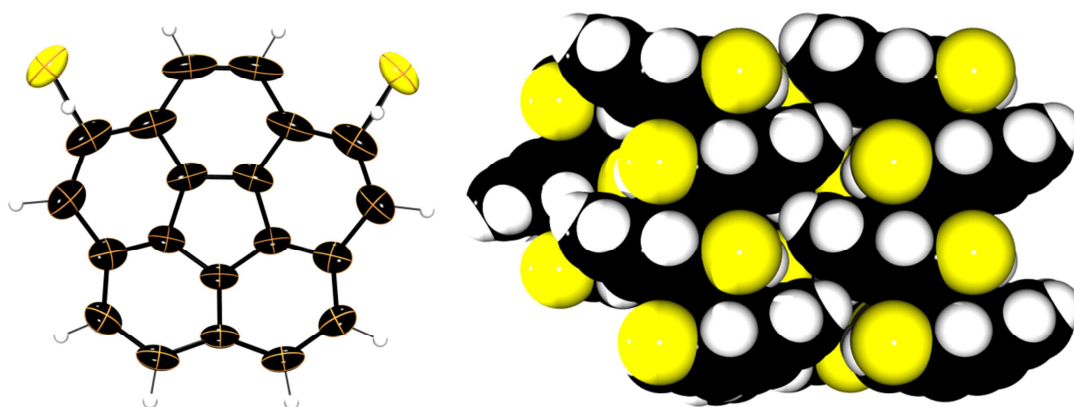
Figure 2.6. Left: Molecular structure of **7**. Right: Schematic representation of the slipped stacking of **7** (space-filling model), the columns going "up" are shown in the front, columns going "down" are behind the plane. **7** features a bowl depth depth of 0.8596(3) Å.

To complete the series of monohalogenated corannulenes, monoiodocorannulene (**8**) was synthesized as well, to obtain a superior precursor molecule to the widely used monobromocorannulene. Like monochlorocorannulene **7**, **8** can be synthesized by treating **1** with gold(III)chloride and the corresponding succinimide in 1,2-dichloroethane.

1.0 equiv NXS

5.0 mol% gold(III)-chloride,
1,2-dichloroethane,
48 h rt, 3 h reflux

7 X = Cl (90 %)
8 X = I (75-99 %)
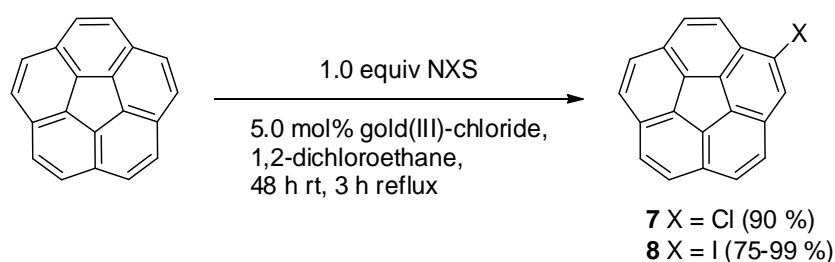
Scheme 2.1. Synthesis of **7** and **8**, applying the halogenation protocol of Wang.[77-78]

To summarize, the introduction of one fluorine, chlorine or bromine[68] atom changes the solid state arrangement of the molecular bowls drastically, but the desired dense packing, which is found for sumanene (**9**), is not observed. The solid state packing of **8** could not be obtained but studies on iodinated sumanenes suggest that the large and strongly polarizable iodine atom prohibits a close stacking in the solid state.[79]

17

2.4. Trifluoromethylation

As described earlier, trifluoromethylation should have a distinct effect on the electron-acceptor properties. Direct trifluoromethylation is still a challenging task, therefore drastic reaction conditions similar to the ones used to trifluormethylate fullerenes were used initially. In a closed vessel, **1** is irradiated with a strong light source (UV) in the presence of copper powder and trifluoroiodomethane, generating CF_3-radicals.[80]
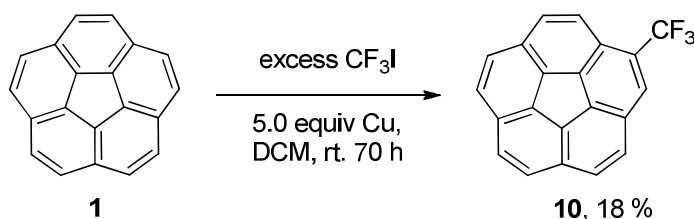
Scheme 2.2. First synthesis of 1-(trifluoromethyl)corannulene (**10**) under harsh free-radical conditions.

A complex mixture of products was obtained that could not be separated by column chromatography on silica gel. 1-(Trifluoromethyl)corannulene (**10**) could be obtained from the mixture by prepurifcation on silica gel and subsequent separation by preparative gel permeations chromatography with chloroform as eluent, albeit in low yield. The needle-like morphology of the crystals of **10** prohibited X-ray analysis because of the dominating growth in only one dimension.

Fortunately, the group of Togni published a direct trifluoromethylation strategy using 1-trifluoromethyl-1,2-benziodoxol-3-(1H)-one (Togni's Acid Reagent) in the presence of methyltrioxorhenium at 80 °C.[81]
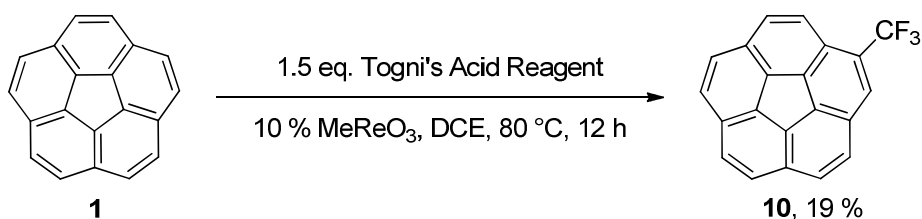
Scheme 2.3. Improved synthesis of **10** by liquid-phase synthesis applying a protocol of Togni's group.[81]

This reaction proceeds under milder conditions and less side products are formed, enabling the isolation of **10** by preparative thin-layer chromatography on silica gel with hexane as eluent. Although only a minor increase of the yield can be noticed, the simplicity and reproducibility are huge advancements and allow full characterization of the compound. Nevertheless, further direct trifluoromethylation of **10** either way would lead to the formation of regioisomers and therefore other methods had to be developed to obtain multi-trifluoromethylated corannulenes.

2.5. Trifluoromethylated fluoranthenes for the generation of trifluoromethylated corannulenes

It seemed reasonable to introduce two trifluoromethyl groups to a precursor molecule of the corresponding corannulene for successive construction of the target molecule. As described earlier, corannulene is formed in general by a ring-closing reaction after obtaining a corresponding fluoranthene, the groups of Scott, Siegel and Rabideau/Sygula use norbornadiene as dieneophile for the construction of the fluoranthene after subsequent CO-loss and Retro-Diels-Alder reaction.[11-12, 19-20] Sygula and co-workers showed that dimethyl acetylenedicarboxylate can be used to synthesize the respective fluoranthene with two dimethyldicarboxylate-groups in *ortho*-position.[82] Therefore hexafluorobutyne should also be applicable because it is a particularly electrophilic acetylene, and hence a potent dienophile.
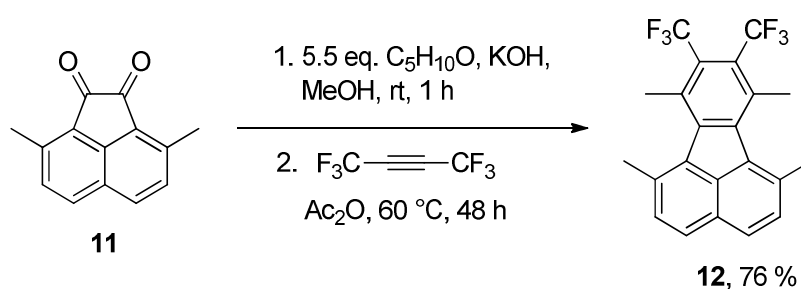
Scheme 2.4. Synthesis of 1,6,7,10-tetramethyl-8,9-bis(trifluoromethyl)fluoranthene (**12**) from 3,8-dimethylacenaphthylene-1,2-dione (**11**) using hexafluorobutyne.

The first step of the reaction is usually carried out in a Schlenk flask. The intermediate product tends to polymerize and can thus not be stored over long time periods; to maximize the yield, it is used immediately.

The crude product is transferred to a glass ampule (diameter 1 cm), connected to the high vacuum line and dried. After addition and degassing of the acetic anhydride, hexafluorobutyne is condensed under vacuum by cooling with liquid nitrogen. The ampule is then flame sealed, allowing the reaction mixture to be heated for the desired time in an oven or bath. It might be noteworthy, that this is the only published reaction, which employs hexafluorobutyne as a dienophile for the construction of compounds bearing two trifluoromethyl groups. This procedure has also been performed by

undergraduate students and found to be a safe and reliable method for the synthesis of **12** in reproducibly good yields. Purification of the product can again be easily achieved by column chromatography on silica gel with pentane as eluent, the product is highly soluble and shows a strong green-blue fluorescence in common organic solvents. Solvent-free crystals suitable for X-ray analysis are obtained by slowly cooling the reaction mixture to room temperature or by evaporation of a dichloromethane/pentane solution. This class of compounds is excellent for studying weak interactions like $\pi\cdots\pi$ interactions, C-H$\cdots\pi$ interactions and of course, C-H$\cdots$F interactions, because stronger forces like hydrogen bonding with carbonyl groups for example, cannot be formed within the crystals. Common distortion modes of this class of compounds are shown schematically (scheme 2.5).

splay   twist C_2-twist
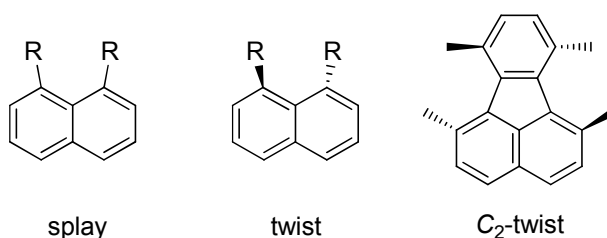
Scheme 2.5. Distortion modes in fluoranthenes and upon *peri*-substituion, according to Siegel and co-workers.[83]

A C_2-twist distortion of the upper, electron-poor part of the molecule can be observed. The lower part is still planar but bent adversely to avoid sterical strain[83] and to engage an opposing molecule by $\pi\cdots\pi$ interactions (centroid-to-centroid distance 3.86 Å for both rings), forming a head-to-head dimer.
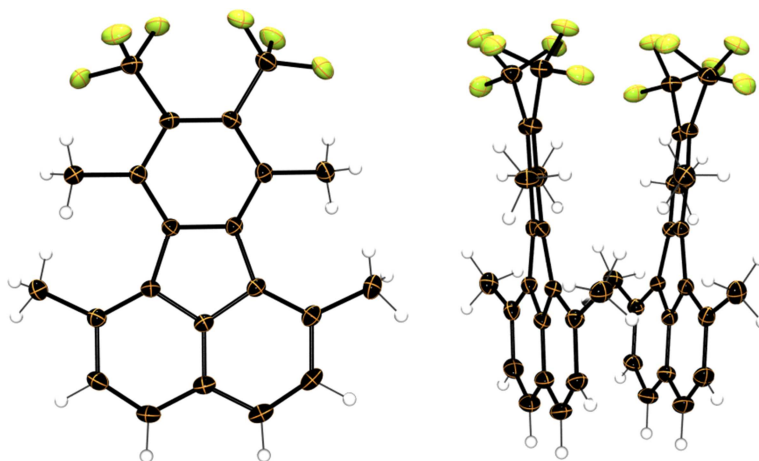
Figure 2.7. Left: The molecular structure of **12**. Right: The dimeric unit (head-to-head dimer) found in the crystal packing of **12**.

A $\pi_F \cdots \pi_F$ interaction is unlikely due to a to distance of 4.37 Å. The dimeric units are engaging in short C-H⋯F interactions of up to 2.54 Å between dimeric units and in C-H⋯π interactions within a strand where the dimers are displaced approximately by 180 °. Intramolecular hydrogen bonding of average lengths from the methyl groups to the trifluoromethyl groups are within a distance of 2.56 - 2.68 Å.
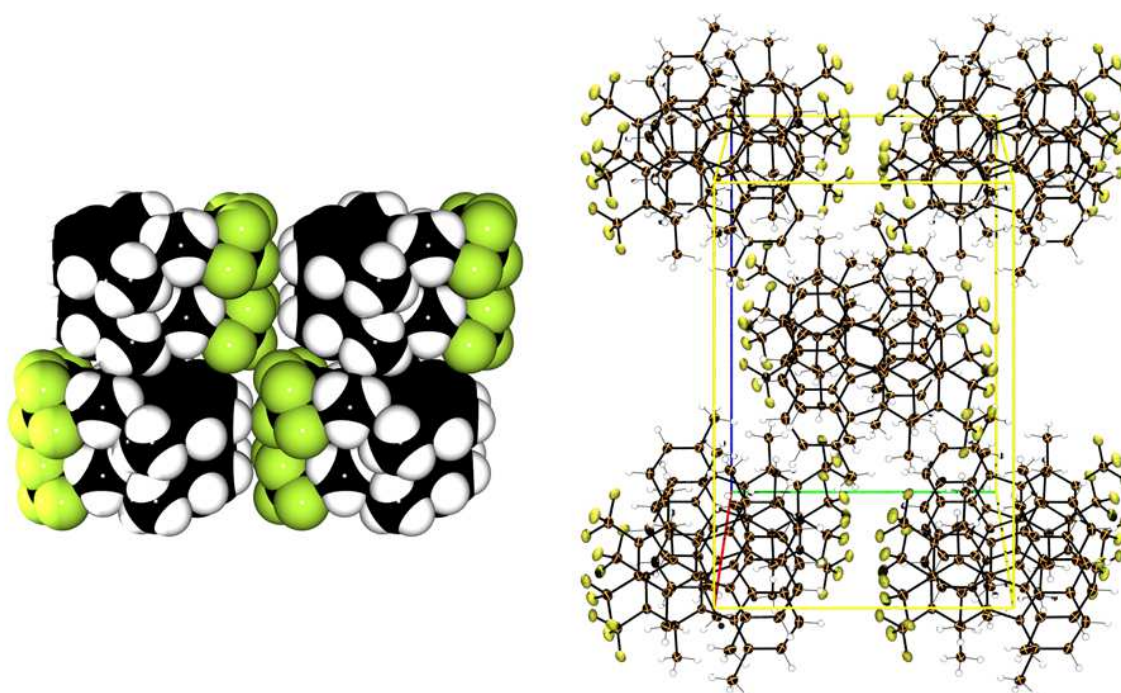
Figure 2.8. Overall solid state packing of **12**. Left: A space-filling model, showing the interactions between dimeric units. Right: View of the unit cell along the crystallographic *c* axis.

Because of the mirror plane, fluoranthene **12** offers two positions where trifluoromethylation according to the protocol of Togni can occur. The sterically demanding methyl group might inhibit an *ortho*-attack and indeed after slight modification of the reaction conditions, 1,6,7,10-tetramethyl-3,8,9-tris(trifluoromethyl)fluoranthene (**13**) can be isolated from the reaction mixture by column chromatography on silica gel in a 36 % yield in high purity.
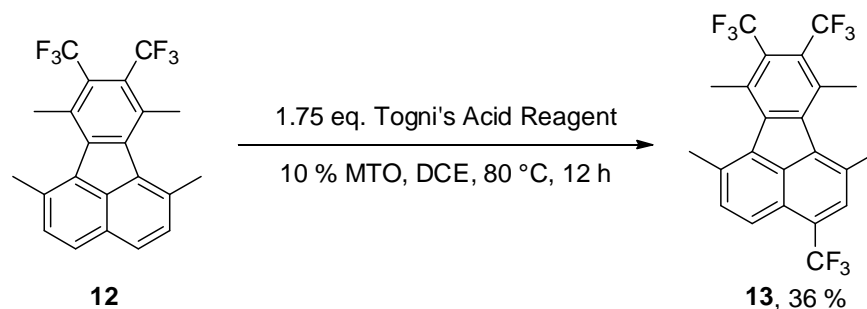
Scheme 2.6. Synthesis of 1,6,7,10-tetramethyl-3,8,9-tris(trifluoromethyl)fluoranthene (**13**) from **12**.

Due to the C_1 symmetry, NMR spectra are comparatively complex, three signals can be observed in the ^{19}F NMR but 23 independent carbon atoms with fluorine couplings are expected for the ^{13}C NMR. Single-crystals suitable for X-ray analysis could be obtained by cooling a dichloromethane/pentane solution to -30 °C.
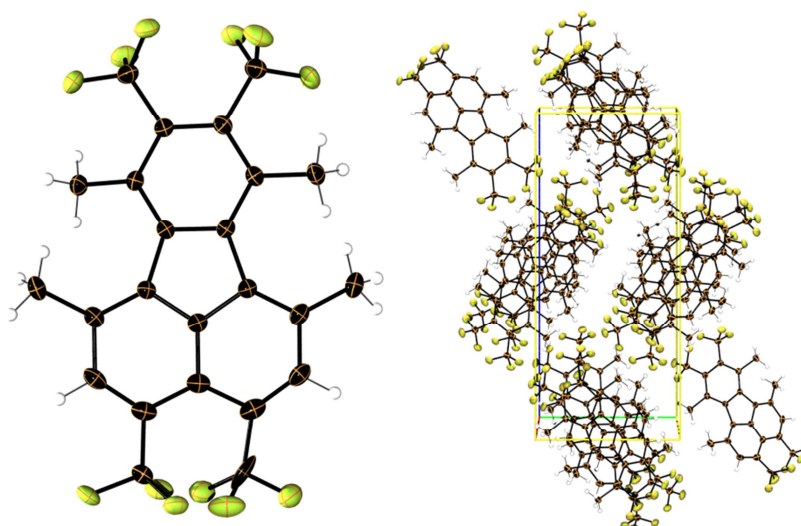
Figure 2.9. Left: The molecular structure of **13**. Right: View of the unit cell along the crystallographic *a* axis.

The solid state structure of **13** suffers from a disorder of the introduced trifluoromethyl group at both possible *peri*-positions (3, 4), giving the visual appearance of a tetrakis-(trifluoromethyl)fluoranthene. The naphthalene-unit of **13** is not deformed, like it would be expected for such a substitution pattern (figure 2.9). Intramolecular C-H···F contacts are present (2.36 – 2.66 Å), as well as intermolecular contacts between neighbouring layers. The overall solid state packing is strand-like, which is supported by π-stacking (short distance of 3.88 Å) of only one of the six-membered rings to the next ring of a rotated molecule (approx. 180 °), giving the off-centred structure. Various interlayer C-H···π contacts can be found as well, ranging from 2.99 – 3.23 Å.

Further trifluoromethylation of **13** is arduous and yields a complex mixture of compounds. The conversion is still in the range of more than 20 % for this reaction. The sterically rather demanding 1,6,7,10-tetramethyl-3,4,8,9-tetrakis(trifluoromethyl)fluoranthene (*sym*-**14**) and 1,6,7,10-tetramethyl-2,4,8,9-tetrakis(trifluoromethyl)fluoranthene (*asym*-**14**) can be identified from the crude NMR. Separation by column chromatography is in this case impossible due to the very similar dipolar moment in all three molecules, **13**, *asym*-**14** and *sym*-**14**. This separation is much more complicated in comparison to the separation of **12** and **13** because in the latter case, a strong dipolar moment is induced in the molecule, whereas no significant change is observed by the introduction of a fourth substituent.

Therefore a separation based on the size (and shape) of the molecules was attempted by using recycling preparative GPC. A size-exclusion gel-permeation chromatography with two JALGEL columns and chloroform as eluent was performed. After 8-10 h, separation of the *sym*-**14** (fastest moving), *asym*-**14** and **13** (slowest moving) could be observed, if around 40 mg of prepurified sample were injected. After several runs, the major product, *asym*-**14**, could be obtained in amounts that allowed a complete characterization of the compound. Again, the C_1-symmetry and the therefore 24 unique carbon atoms with fluorine coupling prevent a precise assignment of each carbon atom, but additionally, single-crystals suitable for X-ray analysis could be obtained.
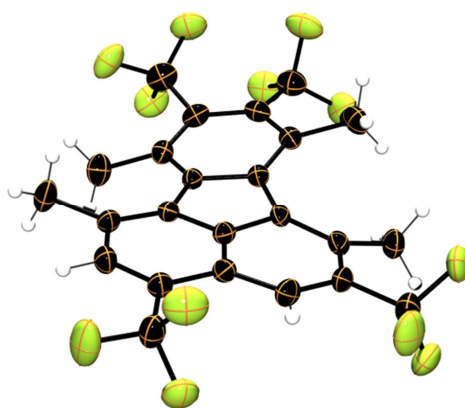
Figure 2.10. The molecular structure of *asym*-**14**. The severe distortion of the lower part of the molecule becomes clearly visible.

Again, a severe C_2-twist distortion is visible. A torsion angle of up to 24 ° is found between a methyl and an adjacent trifluoromethyl group, indicating the out-of-plane bending and additional twist and splay.

The fluoranthene molecules of *asym*-**14** are alternatingly rotated by +90/-90 °, resulting in a strand like packing with elongated intermolecular distances 4.24 Å, suggesting that π-stacking is not a dominant interaction in this system. More likely is the dominant effect of the great number of possible hydrogen bonds to the four trifluoromethyl groups, where each molecule is a donor and acceptor of at least one hydrogen bond. Between two fluoranthenes that form a dimer, which is the smallest repetitive unit of a strand, two hydrogen bonds of a fluorine to a methyl-hydrogen are found (2.55 – 2.78 Å). Intermolecular interaction in this dimeric unit also include C-H···π interactions, for example from a methyl hydrogen of the upper part of the fluoranthene to the naphthalene part of the oppositely facing molecule. These strands, which are produced by repeating the dimeric units, are then interacting by C-H···F contacts in the same plane and even with the upper/lower plane (2.59 – 2.71 Å).
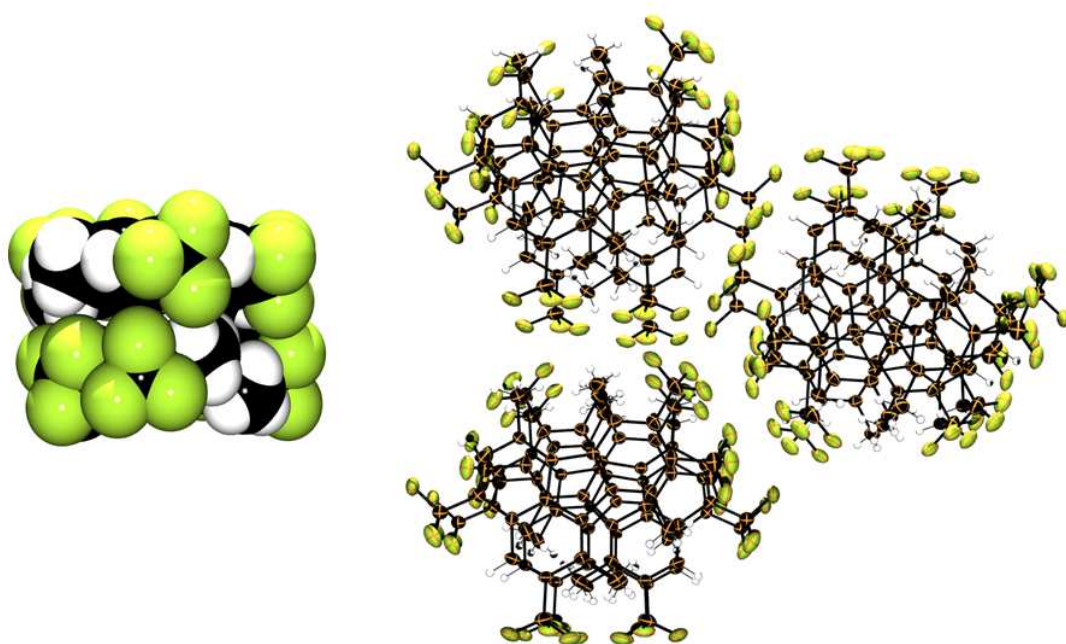
Figure 2.11. Left: A space-filling model of the dimeric unit. Right: Strands of *asym*-**14**, which proceed along the crystallographic *c* axis.

Asym-**14** does not undergo ring-closing reaction to the corresponding corannulene (*cf.* chapter 2.7). To gain access to a highly trifluoromethylated corannulene nevertheless, the focus of attention was the isolation of the *sym*-**14**, which is formed in traces (13 %) upon trifluoromethylation of **13**. Whereas the NMR spectra of *sym*-**14** becomes easier because of its higher symmetry, the solid state structure of *sym*-**14** shows one of the most complex networks found for all studied fluoranthenes. The structure can be solved in the monoclinic space group $P2_1/c$ and the asymmetric unit consists of two independent molecules which show only a partial overlap characteristic for this layered structure. Again, intramolecular hydrogen bonding is observed in the range of 2.70 – 2.79 Å. The *peri*-trifluoromethylgroups show a twist distortion, whereas the overall molecule is heavily contorted.
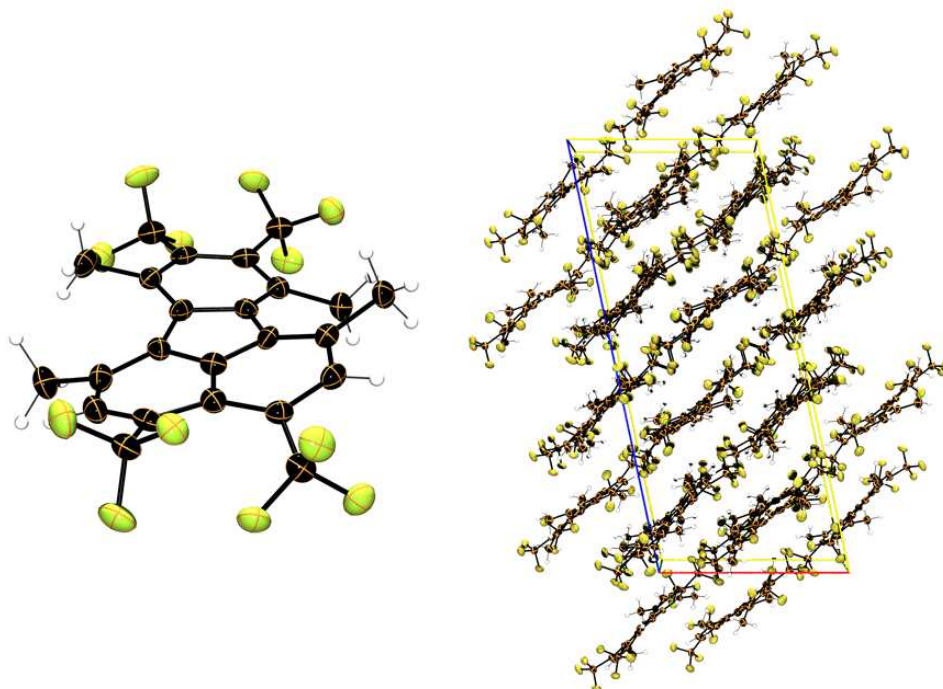
Figure 2.12. Left: The molecular structure of *sym*-**14**. Right: View of the unit cell, along the crystallographic *b* axis, showing the layers of *sym*-**14**.

Within the layers, short hydrogen contacts of 2.55 – 2.63 Å can be observed. One even shorter hydrogen contact of 2.45 Å connects the layers, whereas other interlayer contacts are found in the range of 2.71 – 2.83 Å. All hydrogen contacts are exclusively formed from the hydrogen atoms of the methyl groups, probably because of the favourable geometry. The hydrogen atoms of the methyl groups also engage in interlayer C-H···π interactions in a range of 2.82 – 3.10 Å. In total, the plurality of weak interactions might yield the total stabilization of this structural alignment and cannot be attributed to only one interaction. This concept developed by Nishio[73] should be applicable to at least all fluoranthene- based compounds discussed.

2.6. Synthesis of electron-poor alkynes to generate fluoranthenes

All compounds discussed in the last chapter are based on using hexafluorbutyne for the construction of fluoranthene **12**, which is then further functionalized. Additional dienophiles were synthesized and reacted to yield the corresponding fluoranthenes.

Dicyanoacetylene has been known since the early twentieth century[84] and can be prepared by a reaction of acetylenedicarboxylic acid dimethyl ester (**15**) with concentrated aqueous ammonia at -10 °C giving the dicarboxamide **16** in good yield. Dehydration at 110 °C / 24 mbar of acetylenedicarboxamide **16** with phosphorus pentaoxide suspended with sulfolane gives dicyanoacetylene (**17**), which was collected in a -80 °C trap.[85]
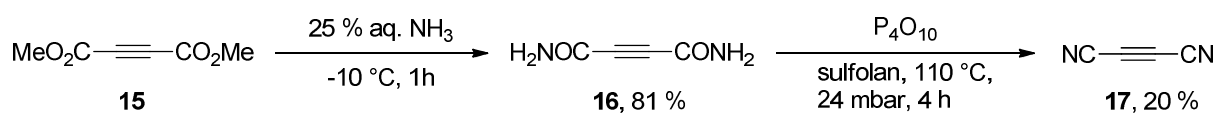
Scheme 2.7. Literature synthesis of dicyanoacetylene (**17**).[85]

For convenient handling and due to its explosive nature, a stock solution with DCE was prepared and stored at -80 °C. **17** was used according to scheme 2.4 and gave the corresponding 1,6,7,10-tetramethylfluoranthene-8,9-dicarbonitrile (**18**) in 88 % yield after workup by column chromatography. The solid state structure of **18** was studied (*cf.* 8.2), but the respective corannulene could not be synthesized.

Diiodoacetylene (**19**) was prepared[86-87] (which also can be used to generate 8,9-diiodo-1,6,7,10-tetramethylfluoranthene (**20**), see 8.4.8) and reacted with pentafluorophenyl-magnesiumbromide (**21**) in the presence of cobalt(II)chloride to yield bis(pentafluorophenyl)acetylene (**22**).
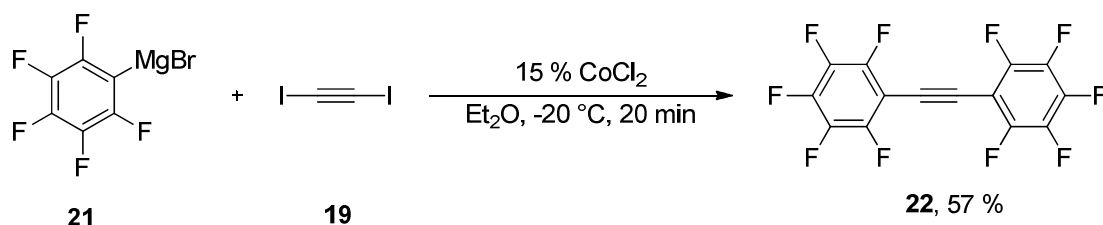
Scheme 2.8. Synthesis of bis(pentafluorophenyl)acetylene (**22**) according to Haszeldine.[88]

Accordingly, the 1,6,7,10-tetramethyl-8,9-bis(perfluorophenyl)fluoranthene (**23**) can be obtained in 54 % isolated yield and was fully characterized, including X-ray crystallography.
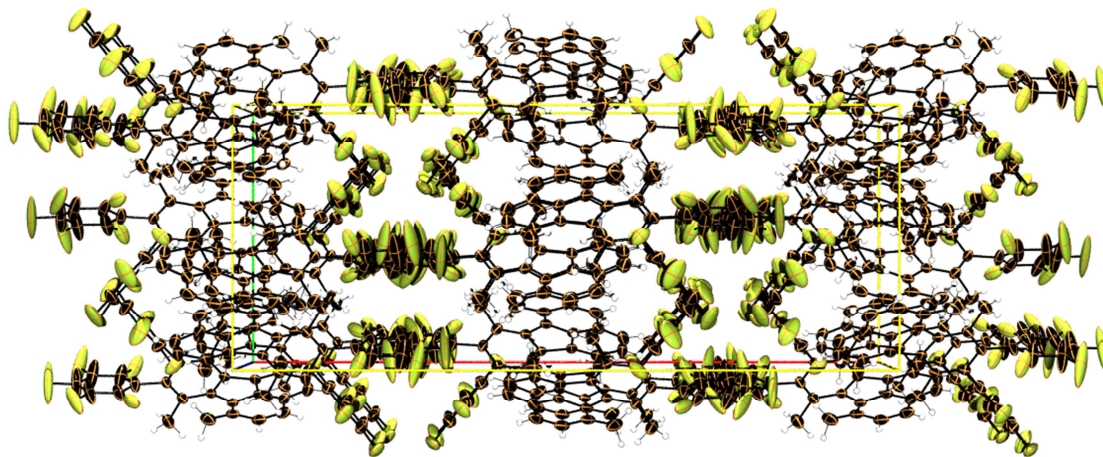
Figure 2.13. View of the unit cell of **23**, along the crystallographic *c* axis, revealing the separation of the fluorocarbon- and hydrocarbon-parts.

Similar to the solid state packing of **12**, fluoranthene units of **23** form dimers. Due to the steric demand of the pentafluorophenyl moeties, which are perpendicular to the fluoranthene plane, head-to-head dimers might be unfavourable (**12**) and the formation of head-to-tail dimers is observed. Within a dimer, elongated π-stacking of the coplanar naphthalene-subunits occurs (3.97 Å) and interactions between dimeric subunits are dominated by C-H⋯π interactions not closer than 3.18 Å. C-H⋯F interactions (2.50 – 2.79 Å) on the other hand arise predominately between the segregated fluorocarbon and hydrocarbon parts connecting the sections (figure 2.13.). Because of the mirror plane in the molecule **23**, ^{19}F NMR spectra show one AA'BB'C-type spectrum, as expected.

2.7. Electron-poor corannulenes generated from fluoranthenes

According to the procedure of Sygula and co-workers, substituted fluoranthenes, like **12**, can be precursor molecules to the corresponding substituted corannulenes.[82]

Therefore Wohl-Ziegler bromination was carried out, using excess of *N*-bromosuccinimide to ensure complete conversion to the 7,10-bis(bromomethyl)-1,6-bis(dibromomethyl)-8,9-bis(trifluoromethyl)-fluoranthene (**24**). Previous studies have shown that similar compounds tend to lose one- or several bromine atoms. Therefore the brominated fluoranthene **24** and all others, were not purified and instead reacted immediately with nickel powder in anhydrous DMF.[89]

1.12.0 eq. NBS, 3.0 % DBPO,
CCl$_4$, *hv*, 80 °C, 24-48 h

2. 8.8 eq. Ni(0),
DMF, 80 °C, 8 h

12 R$_1$ = CF$_3$, R$_2$ = R$_3$ = H
13 R$_1$ = R$_2$ = CF$_3$, R$_3$ = H
14 R$_1$ = R$_2$ = R$_3$ = CF$_3$
23 R$_1$ = C$_6$F$_5$, R$_2$ = R$_3$ = H

25 R$_1$ = CF$_3$, R$_2$ = R$_3$ = H (22 %)
27 R$_1$ = R$_2$ = CF$_3$, R$_3$ = H (16 %)
28 R$_1$ = R$_2$ = R$_3$ = CF$_3$ (11 %)
29 R$_1$ = C$_6$F$_5$, R$_2$ = H (36 %)

1.12.0 eq. NBS, 3.0 % DBPO,
CCl$_4$, *hv*, 80 °C, 28 h

2. 10.0 eq. NaOH,
dioxane/H$_2$O, 110 °C, 20 min

26 R$_1$ = CF$_3$, R$_2$ = R$_3$ = H (78 %)
30 R$_1$ = C$_6$F$_5$, R$_2$ = R$_3$ = H (52 %)
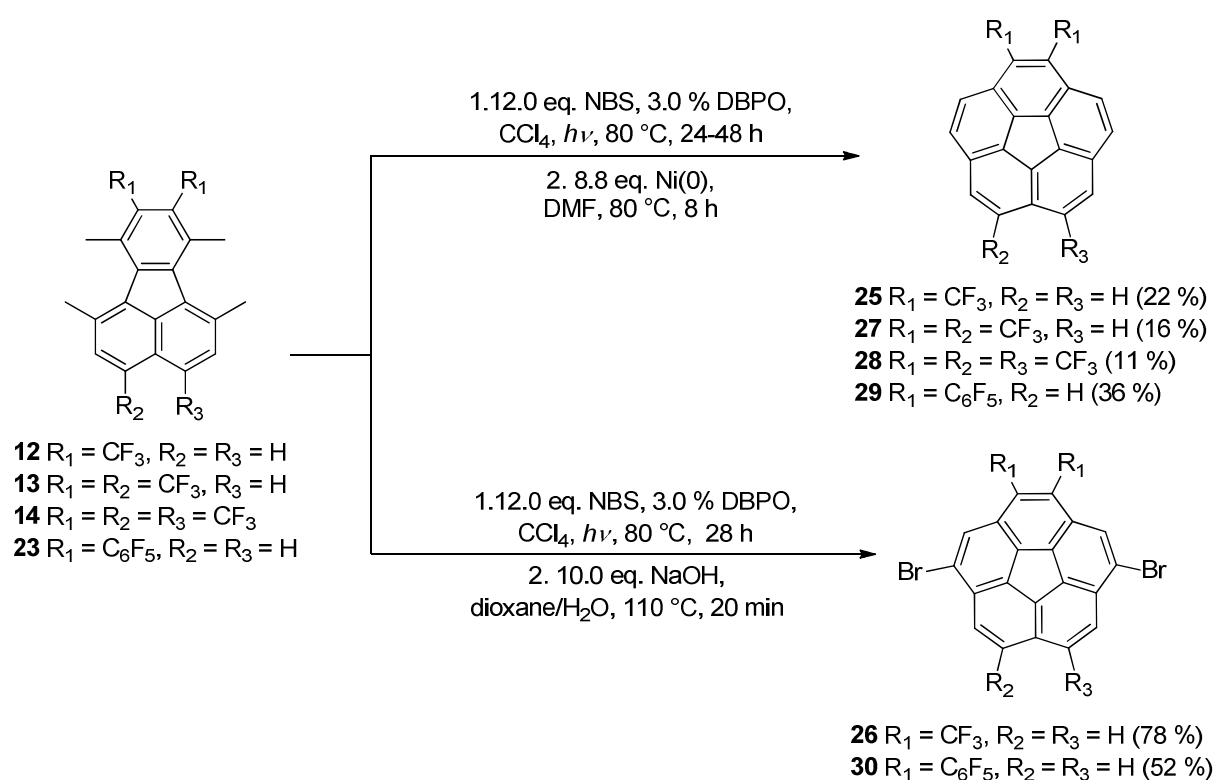
Scheme 2.9. Syntheses of corannulenes **25-30** by liquid-phase protocols.[19a-b, 82]

The mechanism of the ring-closing reaction was not investigated by the group of Sygula, but according to usual reaction patterns, it is likely that a nickel(0) complex abstracts two bromine atoms from the molecule, followed by elimination of hydrogen bromide to give the corannulene, in this particular example 1,2-bis(trifluoromethyl)corannulene (**25**), in moderate yields. **25** can be isolated from the crude mixture after aqueous extraction and column chromatography on silica gel with

pentane as eluent as sole single product. If the column is eluted with a solvent of higher polarity (in this case dichloromethane), an unidentified brown product is obtained, which shows very broad signals in the range of 7 ppm in the ^{1}H NMR and a broad signal in the range of 50 ppm in the ^{19}F NMR and a poor solubility. These probably oligo- or polymeric by-products also indicate the formation of carbene-type intermediates, which was observed for the other corannulenes **27**-**29** as well.
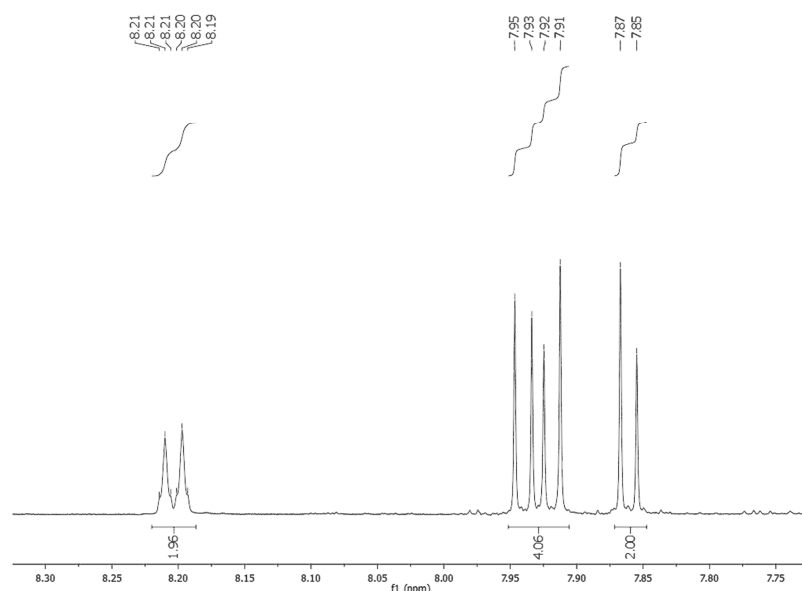
Figure 2.14. ^{1}H NMR of **25**, showing the typical AB-type signals. Note the small ^{19}F couplings of 2.8 Hz of the downfield signal.

The compound **25** is a pale-yellow solid that has a needle-like appearance after slow evaporation of dichloromethane/chloroform solutions and its structure can be solved in the monoclinic space group $P2_1/c$.

The molecular bowls of **25** are aligned into 1D parallel columns along the crystallographic c axis, where neighboring columns have opposite directions. The bowls have a nearly eclipsed conformation (the central five-membered ring is shifted by 8 °). The trifluoromethyl groups are separated by a 140 ° twist (figure 2.15), resulting in a dense arrangement. Surprisingly, despite a rather short distance of approximately 2.5 Å, stabilization by C-H···F interactions between the columns seems to be negligible concerning the rotational disorder of the CF_3 unit in the solid state. Due to the steric demand of the two trifluoromethyl groups, the bowl depth now is flattened to 0.82 Å. The bowl-to-bowl distance as obtained from the centre of the five-membered ring to the centroid of another is 3.73 Å.
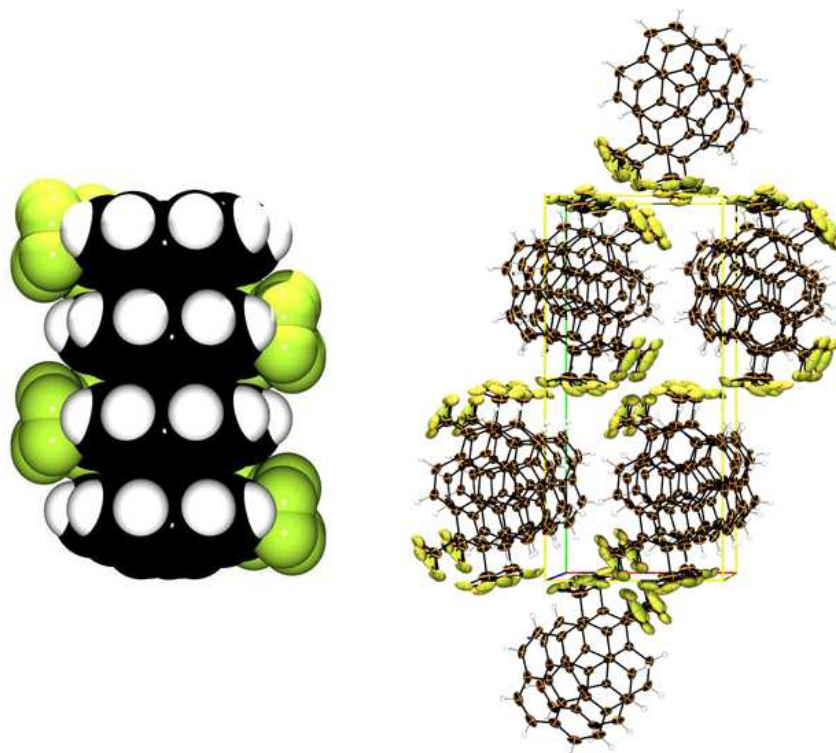
Figure 2.15. Solid state structure of **25**. Left: A schematic representation of the 1D columnar π-stacking (space-filling model). Right: View of the unit cell along the crystallographic *c* axis. The bowl of **25** has a depth of 0.8244(2) Å and the observed bowl-to-bowl distance is 3.725(1) Å.

Further reactions starting from **25** were not studied, as the rather low level of substitution would lead to the formation of isomeric mixtures.

If **12** is brominated and the ring-closing reaction using sodium hydroxide and dioxane is used (scheme 2.9), which in the case of the unsubstituted fluoranthene would yield tetrabromocorannulene,[19] 4,9-dibromo-1,2-bis(trifluoromethyl)-corannulene (**26**) is obtained. Corannulene **26** is poorly soluble in most organic solvents at room temperature (the solubility is estimated to be significantly lower than 1 mg/10 mL), therefore ^{13}C NMR data could not be obtained. Sufficient ^{1}H and ^{19}F NMR data can be obtained at room temperature or by heating a sample to 80 °C in deuterated 1,1,2,2-tetrachloroethane, which also confirms the expected structure. The compound forms long, needle-like crystals that can be solved in the monoclinic space group *P*121/*c*.[90]
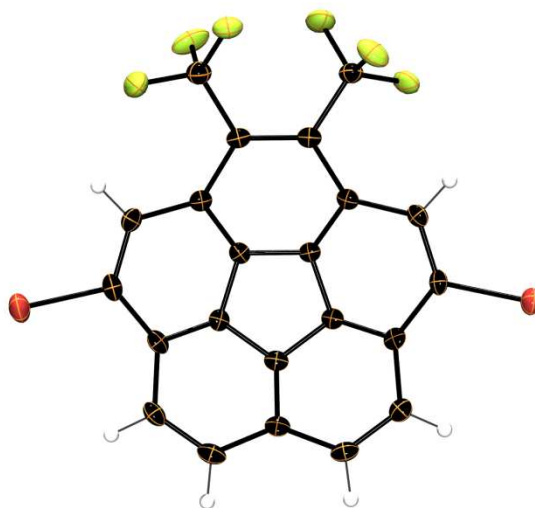
Figure 2.16. Molecular structure of **26**, with a bowl depth of 0.7949(0) Å.

The increasing substitution along the corannulene rim flattens the bowl 0.79 Å and decreases the intermolecular $\pi\cdots\pi$ stacking distance further. The molecular strands are engaging in a few C-H$\cdots$F contacts of about 2.73 Å and no rotational disorder of the trifluoromethyl group occurs. The hydrogen bonding in this crystal is completely dominated by C-H$\cdots$Br contacts within a distance of 2.96 – 3.24 Å, connecting the molecular columns, according to the common sense of the strength of halogens participating in halogen bonding.
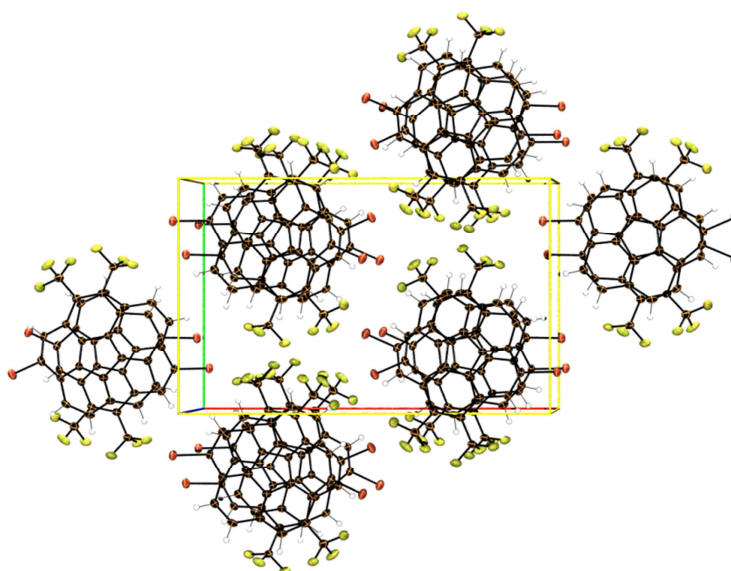
Figure 2.17. View of the unit cell along the crystallographic *c* axis, the dense intermolecular stacking (3.6569(3) Å) of **26** can be seen.

This derivative is a highly promising intermediate for the construction of further functionalized corannulenes, bearing two trifluoromethyl groups. By applying standard cross-coupling reaction conditions, new corannulenes can be synthesized.[90-91] Unfortunately, the reaction yields are very low, suggesting impurities in the obtained starting material **26**. The purity was confirmed by mass spectrometry and NMR for each batch, but the reason for the low yield of consequent reactions is still inscrutable.

Following the presented reaction protocol for **13** (scheme 2.9), the corresponding 1,2,6-tris(trifluoromethyl)corannulene (**27**) can be isolated after column chromatography on silica gel with pentane as eluent. Originating from the C_1-symmetry of the molecule, 23 sets of signals are expected for the ^{13}C NMR. In the ^{1}H NMR protons in *peri*-position to a trifluoromethyl group are visible because of the small ^{5}J coupling of 2 Hz. Due to the predominant crystal growth tendency in only one crystallographic axis, crystals suitable for X-ray analysis could not be obtained.

Surprisingly *asym*-**14**, is not a suitable intermediate for the generation of a tetrakis-trifluoromethylcorannulene. Only yield traces of a didehydrocorannulene and unidentifieds product of probably polymeric nature could be obtained. As apparent (figure 2.10), dibromination of the sterically highly stressed methyl-groups might be unfavourable. Furthermore, the electron-

withdrawing groups increase the stability of the intermediary carbene, which might facilitate polymerisation in favour of rapid intramolecular ring-closing. Trifluoromethylation in both *peri*-positions might release strain from the methyl groups used for ring closing, therefore *sym*-**14** was accumulated from reaction mixtures. After exhaustive bromination of the compound and ring-closing reaction (scheme 2.9), traces of the desired 1,2,6,7-tetrakis(trifluoromethyl)corannulene (**28**) could be obtained after flash column chromatography. The compound is a colourless solid but due to the very small amount obtained, it was only characterized by ^{1}H, ^{19}F NMR and mass spectrometry. Because of the C$_s$-symmetry, spectra of **28** are comparatively simple. Nevertheless, electrochemical data could be obtained and will be discussed together with all other corannulenes in chapter 5.1.

Accordingly pentafluorophenylated corannulenes were prepared. 1,2-bis(perfluorophenyl)-corannulene (**29**) can be synthesized, as well as the corresponding 4,9-dibromo-1,2-bis(perfluorophenyl)corannulene (**30**). The functionalized dibromocorannulene **30** can be methylated[18] to yield a perfluorophenylcorannulene with improved solubility.
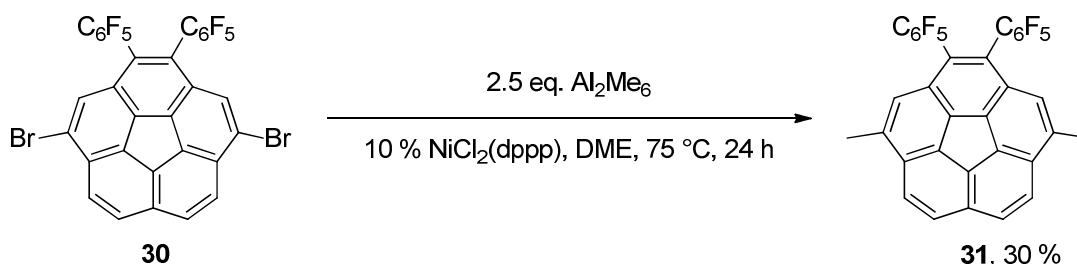
Scheme 2.10. Methylation of **30** yields 4,9-dimethyl-1,2-bis(perfluorophenyl)corannulene (**31**).

Corannulenes **29** and **31** again show a fairly similar ^{19}F NMR to **23**, whereas corannulene **30** was only investigated scarcely, because of the very low solubility in common organic solvents. The electrochemical properties of **29**, will also be discussed in chapter 5.1.

2.8. Excursus: *N*-Substituted imide-fused corannulenes by use of cyclic imides

While the synthesis of a bridging imide (bridging two *peri*-positions) would take several steps it seemed simple to introduce one maleimide, instead of two substituents in *ortho*-position. *N*-subsituted maleimides are usually prepared from maleic anhydride by treatment with amines followed by dehydration and it was decided to synthesize the corresponding electron-poor maleimide first, because of the very low nucleophilicity of (per)fluorinated amines.[92] Two different fluorinated substituents were chosen, based on the research of Würthner's group.[57] The susceptibility to undergo additions across the double bond by Diels-Alder reaction was employed in the common synthetic manner. Usually, this reaction is carried out conveniently in the non-toxic solvent acetic anhydride.
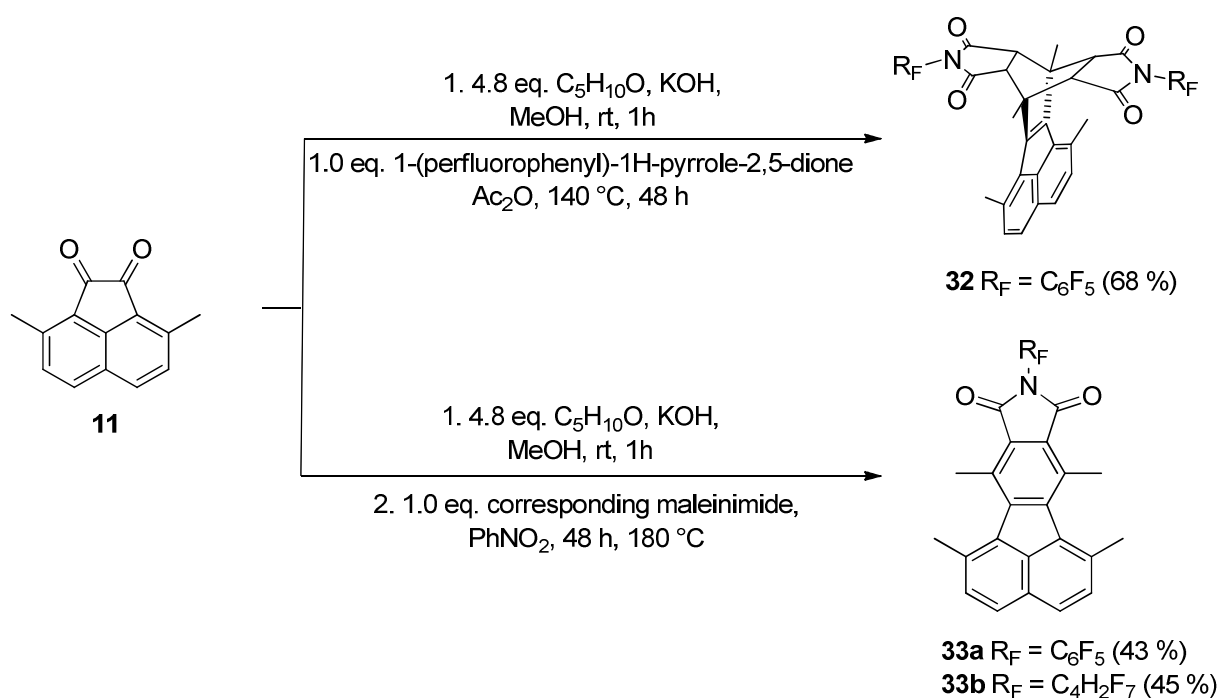
Scheme 2.11. Synthesis of the *N*-substituted, imide-fused fluoranthenes **33a**-**b**.

After workup, the crude reaction mixture showed the expected doublet-like signals in the aromatic region which are characteristic for fluoranthene compounds. The ^{19}F NMR however, was surprising at first, showing four signals instead of expected three sets of signals. Careful considerations suggested an ABCDE-type set of signals instead of the expected AA'BB'C. This can be explained by hindered

rotation of the pentafluorophenyl-moiety giving two chiral rotamers (R_a, S_a).[93] After purification, the ^{1}H NMR showed more signals than expected for the fluoranthene compound. High-resolution mass spectrometry gave no matching results. A single-crystal X-ray analysis finally revealed the true nature of the main product (**32**) of this reaction. In this particular case, the usage of acetic anhydride enables the formation of the adduct **32** with a central bicyclo[2.2.2]oct-2-ene unit (scheme 2.11). It is formed either by reaction of an *exo*-dimer from the condensation reaction or by decarbonylation of the *exo*-adduct and subsequent reaction with a second equivalent of maleimide.[94] Due to the molecular strain and steric repulsion (figure 2.18), the two pentafluorophenyl groups give one distinct set of signals identifiable as a first order ABCDE-type ^{19}F NMR spectrum at room temperature.[93]
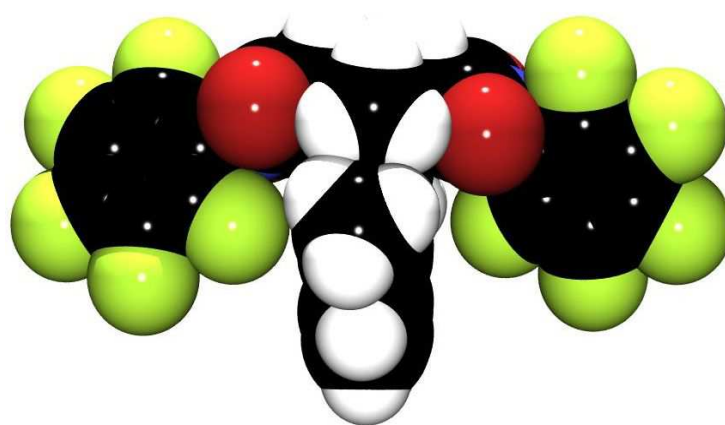
Figure 2.18. A space-filling model of **32** as represented by the asymmetric unit, showing the steric demand of the canted pentafluorphenylgroups. The structure was solved in the monoclinic space group C*c.*

If the reaction runs in nitrobenzene at 180 °C, adduct **32** is not observed and the desired product **33a** and **33b** can be isolated in 43 % and 45 % yield, respectively. The steric hindrance in **32** and **33a** is expected to be similar, but now a fast C_6F_5-rotation is present in **33a** at room temperature, whereas no unusual characteristics are found for **30b**.
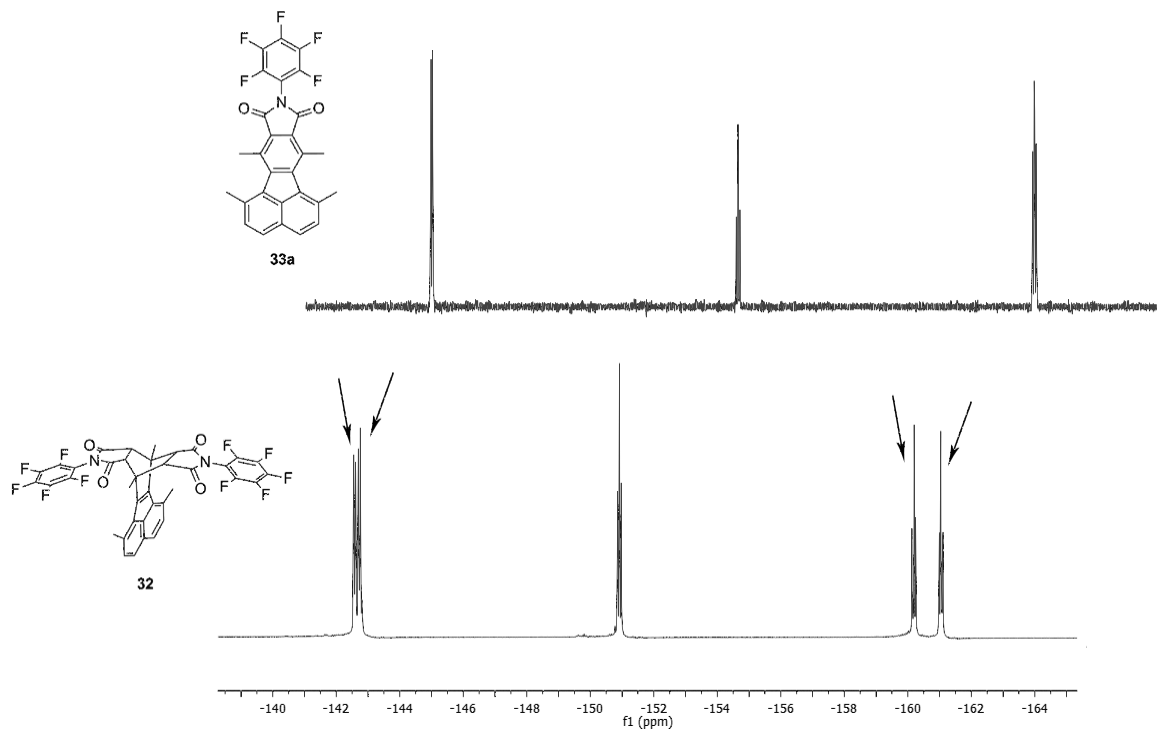
Figure 2.19. ^{19}F NMR of **32** and **33a** showing the different spin systems, AA'BB'C (above) for **33a** and ABCDE for

32 (below).

The higher symmetry of **33a** in comparison to **32** now results in an AA'BB'C-type ^{19}F NMR spectrum.
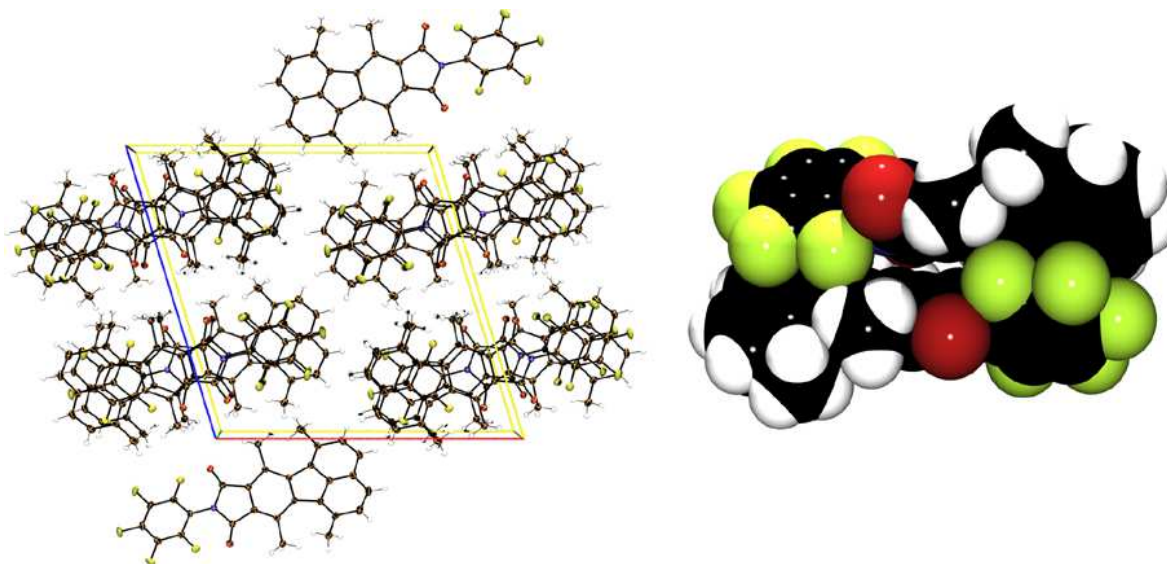
Figure 2.20. Left: View of the unit cell with the dense head-to-tail arrangement in **33a**, which proceeds in

infinite columns along the crystallographic *b* axis. Right: Space-filling model of a dimeric unit.

The solid state structure shows again a C_2-twist and a moderately canted alignment of the perfluorinated phenyl group in **33a**, which opposes the electron rich lower part (naphthalene-part) of an adjacent molecule in the twisted stack (figure 2.20.). This dense head-to-tail crystal packing is supported by C-H···O bonding of the carbonyl groups of approximately 2.48 Å to the opposing molecule and furthermore by relevant C-H···F contacts[64e] of 2.55 Å to the naphthalene-unit of the next column.

Scheme 2.12. Synthesis of the imide-fused corannulenes **34a** and **34b**.

Wohl–Ziegler reaction and subsequent nickel-mediated intramolecular coupling involving complete debromination of the product yield the corresponding corannulenes **34a** and **34b**, likewise. Single crystals of sufficient quality were obtained by slow evaporation of a chloroform solution and solved in the monoclinic space group $P2_1/n$. The bowls of **34a** are aligned into 1D parallel columns (figure 2.21), but unlike, for example indenocorannulenes,[34] they are aligned in a staggered conformation. The bowl direction of the same stack is the same, whereas adjacent columns have an opposite direction. The extended π-system surprisingly results in a shallower bowl depth of 0.83 Å, with the bowls being slightly tilted by 10 °. This alignment is facilitated by C-H···F (2.55 – 2.78 Å) interactions between the anti-parallelly aligned neighboring stacks.
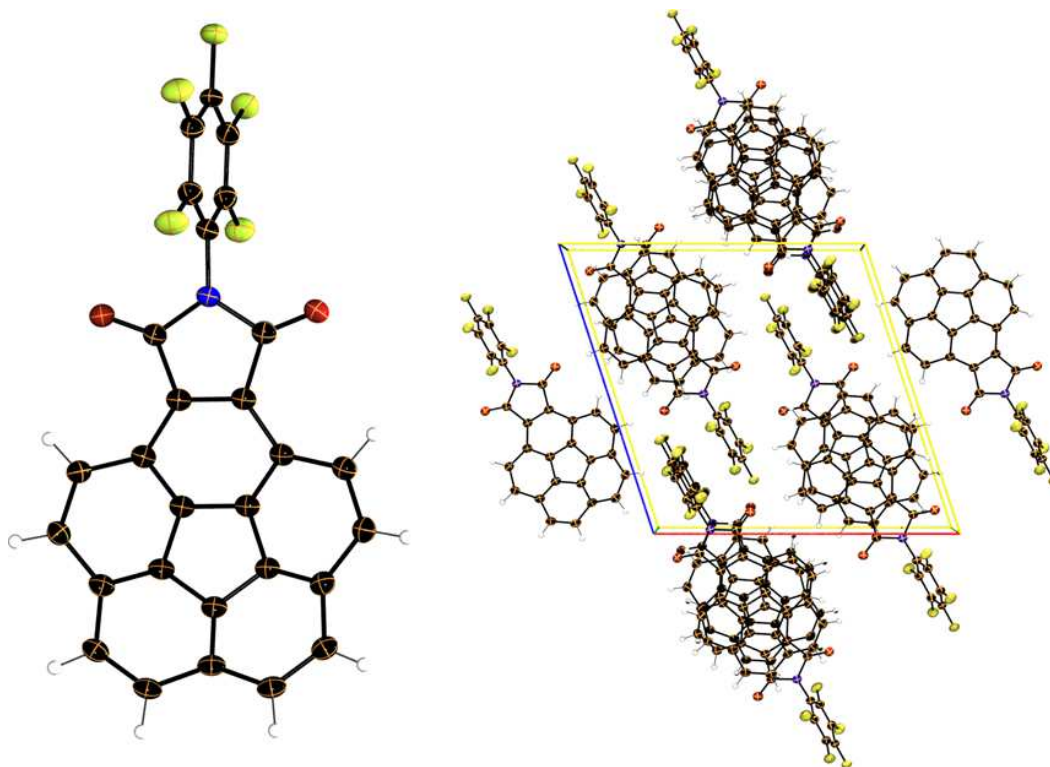
Figure 2.21. Left: The molecular structure of **34a**. Right: View of the unit cell of **34a** along the crystallographic *b* axis, showing the infinite columns. The bowl depth of **34a** is 0.8282(0) Å and with a bowl-to-bowl distance of 3.8783(2) Å. The distance between two bowls is 7.3395(4) Å.

The pentafluorophenyl ring is more canted in comparison to **33a**, with an angle of 76 ° to the imide ring, probably to maximize C-H···F contacts, and because of the absence of the flexible and electron rich surface of **33a**. The ^{19}F NMR spectrum at room temperature suggests again free rotation of the pentafluorophenyl ring of **34a** and the alkyl chain of **34b**. One spoke bond and one flank bond are the shortest (C016–C031) and longest (C019–C034) C–C-bonds of 1.3761(1) and 1.4453(1) Å in the corannulene-bowl, respectively. As a consequence of the decreased curvature, both are marginally longer than in the parent corannulene molecule for **34a**. Within the convex-concave stacks no pitch or roll angle is found, resulting in no transverse shifting.[61] The intermolecular bowl distance calculated between three molecules along the stack is 7.34 Å, which leads to an average bowl-to-bowl distance of 3.67 Å regardless of the small slipping angle. This difference is smaller than previously reported for tetra- and penta-substituted corannulenes, which may result from the steric demand of the arylalkynyl groups attached.[35]

3. Sumanenes with electron withdrawing substituents

3.1. Aromatic fluorination and trifluoromethylation of sumanene

The synthesis of sumanene follows a completely different synthetic approach compared to the kilogram-scale synthesis of the archetypical corannulene (scheme 1.5).
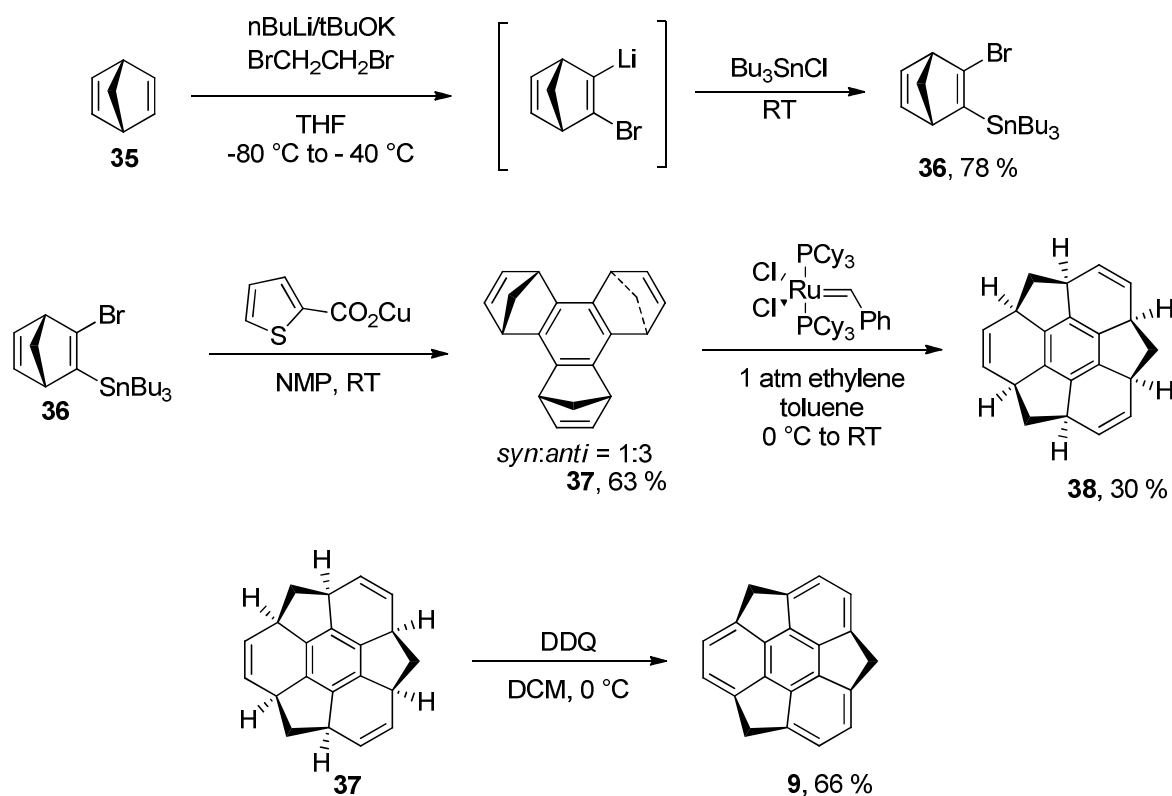
Scheme 3.1. The synthesis of the molecular bowl sumanene (9), $C_{21}H_{12}$.[43]

The synthetic route starting from a three-dimensional framework is mostly based on tetrahedral sp^3 carbons. This strategy resembles the early corannulene synthesis of Barth and Lawton.[9] Trimerization of a norbornadiene **36** yields *syn-* and *anti*-benzotris(norbornadiene) **37**, based on an organocopper-mediated trimerization. Ruthenium-catalyzed tandem ring-opening metathesis (ROM) and ring-closing metathesis (RCM) reaction under an atmospheric pressure of ethylene, yields hexahydrosumanene **38**, which gives finally the required π-conjugated structure **9** by oxidative aromatization, using the strong oxidizer DDQ.[43,47,95]

Naturally, the direct introduction of fluorine, like discussed previously (chapter 2.3), was attempted. A reaction of sumanene with 1.6 equivalents of xenon(II)fluoride in dichloromethane yields a mixture of **9**, monofluorosumanene (**39**) and difluorosumanenes. Here again the purification by column chromatography was not successful and monofluorosumanene could only be obtained by using a buckyprep column. By using the recycling GPC as described for the purification of *asym*-**14** and *sym*-**14** after approximately 8 days, enriched fractions could be collected. The general problem of this method prevails: The peak broadening on the HPLC columns is faster than the separation, giving access only to enriched fractions after very careful purification attempts. Surprisingly, enriched samples, containing only **9** and **39**, as investigated by means of NMR spectroscopy and mass spectrometry, show a tendency to crystallize. Investigations of the needle-like crystals showed that the obtained crystals are not formed by only one compound but instead are co-crystals of the given composition of the bulk-material. If a bulk material of known composition is crystallized, one crystal can be removed and quickly washed with hexane. After drying, the composition can be determined conveniently by ^{1}H NMR integration and shows a deviation of around 10 % which lies in the range of expected error. A crystal suitable for X-ray analysis revealed another surprising effect. The fluorine atom located at the rim of sumanene is small enough to retain the favorable columnar packing of sumanane. Furthermore, the fluorine atom is equally distributed among all possible positions, giving the visual appearance of a hexafluorinated sumanene. A crystal of the pure monofluorosumanene **39** was obtained as well and shows identical behavior in the solid state without the presence of sumanene by maintaining the spacegroup *R*3c.
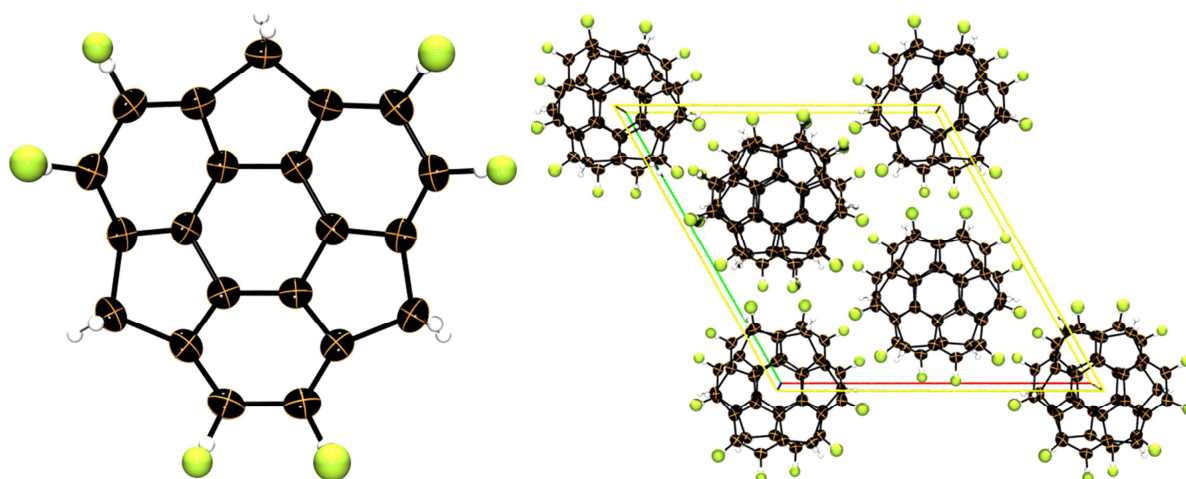
Figure 3.1. Left: The molecular structure of **39**, note the disorder of the fluorine atoms at all possible rim-positions. Right: View of the unit cell, along the crystallographic *c* axis. The bowl depth is 1.100 Å, with a bowl-to-bowl distance of 3.82 Å.

Hydrogen bonding is possible between an *endo* hydrogen atom of the benzylic carbon to a fluorine atom of a neighbouring column (2.53 Å), whereas *exo* hydrogen atoms can interact with a rim fluorine atom underneath (2.48 Å). The bowl itself is slightly flattened by 10 % in comparison to **9**, but in contrast to the corannulene system, the bowl-to-bowl distance increases slightly despite the flattened bowl (3.82 Å).

Further rim-substitution on **9** was carried out by using the previously discussed trifluoromethylation protocol (scheme 2.3) and yields 1-(trifluoromethyl)sumanene (**40**) in a 16 % yield but attempts to obtain crystals suitable for X-ray analysis failed. For unknown reasons, the colourless powder rapidly darkens within a few days in air, suggesting a rather low stability of the compound towards water or sunlight.

To summarize, the latter findings regarding the fluorination of **9**, make **9** an excellent molecule for the design of organic n-type semiconductors, where the electron-acceptor properties and therefore also the threshold values of the bulk material can be fine-tuned, if this trend is persistent for the higher fluorinated species as well.

3.2. Electron withdrawing substituents at the benzylic carbon atoms

As described earlier in the introduction, **9** features three benzylic positions, which allow facile functionalization. Several examples can be found in the literature already, like the stereoselective trisilylation via the corresponding trianion,[47a] benzannulated naphto-sumanenes,[49] π-extended and conjugated sumanenes by condensation with aldehydes[50] and benzylic oxidation yielding "oxosumanenes", a key compound for further transformations.[51a-b]
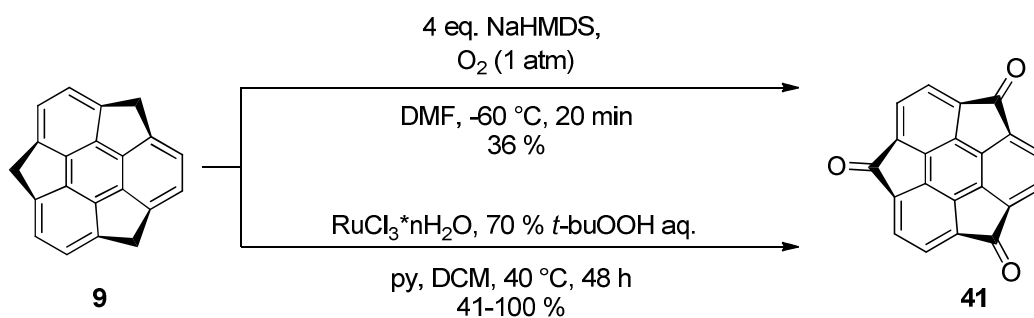
Scheme 3.2. The two synthetic approaches to the sumanenetriketone (**41**).[51a-b]

The synthesis of trione **41** can be carried out using the methods described in the latter scheme. The low temperature oxidation, however, could be only carried out in a small scale with a maximum of 5 mg starting material and gave highly unstable yields. Only in some cases unreacted **9** could be recovered. The synthesis using a ruthenium catalyst also gave unsteady yields, but within the range of 41-68 % (10 runs). This mean value could be increased up to 60-100 %, if the reaction tube was wrapped in aluminium foil and workup was immediately performed after removing the tube from the chemistation slot. It is possible that the ruthenium catalyst or the trione **41** becomes activated by light and subsequent reactions consume generated **41**. The given yields are probably too high, as after very sincere GPC purification a highly pure product was isolated in slightly lower yield, having a pale yellow appearance, in contrast to the bright orange powder that is obtained after purification of the reaction mixture by silica gel chromatography.

Dithianes are excellent precursors for the introduction of fluorine, therefore the transformation to the cyclic dithiane (**42**) was attempted. They are readily fluorinated by (difluoroiodo)benzene derivatives,[96] a combination of an electrophilic halogen and a fluoride ion donor,[97] or even by elemental fluorine.[98]
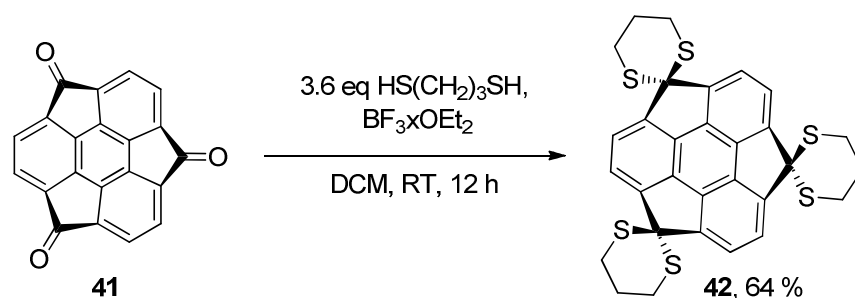
Scheme 3.3. Synthesis of the tris(dithiane) of sumanene (**42**) from the triketone **41**.

Because of the poor solubility of the dithiane **42**, approximately 3 mg of the substance can be purified by PTLC using dichloromethane as eluent, to yield the compound in pure form (colourless powder).

Early attempts using *para*-iodotoluene difluoride led to a low conversion and therefore conditions based on Katzenellenbogen[97a] and Haufe[97c] were tested. Using *N*-iodosuccinimide for the activation and the nucleophilic fluorinating agent pyridine hydrofluoride (Olah's Reagent) was suitable to produce the desired *gem*-dihalo compound, hexafluorosumanene (**43**), in good yield if the reaction was run under anhydrous conditions in a PP-tube. A fast colour change from colourless to pink and finally to purple indicates the formation of iodine, which can be removed during aqueous extraction if a sodium thiosulfate solution is added. Finally the product can be isolated by PTLC on silica gel without the use of HPLC equipment yet again, because the possible byproduct is the corresponding oxosumanene and not the hydrocarbon analogue. If the reaction is carried out in a glass flask instead of a PP-tube, not only **44** in 24 % yield but also tetrafluorosumanenone (**44**) and difluorosumanenedione (**45**) were also obtained in 23 % and 19 % yields, respectively, by nucleophilic attack of the liberated water. In particular, **45** is the first example of a sumanenedione derivative. This allows a comprehensive analysis of all congeners starting from the sumanenetrione **41** to hexafluorosumanene **44**. Again, the simple workup and separation of all compounds by PTLC is a great quality of this reaction design.

43, 24 %   **44**, 23 %   **45**, 19 %
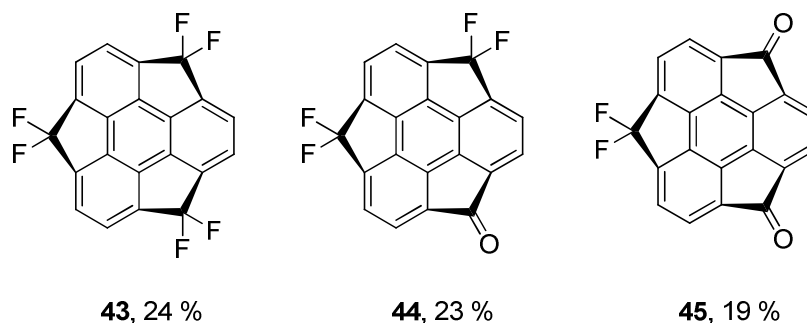
Scheme 3.4. A mixture of products is obtained, if water is liberated during the reaction. Given yields are isolated yields.

The compounds colours range from colourless (**43**) to yellow (**41**), which is accordingly reflected in the UV-vis spectra of the compounds.
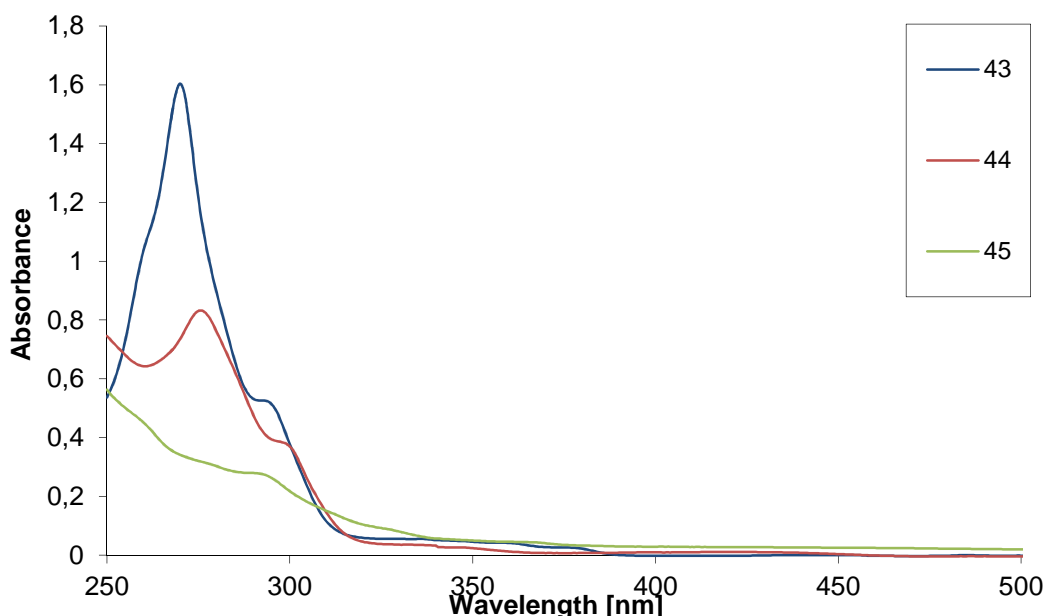
Figure 3.2. UV absorption spectrum of **43**, **44** and **45** in $CHCl_3$, 10^{-4} M.

There was no solvent dependency found for the discussed compounds. In 2012 Sakurai and co-workers investigated the fluorescence of **41** when nanocrystals and nanocrystalline assemblies are formed.[99] The fluorescence spectra of the **41** show two types of emissions: One can be attributed to the monomeric emission, whereas the other, much more broadened band can be assigned to excimer emission phenomena. To investigate possible excimer emission, photoluminescence spectra with different concentrations were measured. In theory, a highly diluted solution does not give an

46

excimer emission because the excited molecule is only surrounded by solvent molecules prohibiting excimer formation during the measurement. Upon raising the concentration, the excimer emission also increases due to the higher compound/solvent ratio.
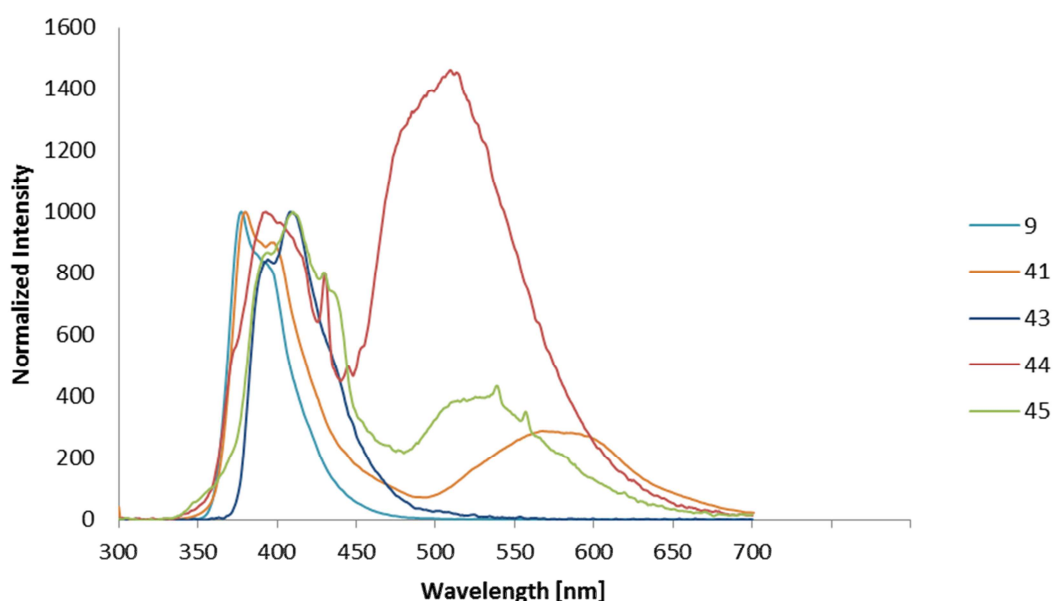
Figure 3.3. Normalized photoluminescence spectra of **9**, **41**, **43**, **44** and **45** in CHCl$_3$.

Hexafluorosumanene shows only the nearly unchanged monomeric emission. Therefore sumanenes with tuneable excimer emissions can now be synthesized.

NMR spectra of **43** are simple due to the C_3 symmetry. Only one signal (δ = 7.28) is observed in the ^{1}H NMR for all equivalent rim-protons. A set of AB signals (^2J = 273 Hz), corresponding to three *endo* and three *exo* benzylic fluorine atoms is observed in the ^{19}F NMR, the doublets deviate by around 25 ppm due to ring current effects (the *exo* fluorine atoms bear significantly more charge than the *endo* fluorine atoms). Likewise, the ^{13}C NMR shows only four signals with fluorine coupling constants of 261, 28 and 8 Hz (benzylic, flank and hub carbon) depending on the distance to the fluorine atoms, the signal for the six rim carbon atoms is broadened. The coupling constants of the ^{13}C NMR of **43** are similar to the ones published for difluorofluorene[100] and support the assignments.

Crystals suitable for single-crystal X-ray analysis were grown by slow evaporation of a chloroform/EtOH solution at room temperature. A thin needle-like crystal was measured using synchrotron radiation. The molecular structure of **43** is shown in figure 3.4. Substitution with bulky

substituents usually results in a shallower bowl depth of the compounds.[46] Surprisingly, the molecular bowl of **43** significantly deepens to 1.24 Å in comparison to 1.12 Å for **9** upon introduction of the six fluorine atoms.
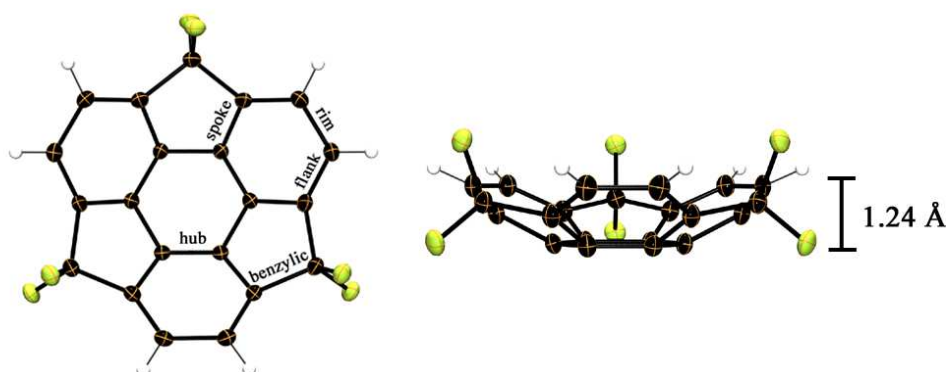
Figure 3.4. The molecular structure of **43** in the solid state. Bowl depth is again defined as the distance between the planes formed by the central hub atoms and the rim carbon atoms, 1.240(12) Å for **43**.

Hexafluorosumanene **43** shows a highly ordered columnar structure formed by concave-to-convex π-π interactions with all 1D columns oriented in the same direction, which surprisingly resembles the favourable packing of sumanene **9**. The central 6-membered rings are fully eclipsed and no slippage of the bowls can be observed, the π-bowls stack perfectly over one another, therefore no transverse shifting occurs. The rim of **43** is rotated by 56 ° to minimize the sterical repulsion of the protruding fluorine atoms, which is identical to the angle found in the solid state structure of **9**.[47a] Short intercolumnar C-H···F interactions of 2.52 Å additionally govern the arrangement of bowls along the columnar stacks, whereas intracolumnar C-H···F interactions exhibit (elongated) distances of around 2.77 Å[74] (figure 3.6). In pristine sumanene the *endo* hydrogen atom of one sumanene interacts with the electron rich 6-membered rings of the sumanene molecule above (distance 2.80 Å for the short CH···π contact, comparable to CH···π (fullerene) contacts).[52b, 74] In **43**, the contact is slightly extended to 3.03 Å and an overall intermolecular distance of 4.16 Å (3.79 − 3.86 Å for **9**) can be observed between two stacked bowls. This increased distance is also reflected by an increase of the estimated volume per C-atom[34] in the structure from 14.31 (**9**) to 16.68 Å^3 (**43**). Overall the introduction of the fluorine atoms does not significantly change the columnar packing motif, although the difference of hydrogen and fluorine atoms causes difference in interactions in the crystals of **9** and **43**.

A striking alteration between the crystal structure of **9** and **43** is the number of molecules in the asymmetric unit. In **9**, one third of the molecule is found in the asymmetric unit, which generates one unique sumanene molecule that forms one column in the crystal.[47] In the case of **43**, the asymmetric unit consists of three-thirds of three independent molecules **43** and thus three different columns in the solid state. The differences between each unit are minor but nevertheless worth mentioning. The gearing of the columns should account for the differences (figure 3.6), otherwise the same space group like for **9** and **43** might have been found.
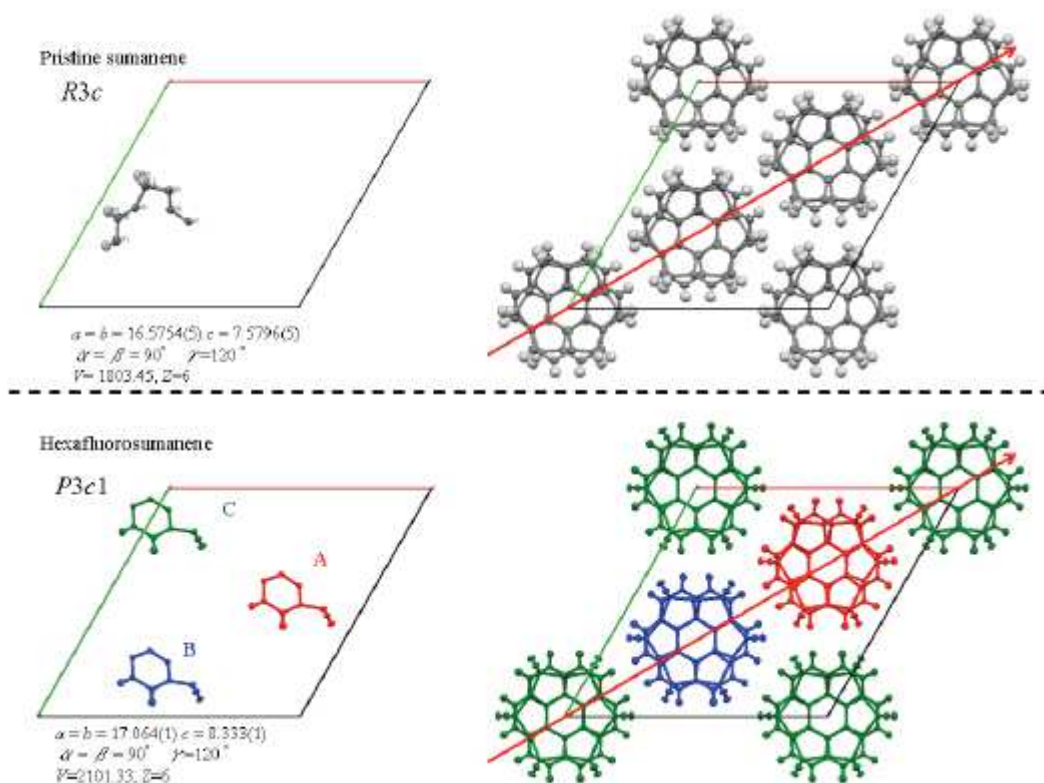
Figure 3.5. A comparison of the crystallographic details of **9** (upper excerpt) and **43** (lower excerpt). For **43** all combinations of the three crystallographically independent molecules are shown and indicated by colour. Image generated by Tatsuhiro Kojima.
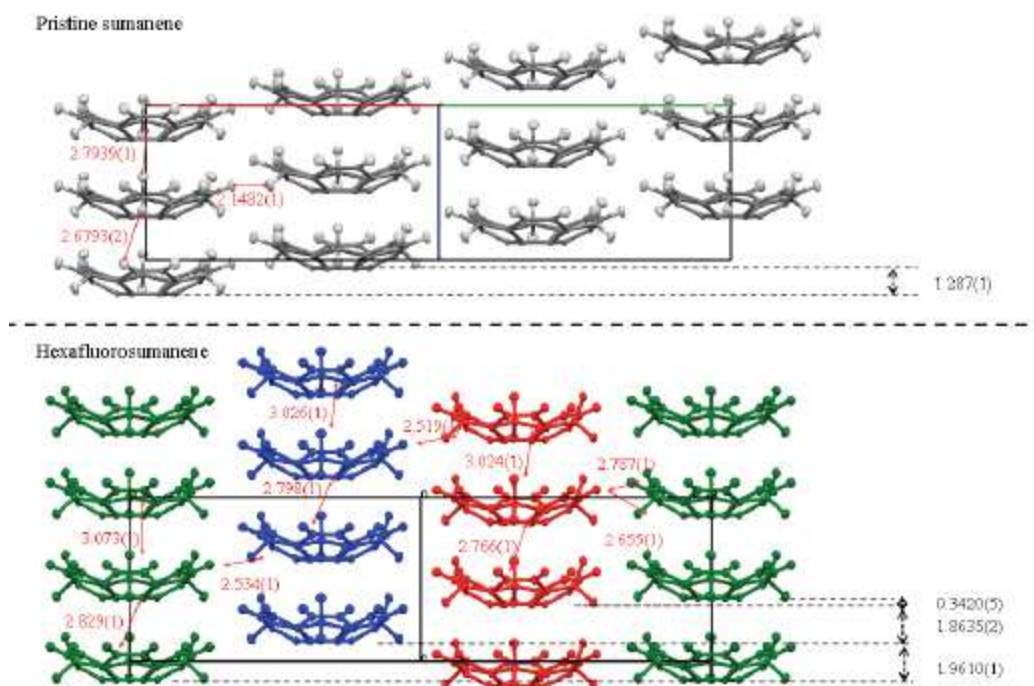
Figure 3.6. An additional comparison of the crystallographic details of **9** (upper excerpt) and **43** (lower excerpt). For **43** all combinations of the three crystallographically independent molecules are shown and indicated by colour. Image generated by Tatsuhiro Kojima.

DFT-calculation on the B3LYP-6-311+G(d,p) level of theory were computed using Gaussian03[101] and are summarized in table 3.1.

Table 3.1. Bond length comparison of selected sumanene derivatives in ångström [Å].

bond	43_{calc}[a]	43_{exp}[b]	9_{exp}[c]	44_{calc}[a]	45_{calc}[a]	41_{calc}[a]
rim	1.431	1.433	1.431	1.430	1.430	1.429
flank	1.390	1.389	1.400	1.392	1.393	1.395
spoke	1.397	1.396	1.396	1.397	1.397	1.399
benzylic	1.553	1.553	1.548	1.554_{CF}	1.554_{CF}	
				1.544_{CO}	1.545_{CO}	1.545
hub$_{short}$	1.380	1.377	1.383	1.379	1.379	1.378
hub$_{long}$	1.439	1.440	1.429	1.439	1.440	1.440

Averaged values are given. [a] DFT calculation (B3LYP/6-311+G(d,p)). [b] Averaged values of all three molecules in the asymmetric unit. [c] From a previously published high-resolution X-ray dataset.[47b]

No deviation of non-equivalent spoke bonds is found, but a pronounced difference in the length deviation of the benzylic bonds. For example in **44** and **45**, a difference of the bonds close to the oxygen atom or to the fluorine atoms can be found. The deviation of the sp^2 or sp^3 carbon bond lengths by changing the substituent may account for the bowl depths change; other bonds are only negligibly changed. The benzylic carbon bonds connected to a CF$_2$-unit are the longest benzylic bonds, both in calculated and experimental data.

A trend generally observed for the compounds discussed is, however, the elongation of benzylic bonds (1.55 Å) in comparison to their planar congeners. In fluorenes[102] and fluorenones,[103] the benzylic bond is significantly shorter (1.50, 1.49 Å, respectively) but it has to be taken into account, that the compounds do not suffer from the steric strain of the bowl-shaped geometry. A planar fluorinated fluorene shows slightly elongated benzylic bonds of averagely 1.52 Å.[104] In both the planar and the curved systems, these bonds are similar for the carbonyl and the hydrocarbon derivatives, whereas the fluorinated congeners show elongated bond lengths (0.005 Å).

It remains unsolved, whether a repulsive effect of the fluorine substituents elongate the bond lengths and account for the deepened bowl.

To investigate the thermal flipping motion of the sumanene bowls of **43**, an optimization of the bowl and flat structures of the compound was carried out using the Gaussian 03 program. The flat

structure has been characterized as the transition state with one imaginary frequency corresponding to the bowl inversion for the respective molecule. The bowl inversion energy was calculated from the difference of the zero-point-corrected energies of the bowl structure and the flat structure,[44] as presented in table 3.2.

Table 3.2. Calculated and experimental bowl depths and inversion energies of selected sumanenes.

	Bowl Depth [Å]	Bowl-to-Bowl Inversion Energy [kcal/mol]
43$_{calc}$[a]	1.219	21.4
43$_{exp}$	1.240(12)	n.d.
9$_{calc}$[b]	1.14	18.3
9$_{exp}$[b]	1.115(2)	19.7-20.4
44$_{calc}$[a]	1.208	n.d.
45$_{calc}$[a]	1.199	n.d.
41$_{calc}$[a]	1.185	n.d.

[a] B3LYP/6-311G**. [b] Bowl-inversion values are solvent dependent and taken from reference 46, calculated bowl depths from reference 52a.

These results (as previously published results) suggest that the inversion energy is usually underestimated giving rise to belief that **43** is an even more rigid bowl than expected. Bowl depth DFT calculations also indicate that the bowl depth of 1.22 Å for **43** is deeper than 1.14 Å for **9** and 1.19 Å for trione **41**, which was the deepest value among substituted sumanenes up to now.[52a] The bowl depths of **44** and **45** are calculated to be in each case about 0.01 Å shallower.

From the data obtained from calculations, the visualization of the electrostatic potential of a single molecule is possible and depicted in the following schemes:
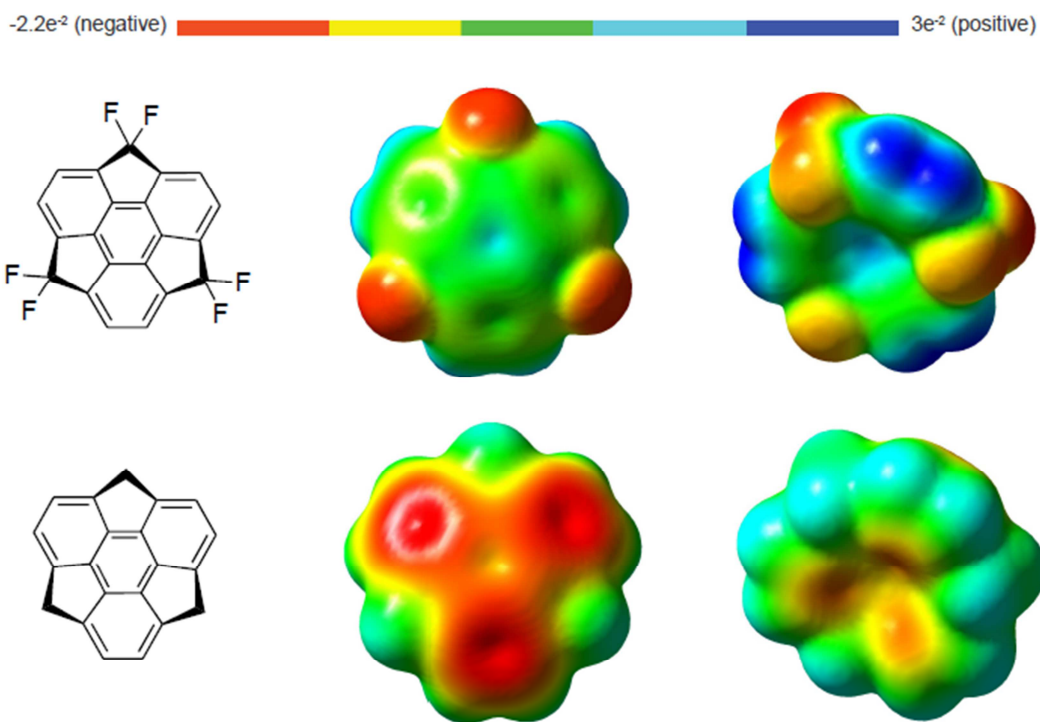
Figure 3.7. Electrostatic potential mapped surfaces of **43** and **9**, generated using Gaussview[105] with an isovalue of 0.0004.

The strong electron withdrawing effect of the fluorine atoms becomes immediately visible. The formerly negative outer six-membered rings become much more electron neutral while the negative electrostatic potential is now located at the *exo* fluorine atoms. In general, sumanene **43** is much more polarized now.
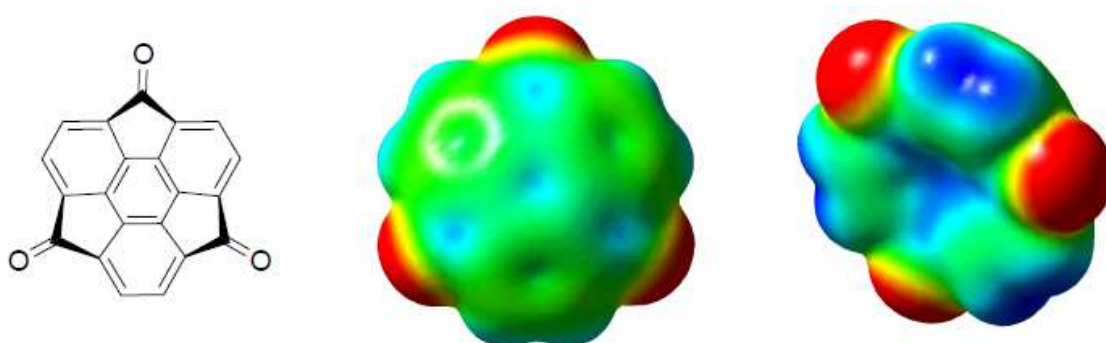
Figure 3.8. Electrostatic potential mapped surfaces of **41**, generated using Gaussview[105] with an isovalue of 0.0004. For the colour legend, see figure 3.7.

53

The strongly conjugated carbonyl groups of **41** show a similar effect on the overall molecule. Its fascinating properties will also be discussed in the electrochemistry section 5.2.

To summarize, the introduction of the fluorine atoms does not significantly change the columnar packing motif, although the difference of hydrogen and fluorine atoms causes dissimilarities in interactions in the crystals of **9** and **43**. The crystal packing of **43** makes this system highly promising for tailor made molecular electronics, as well as the low reduction potential, concomitant with electron acceptor abilities.

The first directly fluorinated sumanene compounds were synthesized and revealed a columnar packing structure, as well as low reduction potential for all members of the family. The very electron deficient molecule **43** is not only the deepest sumanene derivative, but also a candidate for n-type semiconductor application under ambient conditions, due to the efficient shielding of the molecular columns by the fluorine atoms. It is of great interest in regard to crystal engineering, because the favourable columnar structure is completely maintained, although six functional groups are introduced. For **39**, only minor changes in the crystal structure can be found, which contrasts strongly with the corannulene system (**1** and **6**) where the overall packing motif is completely changed. Furthermore, the sumanene system allows doping by mixing the compounds in different ratios.

4. Molecular electronics?

Previously, different corannulenes and sumanenes were discussed to possess suitable properties for electronic applications. A variety of structures and different solid state architectures were presented and theoretically evaluated.
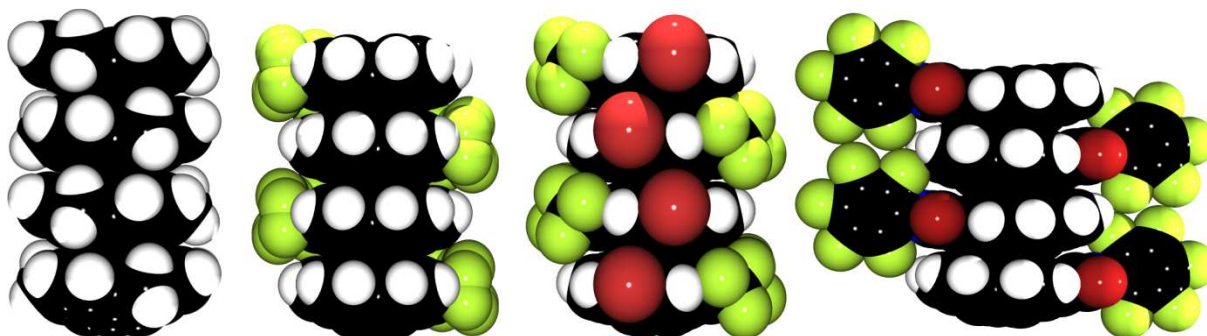
Figure 4.1. Space-filling models of the compounds with columnar structure. **9**, **25**, **26** and **34a** (from left to right).

Some aforementioned compounds are not suitable for conductivity measurements, for example corannulene **26**, whose bromide-substituents will act as electron holes, trapping the major charge carriers. It was shown that even ~2 % of monobromosumane (**46**) as dopant are sufficient to inhibit charge carrier mobility.[48] But not only substituents are important, the intermolecular distance and overlapping areas of the molecule also influence the ability of organic charge transport. Therefore, *ortho*-bis(trifluoromethylated) **25** was chosen for charge transport measurement, because it can be synthesized on a relatively large scale and possess a good solubility in common chlorohydrocarbons. Corannulene **34a** would possibly have been an appropriate choice as well.

On the basis of the confined columnar stacking structure of **25** in the solid state and the close intermolecular distance of 3.73 Å, the charge carrier transport properties were examined by an electrode-less microwave conductivity measurement. Flash-photolysis TRMC (FP-TRMC) technique utilizes exciton dissociation into charges as a charge carrier injection method, providing the elucidation of intrinsic charge carrier mobility in a wide variety of organic and inorganic electronic materials.

The significant assets and drawbacks of this electrode-less measurement is the ability of showing the intrinsic charge transport properties.[106] The best known and widely used time-of-flight (TOF) methods consist of a rather simple setup following the general to use injection, accumulation, and retraction of charge as a way to measure the charge carrier mobility, for example charge-retraction time-of-flight (CR-TOF).[107] For photocurrent time-of-flight measurements, which are more similar to the method used for evaluation of **25**, the charge is directly induced without using a blocking layer by a short laser pulse. Both the TOF methods are not only time consuming but the sample is also subjected to significant stress during sample deposition as well as during the thermal evaporation of the gold electrodes by vapor deposition. Furthermore, defects (scratches etc.) of the prepared device adulterate the measurement results together with the attached electrodes. On the other hand, much more realistic results are obtained in contrast to the intrinsic results of TRMC.

For the preparation of the sample by TRMC, **25** and **1** were scrupulously purified by recycling GPC to remove any possible brominated trace impurities, which are likely to be present considering the given reaction conditions.

Upon excitation at 355 nm, solid **25** in polycrystalline state exhibits clear signature of photoconductivity (figure 4.2), which is in striking contrast of a three orders of magnitude lower conductivity transient observed for corannulene **1** as an amorphous analogue of the identical conjugated buckybowl core. This is strongly indicative that the corannulene moieties also provide a highly electric conductive pathway in case of their columnar form of intermolecular π-stacking, as reported for sumanene **9**. Unlikely compared to the photo-conductivity transient observed in a single crystal of **9**, the transient in crystalline **25** displays a significant delay of photo-carrier generation reflected as a considerable increase of transient conductivity over a few μs, indicating that triplet-triplet annihilation processes predominantly yield free charge carriers in polycrystalline state of **25**.[108]
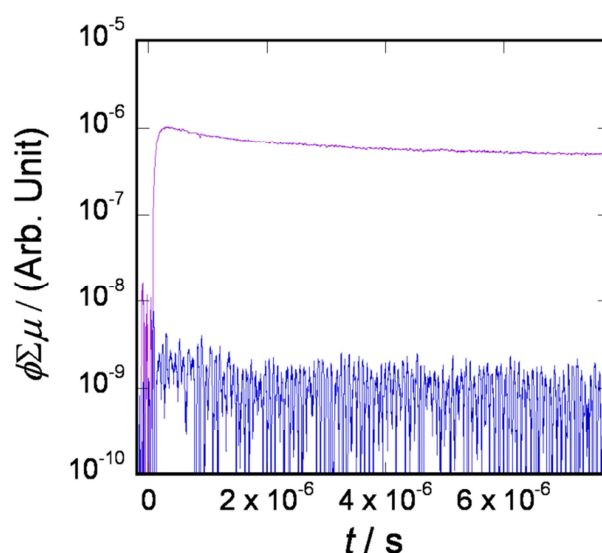
Figure 4.2. (a) Conductivity transients observed from a polycrystalline film of **25** (violet) and of **1** in solid film (blue). Excitation was carried out at 355 nm, 2.1 × 10^{15} and 2.8 × 10^{15} photons cm^{-2}, respectively. Image generated by Shu Seki.

Based upon this data and transient absorption spectra the minimum limit of charge carrier mobility as $\Sigma\mu$ > 0.9 cm^2 V^{-1} s^{-1} in **25** (intra-columnar) and $\Sigma\mu$ > 5 × 10^{-4} cm^2 V^{-1} s^{-1} in **1**, respectively. This value is even higher compared to those observed in crystalline sumanene,[48] proving that the presented concept is highly successful. (table 4.1).

Table 4.1. Selected charge carrier mobilities are presented for comparison.

	$\Sigma\mu$ [cm^2 V^{-1} s^{-1}]	Comment
Poly(hexylphenyl)silane in benzene[109]	0.30	-
Amorphous silicon[110]	1-10	-
HBC-TNF coassembled nanotube[a][111]	3.0	-
Carbon Nanotubes[5]	100,000	mixture
Rubrene[112]	0.052	single crystal
Sumanene (**9**)[48]	0.75	single crystal
Sumanene (**9**) /Br$_1$-sumanene (**46**) (99:1)[48]	<5 × 10^{-4}	single crystal
Corannulene (**1**)[108]	>5 × 10^{-4}	film
1,2-(CF$_3$)-Corannulene (**25**)[108]	0.9	film

[a] Hexa-*peri*-hexabenzocoronene (HBC), trinitrofluorenone (TNF) coaxial nanotubular structure, consisting of π-stacks of a HBC core laminated by TNF outer/inner layers.

5. Electrochemistry

5.1. Corannulenes

To study the electron acceptor abilities of the new corannulenes and sumanenes, cyclic voltammetry and square-wave measurements (if available) were conducted. Strictly anhydrous conditions were necessary to observe (reversible) reductions for all studied compounds. In all cases, the conductive salt used was tetra-*n*-butyl ammonium hexafluorophosphate. The mean value between the anodic and cathodic potential was used as an estimation for the redox potentials or obtained from the peak maximum of a square-wave measurement of the same sample. The solvent was THF or DCM, and all potentials were referenced versus the ferrocene/ferrocenium (Fc/Fc$^+$) redox couple (internal standard).

To achieve oxidation of a sample, usually a solvent like acetonitrile with a broad cathodic window is used, but most samples of this study were (almost) insoluble and did not give satisfying measurements.
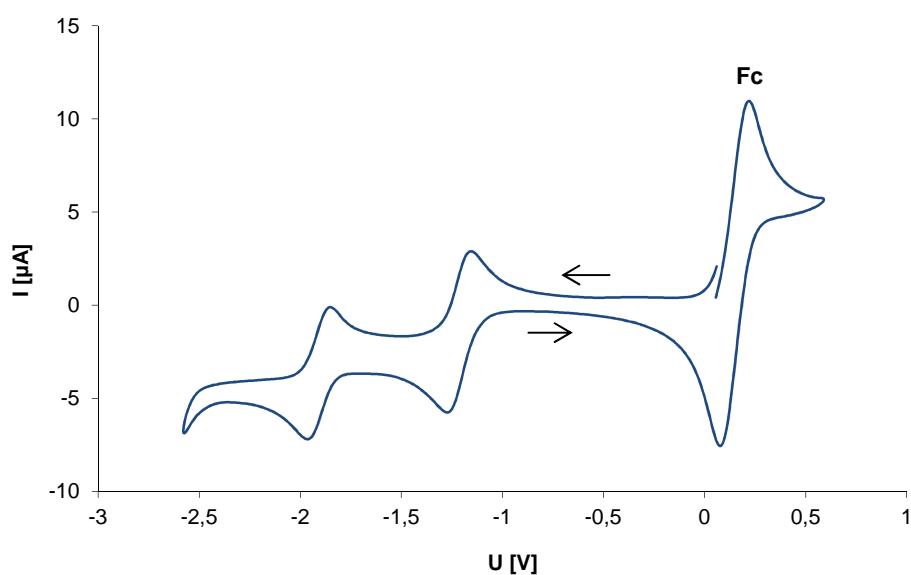
Figure 5.1. Cyclic voltammogram of **34a** in THF, scanrate 100 mV/s, analyte concentration $5*10^{-3}$ M.

Corannulene **1** has been investigated by other groups before,[113] but was measured in this setup again for comparison. Usually all compounds showed at least one reversible reduction. The half-wave reduction potentials are -2.47 for **1**, -2.20 for **10**, -1.86 for **25**, -1.66 for **27**, and -1.48 V for **28**. As previously reported by the Wang group[114] and the Petrukhina group,[115] the introduction of perfluoroalkyl substituents to an aromatic system shifts the reduction towards higher potentials, hence inducing a stronger electron-accepting ability. Values presented here for the systematically trifluoromethylated compounds agree with these observations. Already through the introduction of one trifluoromethyl group, the $E_{1/2}$ value of the reduction is shifted by 0.28 V towards higher potentials relative to corannulene **1**. For pentakis(trifluoromethyl)corannulene, Petrukhina and co-workers observed a shift of 0.95 V,[115] which corresponds to a shift of 0.19 V per trifluoromethyl group. Through the selective substitution in specific positions and the resulting lower symmetry, this shift can be increased to 0.25 V per trifluoromethyl group on average. Because of the different substitution pattern, no strictly linear increase of the electron accepting ability can be expected. For the corannulene **27** with three trifluoromethyl groups, and for **28** with four, a shift of 0.82 and 1.0 V is observed compared to **1**; this shift surpasses the shift of pentakis(trifluoromethyl) corannulene (0.95 V).
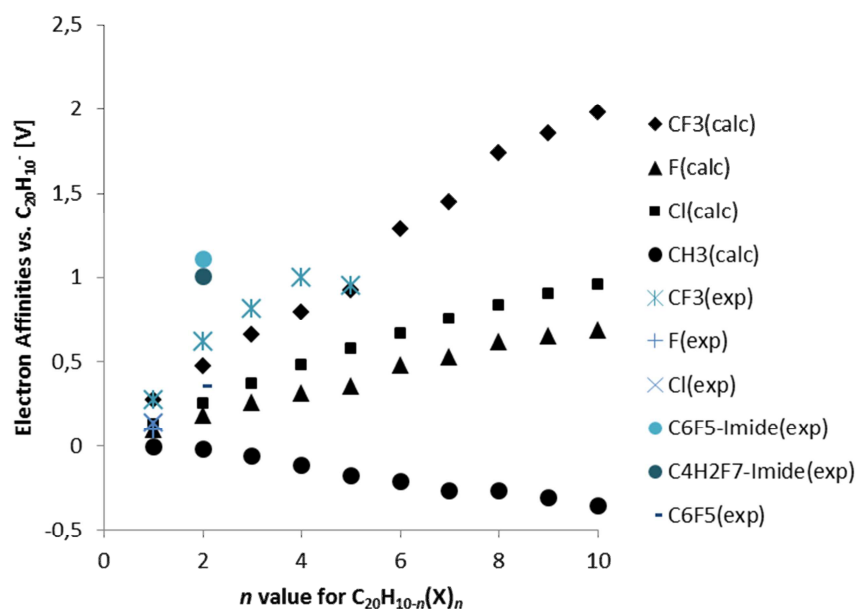
Figure 5.2. A comprehensive comparison of experimentally obtained data in this work (blue), except for CF$_3$ with n = 5, which is an experimental value but taken from the Petrukhina group[115] and calculated electron

affinities (black). Calculated substitution patterns for n=2 (1,5), n=3 (1,3,7), n=4 (1,3,5,7), n=5 (1,3,5,7,9), because significant variation of electron affinities were not expected by the authors, if the added groups are distributed more or less uniformly.[115]

If all given values are referenced against the first reduction of **1**, like described in the afore-mentioned discussion, a comparison with calculated values of the Petrukhina group[115] is possible. Although the DFT calculated data for the gas-phase uses acetonitrile as notional solvent, the experimental data blends well with the calculated values. The cyclic imides **34a** and **34b** were added with a value of two for the substituents count on the corannulene rim.

Table 5.1. Electrochemical potentials of synthesized corannulenes.

Compound	$E_{1/2}$ *vs.* ferrocene [V][a]
1	-2.47
6	-2.38
7	-2.34
10	-2.20
25	-1.86
26	-1.66
28	-1.48
29	-2.11
34a	-1.36
	-2.06
34b	-1.47
	-2.15

[a] The potentials are referenced to the ferrocene/ferrocinium (Fc/Fc$^+$) couple, used as an internal standard, and uncorrected for ohmic drop.

The influence on the electron affinities of the substituents studied, follow the rough order of CF_3 > C_6F_5 > Cl > F, which might cause amazement at first. Fluorine, having the highest electronegativity of all elements, induces a strongly polarized C-F single bond, thus causing a dipole moment along the C-F-bond axis. Fluorine is a strong σ-acceptor and to some extent, a π-donor. The trifluoromethyl group

as a substituent is both a strong σ- and π-acceptor and induces a stronger dipole moment than just one fluorine atom.[116] For a,ß-unsaturated systems and also for allenes,[117] this phenomenon is known as negative hyperconjugation, which might be a possibility to explain the experimentally obtained values (table 5.1).

Fluorine atoms have a much smaller effect than CF_3 groups and a smaller effect than chlorine atoms, the opposite of what was found for $C_{60}F_n$ *vs.* $C_{60}(CF_3)_n$.[118] The difference might be due to the difference between substituents on carbon sp^2 atoms in conjugation with an extensive π-system in corannulene and substituents on carbon sp^3 atoms, like for fluorinated fullerenes. DFT calculations revealed further, that addition patterns with double bonds in five-membered rings having two sp^2 neighbors result in the strongest electron acceptors.[118] This offers an explanation, why the studied *ortho*-bis(trifluoromethylated) corannulenes are even stronger electron-acceptor molecules, than predicted for the isomers taken from reference 115, despite a possible solvent effect. The very precise predictions of **6**, **7** and **10** (only one possible isomer) however, suggests a minor solvent effect and indicate the crucial role of the substitution pattern.

5.2. Sumanenes

The redox properties of all new fluorous sumanenes were studied by cyclic voltammetry and square wave voltammetry in THF solutions. The fluorine substitution was shown to have a drastic effect on the first reduction of the sumanene bowl. Upon introduction of six fluorine atoms, the redox potential of **43** remains irreversible but is shifted from -3.21 V of **9** to -1.79 V. An even stronger effect can be observed for the monoone **44** and the dione **45**. Both undergo a reversible reduction in THF solution at -1.36 and -1.13 V, respectively, which is expected to take place at the carbonyl group. Hence, the irreversible reduction of **43** to the radical anion should be accompanied by immediate loss of a fluorine atom upon reduction. The strongest change of the electron acceptor properties is observed for the heavily conjugated **41**.

Table 5.2. Electrochemical potentials of studied sumanenes.

Compound	$E_{1/2}$ *vs.* ferrocene [V][a]
43	-1.79[b]
9	-3.21[b]
41	-0.94
44	-1.36
45	-1.13

[a] The potentials are referenced to the ferrocene/ferrocinium (Fc/Fc$^+$) couple, used as an internal standard, and uncorrected for ohmic drop.[b] An irreversible reduction occurs in THF.

6. Summary

This work has demonstrated the influence of electron withdrawing groups on non-planar polycyclic hydrocarbons, also called buckybowls.

The molecular bowl corannulene ($C_{20}H_{10}$) was synthesized and substituents were introduced directly by using xenon(II)fluoride or known trifluoromethylation protocols. If more than one substituent was introduced, inseparable (regio)isomeric mixtures were obtained.

Therefore, trifluoromethylated corannulenes were synthesized by accessing suitable precursor molecules, bearing several trifluoromethyl groups. The obtained fluoranthenes were studied crystallographically and discussed with respect to their weak molecular interactions (π-stacking, C-F···H-C interactions).

The strategy of constructing fluoranthenes by using hexafluorobutyne was extended to other electron-poor alkynes for example bis(pentafluorophenyl)acetylene, providing the corresponding fluoranthenes.

Fluoranthenes bearing up to four trifluoromethyl groups were reacted to yield the desired perfluoroalkylated corannulenes, fluoranthenes derived from bis(pentafluorophenyl)-acetylene gave access to pentafluorophenylated corannulenes and even extended corannulenes were synthesized by using *N*-substituted maleimides. These compounds were studied by multi-nuclear NMR spectroscopy and X-ray crystallography. Electrochemical investigations revealed their strong electron-acceptor properties in solution. A corannulene bearing two trifluoromethyl groups in *ortho*-position was shown to be an eminently conductive material, with high charge-carrier mobility along the molecular columns, which are formed by convex-concave π-stacking interactions of the molecular bowls.

The molecular bowl sumanene ($C_{21}H_{12}$) was fluorinated directly and trifluoromethylated accordingly. Monofluorosumanene was isolated and found to have an unaltered crystal structure, identical with the parent sumanene molecule, even allowing doping with the latter, resulting in mixed crystals of various percentages.

By using the unique chemical reactivity of sumanene, originating from its three benzylic carbon atoms, six fluorine atoms could be introduced in one step by choosing the appropriate precursor molecule, a cyclic dithiane. Slightly modified reaction conditions allowed for isolation of two oxo-fluoro-sumanenes, which were isolated and studied.

7. Zusammenfassung

In dieser Arbeit wurde der Einfluss elektronenziehender Gruppen auf nicht-planare, polyzyklische, aromatische Kohlenwasserstoffe untersucht.

Das schalenförmige Molekül Corannulen ($C_{20}H_{10}$) wurde dargestellt, durch direkte Methoden fluoriert und trifluormethyliert. Bei Einführung mehrerer Substituenten auf diese Weise wurden untrennbare Mischungen von Regioiosmeren erhalten, daher wurde die isomerenreine Darstellung von geeigneten Vorstufen, Fluoranthenen, angestrebt, um die gewünschten Corannulene zu erhalten. Alle dargestellten Fluoranthene wurden röntgenkristallographisch untersucht und ihre Strukturen in Hinblick auf schwache intermolekulare Wechselwirkungen eingehend diskutiert (π-stacking, C-F···H-C-Interaktionen). Die Strategie zum Aufbau trifluormethylierter Fluoranthene durch Nutzung von Hexafluorbutin wurde auf die Nutzung anderer, elektronenarmer Alkine, wie z.B. Bis(pentafluorphenyl)acetylen, erweitert.

Trifluormethylierte Fluoranthene wurden durch Ringschlussreaktionen zu perfluoralkylierten Corannulenen reagiert. Fluoranthene, die unter Nutzung von Bis(pentafluorphenyl)acetylen dargestellt wurden, gaben pentafluorphenylierte Corannulene. Unter Verwendung *N*-substituierter Maleinimide zur Konstruktion von Fluoranthenen, wurden analog erweiterte Corannulene erhalten.

Alle erhaltenen Substanzen wurden mit Hilfe von NMR-Spektroskopie untersucht teilweise auch röntgenkristallographisch. Elektrochemische Messungen offenbarten unerwartet hohe Werte für die Elektronenaffinität der dargestellten, trifluormethylierten Corannulene.

Des Weiteren konnte gezeigt werden, dass 1,2-Bis(trifluromethyl)corannulen im Festkörper eine günstige Anordnung der molekularen Schalen durch π-Wechselwirkungen verknüpfte Stränge bildet, welche eine hohe Ladungsträgermobilität ermöglichen.

Ergänzende Untersuchungen erfolgten am ebenfalls schalenförmigen Molekül Sumanen ($C_{21}H_{12}$). Dieses wurde ebenso direkt fluoriert und trifluormethyliert. Dabei zeigte sich, dass die vorteilhafte Festkörperstruktur nach Fluorierung sich, nicht ändert und sogar Dotierung in beliebigen Verhältnissen möglich ist.

Die benzylischen Positionen von Sumanen wurden genutzt, um durch geeignete Funktionalisierung einen Dithian-Vorläufer darzustellen, welcher die Einführung von sechs Fluoratomen in einem Reaktionsschritt ermöglicht.

8. Experimental section

8.1. General

8.1.1. Techniques

All experiments were carried out under standard Schlenk conditions and argon atmosphere or by working in either an argon-filled MBraun glove box model LAB master SP or a nitrogen-filled MBraun glove box model UNIlab 2000. The amount of gaseous compounds was determined using pVT techniques.

8.1.2. Chemicals

Tetrahydrofuran, was freshly distilled from sodium/benzophenone ketyl prior to use and further purified by trap-to-trap distillation for electrochemical use, 1,2-dichloroethane (DCE) and *N,N*-dimethylformamide were distilled from phosphorus pentoxide, and stored over molecular sieve (3 Å) or purchased anhydrous and used as received. Dichloromethane was dried over activated alumina using an MBraun solvent system model MB SPS-800 or a Glass Contour Solvent Purification Systems. Methanol was purchased anhydrous and used as received.

Nickel powder (99.5 %, 150 micron), gold(III)chloride and hexafluorobutyne were obtained from ABCR GmbH & Co. KG, methyltrioxorhenium(VII) (MTO) from ABCR GmbH & Co. KG or TCI, *N*-iodosuccinimide from molecula, *N*-bromosuccinimide and pentan-3-one from Acros Organics. AIBN was purchased from TCI, DBPO from Alfa Aesar.

Dicyanoacetylene (**17**)[85], diiodoacetylene (**19**)[86] and bis(pentafluorophenyl)acetylene (**22**)[88] were synthesized by literature procedures. **19** and **22** should be handled with special care due to their toxicity and explosive nature. Xenon(II)fluoride was obtained from the elements or purchased from Sigma-Aldrich. 1-Trifluoromethyl-1,2-benziodoxol-3-(1H)-one was synthesized by literature procedure starting from 2-iodobenzoic acid[119] or purchased from TCI.

N-pentafluorophenyl maleimide was synthesized from maleic anhydride and pentafluoroaniline,[93] *N*-heptafluorobutylmaleimide was synthesized by the same procedure using 2,2,3,3,4,4,4-Heptafluorobutylamine instead of pentafluoroaniline.

Pyridine hydrofluoride (Olah's Reagent, HF-py), density 1.1, is available from Sigma-Aldrich, a 7:3 w/w mixture of anhydrous HF and pyridine with a molecular weight of 263 gmol^{-1}, formulated as $C_5H_5N(HF)_{9.2}$, as proposed by Umemoto and co-workers[120] was used for stoichiometric calculations.

Corannulene (IUPAC dibenzo[ghi,mno]fluoranthene) (**1**),[20,69] sumanene (IUPAC 4,7-dihydro-1H-tricyclopenta[def,jkl,pqr]triphenylene) (**9**),[43] and sumanenetrione (IUPAC 1H-tricyclopenta[def,jkl,pqr]triphenylene-1,4,7-trione) (**41**)[51] were synthesized according to the previously published methods.

8.1.3. Instrumentation

Melting points were determined on a Gallenkamp Melting Point Apparatus or Stanford Research Systems MPA100 and are not corrected. IR spectra were recorded on a Nicolet 5 SXC FTIR spectrometer equipped with a DTGS detector or on a JASCO FT IR-4100 spectrometer (signals are denoted as following, s (strong), m (middle) and w (weak)).

^{1}H, ^{19}F and ^{13}C-NMR spectra were measured on a JEOL ECS 400/500 spectrometer or on a Bruker Instruments AVIII 700 at 23 °C. CDCl$_3$ and CD$_2$Cl$_2$ were used as solvents, if not stated otherwise, and the residual solvent peak was taken as an internal standard (^{1}H NMR: CDCl$_3$ 7.26, CD$_2$Cl$_2$ 5.30 ppm; ^{13}C NMR: CDCl$_3$ 77.0 ppm, CD$_2$Cl$_2$ 54.0 ppm; always proton-decoupled). Chemical shifts are reported in ppm (δ) relative to TMS, ^{19}F NMR spectra were referenced against external CFCl$_3$.

Mass spectra were measured on a MAT CH7A (EI, 80 *e*V, 3 kV), at the given temperature for each sample or on a on a JEOL JMS-777V. High resolution masses were determined by peak match method against perfluorokerosene.

Gel permeation chromatography (GPC) was performed on JAIGEL 1H and 2H using a JAI Recycling Preparative HPLC LC-908W and chloroform as eluent. HPLC analysis and separation was performed using a JASCO LC-2000 HPLC using Cosmosil Buckyprep columns.

TLC (precoated) analysis and PTLC (precoated and self-made) was performed using Merck Silica gel 60 F$_{254}$ or Wako Wakogel B-5F.

Some reactions were carried out using personal parallel chemical reactors (EYELA Chemistation series) and low-temperature reactors (EYELA PSL series).

Single-crystal X-ray structure determination was performed on a Bruker-AXS SMART 1000 fitted with a CCD Data collection, reduction and empirical absorption correction were performed using the SMART, SAINT and SADABS programs, respectively;[121] the SHELX program package[122] was used for structure solution and refinement. ORTEP[123] was employed for structure visualization and images were rendered using POVray.[124] Thermal-motion probability ellipsoids were set to 50 % in all cases.

The single-crystal X-ray crystallographic analysis of *asym*-**14** and *sym*-**14** was performed on a Rigaku Mercury-CCD. Data were collected and processed by using CrystalClear software (Rigaku).[125] The structure was solved by direct methods (SIR200824) and expanded by Fourier techniques. Refinements were performed by the full-matrix least-squares methods. Hydrogen atoms of methyl groups were calculated and refined as riding atoms.

The crystal of **43** was coated with paratone-*N* oil and the diffraction data measured at 100K with synchrotron radiation (λ = 0.69000 Å) on a ADSC Quantum-210 detector at 2D SMC with a silicon (111) double crystal monochromator (DCM) at the Pohang Accelerator Laboratory, Korea. The ADSC Q210 ADX program[126] was used for data collection (detector distance is 62 mm, omega scan; Δω = 1º, exposure time is 10 s per frame) and HKL3000sm (Ver. 703r)[127] was used for cell refinement, reduction and absorption correction. The crystal structure of **43** was solved by the superflip[128] program and refined by full-matrix least-squares calculations with SHELXL-97.[122]

Additional supplementary data for each compound is available from the attached CD-ROM in cif-format. Data of already published structures was deposited and can be obtained free of charge from The Cambridge Crystallographic Data Centre *via* www.ccdc.cam.ac.uk/data_request/cif, **25** (892586), **32** (876634), **33**a (876633), **34**a (876635) and **43** (909608).

8.2. X-ray crystallographic tables

Table 8.1. X-ray crystallographic details for the compounds **6**, **12-13** and *asym*-**14**.

Compound reference	**6**	**12**	**13**	*asym*-**14**
Chemical formula	$C_{20}H_9F$	$C_{22}H_{16}F_6$	$C_{23}H_{15}F_9$	$C_{24}H_{14}F_{12}$
Formula Mass	268.27	394.35	462.35	530.36
Crystal system	Monoclinic	Monoclinic	Monoclinic	Monoclinic
a/Å	17.700(7)	16.028(5)	8.943(2)	11.817(3)
b/Å	9.540(4)	12.352(4)	9.827(2)	21.237(4)
c/Å	7.308(3)	17.520(5)	21.451(5)	8.2580(16)
α/°	90	90	90	90
β/°	90.063(9)	104.455(19)	97.064(5)	97.474(2)
Unit cell volume/Å^3	1234.0(9)	3358.8(18)	1870.8(7)	2054.9(7)
Temperature/K	293(2)	108(2)	100(2)	153
Space group	$P2_1$/c	C2/c	$P2_1$/c	$P2_1$/c
Z	4	8	4	4
No. of reflections measured	11020	19536	14069	7879
No. of independent reflections	11020	4176	3819	4015
R_{int}	0.0000	0.0229	0.0241	0.0162
Final R_1 values ($I > 2\sigma(I)$)	0.0670	0.0352	0.0474	0.0504
Final $wR(F^2)$ values ($I > 2\sigma(I)$)	0.1700	0.0883	0.1089	
Final R_1 values (all data)	0.0894	0.0516	0.0538	
Final $wR(F^2)$ values (all data)	0.1841	0.1009	0.1116	0.0599
Goodness of fit on F^2	1.060	1.040	1.218	3.246

Table 8.2. X-ray crystallographic details for of compounds *sym*-**14**, **18**-**19** and **22**.

Compound reference	*sym*-**14**	**18**	**19**	**22**
Chemical formula	$C_{48}H_{28}F_{24}$	$C_{22}H_{16}N_2$	$C_{20}H_{16}I_2$	$C_{32}H_{16}F_{10}$
Formula Mass	1060.70	308.37	510.13	590.45
Crystal system	Monoclinic	Monoclinic	Orthorhombic	Orthorhombic
a/Å	12.479(2)	12.017(2)	7.6106(19)	30.365(11)
b/Å	11.3269(19)	7.1071(14)	12.657(3)	12.085(4)
c/Å	29.181(5)	35.635(7)	17.202(4)	13.365(4)
α/°	90	90	90	90
β/°	101.941(2)	92.848(5)	90	90
Unit cell volume/Å³	4035.5(12)	3039.7(10)	1657.0(7)	4905(3)
Temperature/K	123(2)	133(2)	133(2)	133(2)
Space group	$P2_1/c$	C2/c	$P2_12_12_1$	Pccn
Z	4	8	4	8
No. of reflections measured	8738	14214	26496	36886
No. of independent reflections	8738	4509	5040	4318
R_{int}	0.0000	0.0227	0.0227	0.0556
Final R_1 values ($I > 2\sigma(I)$)	0.0510	0.0462	0.0235	0.1019
Final $wR(F^2)$ values ($I > 2\sigma(I)$)	0.1069	0.1194	0.0491	0.2290
Final R_1 values (all data)	0.0643	0.0596	0.0278	0.1305
Final $wR(F^2)$ values (all data)	0.1255	0.1313	0.0506	0.2473
Goodness of fit on F^2	0.992	1.062	1.092	1.077

Table 8.3. X-ray crystallographic details for the compounds **25-26** and **32-33a.**

Compound reference	**25**	**26**	**32**	**33a**
Chemical formula	$C_{22}H_8F_6$	$C_{22}H_6Br_2F_6$	$C_{38}H_{20}F_{10}N_2O_4$	$C_{28}H_{16}F_5NO_2$
Formula Mass	386.28	544.09	758.56	493.42
Crystal system	Monoclinic	Monoclinic	Monoclinic	Monoclinic
$a/Å$	9.701(3)	18.9513(6)	12.407(4)	16.691(5)
$b/Å$	21.131(6)	12.3654(4)	27.476(8)	7.731(2)
$c/Å$	7.447(2)	7.3171(3)	9.607(3)	16.655(5)
$α/°$	90	97.0400(10)	90	90
$β/°$	97.645(8)	90	110.687(6)	107.022(6)
Unit cell volume/$Å^3$	1513.0(8)	1701.76(10)	3063.9(15)	2055.0(11)
Temperature/K	153(2)	100.0(2)	133(2)	293(2)
Space group	$P2_1/c$	$P2_1/c$	Cc	$P2_1/c$
Z	4	4	4	4
No. of reflections measured	6546	13550	17831	15784
No. of independent reflections	3064	3109	3125	3602
R_{int}	0.0261	0.0413	0.0565	0.0566
Final R_1 values ($I > 2\sigma(I)$)	0.0585	0.0279	0.0463	0.0409
Final $wR(F^2)$ values ($I > 2\sigma(I)$)	0.1443	0.0634	0.1139	0.1078
Final R_1 values (all data)	0.0919	0.0417	0.0648	0.0725
Final $wR(F^2)$ values (all data)	0.1656	0.0680	0.1235	0.1324
Goodness of fit on F^2	1.032	1.055	1.061	1.038

Table 8.4. X-ray crystallographic details for the compounds **34a, 39** and **43.**

Compound reference	**34a**	**39**	**43**
Chemical formula	$C_{28}H_8F_5NO_2$	$C_{21}H_{11}F$	$C_{21}H_6F_6$
Formula Mass	485.35	282.30	372.26
Crystal system	Monoclinic	Trigonal	Trigonal
a/Å	16.4353(5)	16.868(3)	17.0640(10)
b/Å	7.3459(2)	16.868(3)	17.0640(10)
c/Å	16.4520(4)	7.647(2)	8.3330(10)
α/°	90	90	90
β/°	108.036(2)	90	90
Unit cell volume/Å^3	1888.68(9)	1884.5(7)	2101.3(3)
Temperature/K	100(2)	133(2)	100(2)
Space group	$P2_1/n$	$R3c$	$P3c1$
Z	4	3	6
No. of reflections measured	17814	5838	43736
No. of independent reflections	3211	836	4447
R_{int}	0.0530	0.0335	0.0567
Final R_1 values ($I > 2\sigma(I)$)	0.0373	0.0453	0.0457
Final $wR(F^2)$ values ($I > 2\sigma(I)$)	0.0883	0.1090	0.1134
Final R_1 values (all data)	0.0535	0.0525	0.0544
Final $wR(F^2)$ values (all data)	0.0961	0.1150	0.1187
Goodness of fit on F^2	1.019	1.084	0.986

8.3. Electrochemical data

All electrochemical experiments were carried out at 25 °C. Cyclic voltammetry and square wave were measured on a ALS/CH Instruments Electrochemical Analyzer Model 620c or a MaterialsM 510 using a Schlenk measuring cell with three platinum wires as electrodes. Measurements were conducted in dry and degassed THF with tetra-*n*-butylammonium hexafluorophosphate (0.1 M) as conducting salt and a concentration of $5*10^{-4}$ M was used for the investigated compounds.

Table 8.5. Electrochemical potentials of synthesized buckybowls.

Compound	$E_{1/2}$ vs ferrocene [V][a]
1	-2.472[b]
6	-2.375
7	-2.339
9	-3.21[b]
10	-2.196
25	-1.856
27	-1.656
28	-1.476
29	-2.114
34a	-1.364
34b	-1.468
41	-0.94
43	-1.79[b]
44	-1.36
45	-1.13

[a] The potentials are referenced to the ferrocene/ferrocinium (Fc/Fc$^+$) couple, used as an internal standard, and uncorrected for ohmic drop. [b] An irreversible reduction occurs in THF.

8.4. Preparations

8.4.1. Monofluorocorannulene (6)
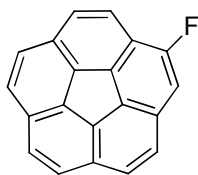
6 Corannulene (98.8 mg, 0.39 mmol, 1.0 eq.) was dissolved in dichloromethane (5 mL) and cooled to -78 °C. Solid xenon(II)fluoride (92.0 mg, 0.54 mmol, 1.38 eq.) was added at one and the flask was sealed again. The mixture was allowed to warm to room temperature during 3 hours. The green slurry diluted with 30 mL dichloromethane and silica gel was added. The solvent was removed under reduced pressure and the crude product was purified by flash column chromatography (pentane/ethyl acetate: 20/1) to yield **5** together with unreacted corannulene and small amounts of the regioisomers of $C_{20}H_8F_2$ (as indicated by a series of doublets between -116 and -119 ppm exhibiting $^3J(^1H\text{-}^{19}F)$ coupling constants of ~13 Hz) as an amorphous powder (34 % conversion by crude NMR). **5** was further purified by RP-HPLC to give analytically pure **6** (Gemini C18, methanol/water: 9/1), using a flow rate of 1 mL/min at 148 bar, with an Rt of 10.9 minutes.

Mp: 226 °C; **^{1}H NMR** (400 MHz, CDCl$_3$): δ = 7.39 (d, $^3J_{F\text{-}H}$= 13 Hz, 1H), 7.78–7.88 (m, 7 H), 7.96 (d, ½ AB, ^3J = 8.8 Hz, 1H); **^{19}F NMR** (376 MHz, CDCl$_3$): δ = -118.3 (d, $^3J_{F\text{-}H}$= 13 Hz, 1F); **^{13}C NMR** (101 MHz, CDCl$_3$): δ = 160.00 (C_F, d, ^1J = 260 Hz, 1C), 135.53 (C_{hub}, d, J = 9 Hz, 1C), 136.21 (C_{hub}, 1C), 135.38 (C_{hub}, 1C), 134.80 (C_{hub}, d, J = 5 Hz, 1C), 132.70 (C_{flank}, 1C), 132.16 (C_{flank}, d, J = 10 Hz, 1C), 131.11 (C_{flank}, 1C), 130.87 (C_{flank}, 1C), 130.28 (C_{flank}, 1C), 127.85 (C_{rim}, 1C), 127.78 (C_{rim}, 1C), 127.51 (C_{rim}, 1C), 127.26 (C_{rim}, 1C), 127.02 (C_{rim}, 1C), 126.71 (C_{rim}, d, ^3J = 4 Hz, 1C), 126.64 (C_{rim}, 1C), 121.80 (d, ^2J = 22 Hz, 1C), 112.36 (1C), 109.83 (d, ^2J = 109.8 Hz, 1C); **MS** (EI °C): m/z 268.0677 (found), 268.0688 (calc'd), 268 (100 %, [M]$^+$), 134 (15 %,[M]$^{2+}$); **IR**: ν = 2921 (m), 2845 (m), 1620 (s), 1438 (s), 1376 (s), 1108 (s), 997 (m), 824 (m), 566 cm^{-1} (m).

8.4.2. Monochlorocorannulene (7)
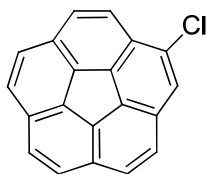
7   Corannulene (18.0 mg, 0.07 mmol, 1.0 eq.), *N*-chlorosuccinimide (9.6 mg, 0.07 mmol, 1.0 eq.) and gold(III)chloride (3.0 mol%) were dissolved in DCE (1 mL). The mixture immediately turned dark green. After stirring the mixture for 24 h at 60 °C, the mixture was diluted with DCM (10 mL) and silica gel was added. The solvent was removed under reduced pressure and the crude product was purified by flash column chromatography (n-pentane/ethyl acetate: 20/1) to yield **7** together with unreacted **1** as an amorphous powder. Chromatography on silica gel with cyclohexane gives **7** as pale yellow needles (18.4 mg, 90 %).

Mp: 191 °C; **^{1}H NMR** (700 MHz, CDCl$_3$): δ = 7.72 (d, ½ AB, ^3J = 8.7 Hz, 1H), 7.78 – 7.82 (m, 4H), 7.82 (d, ½ AB, ^3J = 8.7 Hz, 1H), 7.84 (d, ½ AB, ^3J = 8.7 Hz, 1H), 7.88 (d, ½ AB, ^3J = 8.7 Hz, 1H), 8.01 (d, ½ AB, ^3J = 8.7 Hz, 1H); **^{13}C NMR** (175 MHz, CDCl$_3$): δ = 136.02 (C$_{hub}$, 1C), 135.89 (C$_{hub}$, 1C), 135.70 (C$_{hub}$, 1C), 135.05 (C$_{hub}$, 1C), 134.93 (C$_{hub}$, 1C), 131.90 (C$_{flank}$, 1C), 131.52 (C$_{flank}$, 1C), 131.09 (C$_{flank}$, 1C), 131.05 (C$_{flank}$, 1C), 130.79 (C$_{flank}$, 1C), 128.85 (C$_{Cl}$, 1C), 127.93 (C$_{rim}$, 1C), 127.74 (C$_{rim}$, 2C), 127.23 (C$_{rim}$, 1C), 127.19 (C$_{rim}$, 1C), 127.04 (C$_{rim}$, 1C), 126.22 (C$_{rim}$, 1C), 126.03 (C$_{rim}$, 1C), 124.74 (C$_{rim}$, 1C); **MS** (EI, 90 °C): *m/z* 284.0395 (found), 284.0393 (calc'd), 248 (100 %, [M]$^{+\cdot}$), 124 (12 %, [M-HCl]$^{+\cdot}$), 124 (12 %, [M-HCl]$^{2+}$); **IR**: ν = 2920 (m), 2850 (m), 1615 (w), 1298 (w), 1070 (m), 1030 (m), 861 (m), 824 (s), 782 (s), 559 cm^{-1} (s).

8.4.3. 1-(Trifluoromethyl)corannulene (10)
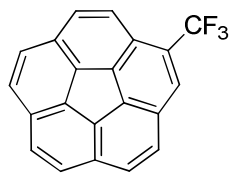
Corannulene (20.0 mg, 0.08 mmol, 1.0 eq.) was added to a flame-dried 10 mL Schlenk tube and taken into a glovebox, where 1-trifluoromethyl-1,2-benziodoxol-3-(1H)-one (25.3 mg, 0.08 mmol, 1.0 eq.) and methyltrioxorhenium (2.0 mg, 0.008 mmol, 0.1 eq.) were added. The reaction is stirred at 80 °C for 8 h under argon upon addition of 2 mL abs. DCE. After 30 minutes, the solution darkened. The reaction mixture was allowed to cool to room temperature before the solvent was evaporated under reduced pressure. The product was finally purified by PTLC with silica gel and hexane as eluent, to give a pale yellow solid 4.9 mg (19 %).

Mp: 169-172 °C; **^{1}H-NMR** (400 MHz, CDCl$_3$): δ = 8.22 (q, ^4J = 1.1 Hz, 1H), 8.03 (dd, ½ AB, ^4J = 1.9, ^3J = 8.9 Hz, 1H), 7.91 (d, ½ AB, ^3J = 8.9, 1H), 7.87-7.81 ppm (m, 6H); **^{19}F-NMR** (376 MHz, CDCl$_3$): δ = -57.41 ppm (s, CF$_3$, 3F); **^{13}C{^{1}H}-NMR** (126 MHz, CDCl$_3$): δ = 137.22 (C$_{hub}$, 1C), 136.43 (C$_{hub}$, 1C), 135.98 (C$_{hub}$, 1C), 135.61 (C$_{hub}$, 1C), 135.51 (C$_{hub}$, 1C), 132.16 (C$_{flank}$, 1C), 131.28 (C$_{flank}$, 1C), 131.12 (C$_{flank}$, 1C), 128.81 (C$_{flank}$, 1C), 128.36 (C$_{rim}$, 1C), 128.34 (C$_{rim}$, 1C), 128.13 (C$_{rim}$, 1C), 128.03 (C$_{rim}$, 1C), 127.50 (C$_{rim}$, 1C), 127.40 (C$_{rim}$, 1C), 127.26 (C$_{rim}$, 1C), 126.44 (C$_{rim}$, 1C), 126.29 (C$_{flank}$, 1C), 125.43 ppm (C$_{rim}$, 1C). CF3 and the corresponding ipso C-CF3 cannot be observed due to strong coupling and low S/N-ratio; **MS** (EI): m/z 318.0651 (found), 318.0656 (calc'd), 318 (100 %, [M]$^{+\cdot}$), 299 (15 %, [M-F$^-$]$^+$), 248 (9 %, [M-HCF$_3$]$^{+\cdot}$), 159 (10 %, [M]$^{2+}$); **IR**: ν = 2958 (m), 2924 (s), 2850 (m), 1650 (m), 1631 (m), 1280 (s), 1160 (m), 1106 (s), 890 (w), 828 (s), 720 (w), 666 (w), 547 cm^{-1} (m).

8.4.4. 1,6,7,10-Tetramethyl-8,9-bis(trifluoromethyl)fluoranthene (12)
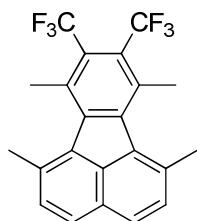
12

3,8-Dimethylacenaphthequinone (1.00 g, 4.76 mmol, 1.00 eq,) and 2.78 mL 3-pentanone (2.25 g, 26.16 mmol, 5.5 eq) were suspended in 28 mL methanol. A solution of potassium hydroxide (2.20 g, 7.84 mmol, 1.65 eq) in 11 mL methanol was added in one portion whereupon a yellow solution was formed. The solution was stirred for one hour at room temperature. 120 mL dichloromethane and 80 mL 10 % HCl were added, the organic layer was subsequently washed three times with 100 mL water and dried with sodium sulfate. After removal of the solvent, a glass ampule (diameter 1cm) was charged quickly with the crude product in 8 mL acetic anhydride and connected to the high vacuum line. After degassing, hexafluorobutyne (3.01 g, 18.56 mmol, 3.90 eq) was condensed under vacuum by cooling with liquid nitrogen. The ampule was flame sealed and the mixture was reacted for two days at 60 °C.

Upon cooling, the ampule was opened and the crude product was transferred to a flask using dichloromethane. After evaporation of the solvents, the crude product was purified column chromatography on silica gel using pentane as eluent, yielding 1.43 g of **12**, (76 %) as a yellow solid.

Mp: 203-210 °C; **^{1}H-NMR** (400 MHz, CDCl$_3$): δ = 7.58 (AB, ^3J = 8.2 Hz, 4H), 2.77 (s, 6H), 2.75 ppm (s, 6H); **^{19}F-NMR** (376 MHz, CDCl$_3$): δ = -52.40 ppm (s, CF$_3$, 6F); **^{13}C{^{1}H}-NMR** (101 MHz, CDCl$_3$): 143.51 (1C), 134.48 (2C), 134.20 (C$_{ipso}$, 2C), 132.99 (1C), 132.08 (CH$_{arom}$, 2C), 130.53 (2C), 127.89 (CH$_{arom}$, 2C), 126.62 (C$_{ipso}$, 2C), 124.81 (q, ^1J = 276 Hz, CF$_3$, 1C), 25.09 (2C, CH$_3$), 22.84 ppm (2C, CH$_3$); **^{13}C {^{1}H, ^{19}F}-NMR** (101 MHz, CDCl$_3$): δ = 143.52 (1C), 134.49 (2C), 134.48 (C$_{ipso}$, 2C), 133.00 (1C), 132.08 (CH$_{arom}$, 2C), 130.54 (2C), 128.16(C$_{ipso}$, 2C) 127.89(CH$_{arom}$, 2C), 126.63 (C$_{ipso}$, 2C), 124.81 (1C, CF$_3$), 25.09 (2C, CH$_3$), 22.84 ppm (2C, CH$_3$); **MS** (EI, 60 °C): *m/z* 394.1159 (found), 394.1156 (calc'd), 394 (100 %, [M]$^+$), 379 (47 %, [M-CH$_3$]$^+$), 325 (39 %, [M-CF$_3$]$^+$), 239 (13 %); **IR**: ν = 2917 (m), 2847 (m), 1741 (m), 1619 (w),

1563 (w), 1459 (m), 1384 (m), 1364 (s), 1363 (s), 1350 (s), 1305 (s), 1181 (s), 1142 (s), 1122 (s), 1018 (m), 988 (s), 968 (s), 925 (w), 907 (w), 796 (s), 757 (m), 717 (s), 643 (m), 633 (m), 590 cm^{-1} (m).

8.4.5. 1,6,7,10-Tetramethyl-3,8,9-tris(trifluoromethyl)fluoranthene (13)
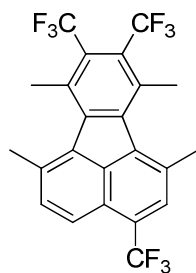
13   Fluoranthene **12** (0.60 g, 1.52 mmol, 1.00 eq), methyltrioxorhenium (38.00 mg, 0.15 mmol, 0.10 eq), and 1-(trifluoromethyl)-1,2-benziodoxol-3(1H)-one (0.84 g, 2.66 mmol, 1.75 eq) were charged into a flame-dried Schlenk tube and dissolved in 30 mL abs. DCE. Under an argon atmosphere the reaction mixture was stirred at 80 °C for 12 hours. After 60 minutes the colour turned from yellow to black. The solvent was evaporated and the crude product was purified by column chromatography on silica gel using pentane:dichloromethane (10:1) as eluent. The product **13** was isolated as a pale yellow solid, 146.5 mg (20.8 %).

Mp: 191 °C; **^{1}H-NMR** (400 MHz, CDCl$_3$): δ = 7.79 (½ AB, ^{3}J = 8.6 Hz, 2H), 7.78 (s, 1H), 2.81 (s, 3H), 2.78 (s, 3H), 2.77 (s, 3H), 2.77 ppm (s, 3H). The peaks of the downfield part of the AB signal show weak ^{19}F couplings; **^{19}F-NMR** (376 MHz, CDCl$_3$): -52.67 − (-52.81) (m, CF$_3$, 6F), -57.87 ppm (s, CF$_3$, 3F); **^{13}C{^{1}H}-NMR** (176 MHz, CDCl$_3$): δ = 144.35 (1C), 142.57 (1C), 136.95 (1C), 135.38 (1C), 134.79 (1C), 133.61 (CH$_{arom}$, 1C), 132.77 (1C), 131.37 (1C), 130.87 (1C), 130.21 (q, J = 5 Hz, CH$_{arom}$, 1C), 129.53–128.73 (m, 2C), 126.57 (q, J = 31 Hz, 1C), 125.05 (CH$_{arom}$, 1C), 124.51 (q, ^{1}J = 273 Hz, CF$_3$, 2C), 124.47 (q, ^{1}J = 273 Hz, CF$_3$, 1C), 122.50 (1C), 24.97 (CH$_3$, 1C), 24.96 (CH$_3$, 1C), 22.87–22.82 ppm (m, CH$_3$, 2C); **MS** (EI, 50 °C): *m/z* 426.10809 (found), 462.10300 (calc'd), 462 (100 %, [M]$^{+\cdot}$), 394 (69 %, [M-CF$_3$]$^{+\cdot}$), 447 (55 %, [M-CH$_3$]$^{+\cdot}$), 69 (34 %, [CF$_3$]$^{+\cdot}$), 320 (25 %), 309 (20 %), 178 (17 %), 91 (17 %), 131 (14 %), 443 (14 %, [M-F]$^{+\cdot}$), 277 (12 %); **IR**: ν = 3000 (w), 1616 (w), 1558 (w), 1506 (w), 1469 (m), 1445

(m), 1365 (m), 1278 (s), 1213 (m), 1139 (s), 1112 (s), 1048 (s), 919 (m), 886 (m), 870 (m), 821 (m), 702 (m), 622 (m), 534 (s) cm^{-1}.

8.4.6. 1,6,7,10-Tetramethyl-3,4,8,9-tetrakis(trifluoromethyl)fluoranthene (*sym*-14) and 1,6,7,10-tetramethyl-2,4,8,9-tetrakis(trifluoromethyl)fluoranthene (*asym*-14)
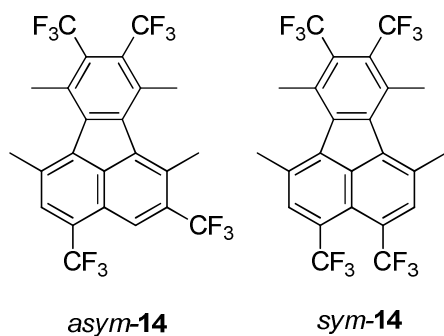
*asym*-**14**   *sym*-**14**   1,6,7,10-Tetramethyl-3,8,9-tris(trifluoromethyl)fluor-

anthene (**13**) (67.4 mg, 0.15 mmol, 1.00 eq), methyltrioxorhenium (3.6 mg, 0.015 mmol, 0.10 eq), and 1-(trifluoromethyl)-1,2-benziodoxol-3(1H)-one (81.0 mg, 0.26 mmol, 1.75 eq) were charged into a flame-dried Schlenk tube and dissolved in 4 mL abs. DCE. The reaction mixture was stirred at 80 °C for 12 hours under an argon atmosphere. During the first 60 minutes, the colour turned from yellow to black. The solvent was evaporated and the crude product was prepurified by filtration through a short silica gel plug with pentane:dichloromethane (1:1). The crude product (consisting of a mixture of **13** and **14**) was subjected to purification by GPC (eight cycles in average) to yield the both the products *asym*-**14** (23.6 mg, 31 %) and *sym*-**14** (9.9 mg, 13 %) as well as remaining starting material **14** (21.9 mg, 32 %) as a pale yellow solids.

1,6,7,10-tetramethyl-2,4,8,9-tetrakis(trifluoromethyl)fluoranthene (*asym*-14)

Mp: 153 °C; **^{1}H-NMR** (400 MHz, CDCl$_3$): δ = 8.46 (s, 1H), 7.83 (s, 1H), 2.82 (s, 3H), 2.80–2.75 (m, 6H), 2.74–2.69 ppm (m, 3H); **^{19}F-NMR** (376 MHz, CDCl$_3$): δ = -52.88 (br s, 6F), -57.90 (s, 3F), -60.13 ppm (s, 3F); **^{13}C{^{1}H}-NMR** (126 MHz, CDCl$_3$): δ = 144.35 (1C), 143.56 (1C), 137.37 (1C), 137.09 (1C), 136.51 (1C), 135.67 (1C, CH), 133.30 (1C), 132.30–130.58 (m, 1C, C-CF$_3$), 132.17 (1C, CH), 128.48–127.06 (m, 2C, C-CF$_3$), 126.04 (1C, C-CH$_3$), 124.89–124.71 (m, 1C, C-CF$_3$), 124.79 (1C), 124.10 (1C, C-CH$_3$), 123.57 (1C, C-CH$_3$), 126.63 (1C, C-CH$_3$), 25.68 (2C, CH$_3$), 23.46 – 23.32 (m, 1C, CH$_3$), 21.30 ppm (q, *J* = 3.0 Hz, CH$_3$), the CF3 carbons cannot be

assigned due to the strong coupling with large coupling constants and the consequent low S/N-ratios; **MS** (EI): *m/z* 530.0906 (found), 530.0904 (calc'd), 530 (100 %, [M]$^{+\cdot}$), 515 (30 %, [M-CH$_3$]$^+$), 461 (25 %, [M-CF$_3$]$^+$); **IR**: ν = 2994 (w), 2967 (w), 1469 (w), 1372 (w), 1344 (m) 1280 (s), 1207 (m), 1109 (s), 1051 (s), 990 (m), 916 (m), 742 cm^{-1} (m).

1,6,7,10-tetramethyl-3,4,8,9-tetrakis(trifluoromethyl)fluoranthene (*sym*-14)

Mp: 198 °C; **^{1}H-NMR** (400 MHz, CDCl$_3$): δ = 8.00 (s, 2H), 2.74 (s, 6H), 2.72 ppm (s, 6H); **^{19}F-NMR** (376 MHz, CDCl$_3$): δ = -52.94 (s, 6F), -55.08 ppm (s, 6F); **^{13}C{^{1}H}-NMR (126 MHz, CDCl$_3$)**: δ = 143.14 (2C), 137.71 (2C), 136.48 (2C), 135.04 (2C), 133.36 (2CH), 131.50 (2C), 118.64 (1C), 24.04 (2CH$_3$), 22.29 ppm (2CH$_3$), CF3 and the corresponding C-CF3 cannot be observed due to strong coupling and the consequent low S/N-ratios; **MS** (EI): *m/z* 530.0903 (found), 530.0904 (calc'd), 530 (100 %, [M]$^{+\cdot}$), 515 (15 %, [M-CH$_3$]$^+$), 461 (24 %, [M-CF$_3$]$^+$); **IR**: ν = 3001 (w), 2967 (w), 1604 (w), 1509 (w), 1472 (w), 1344 (m), 1280 (s), 1210 (s), 1115 (s), 1045 (s), 993 (s), 745 (m), 724 cm^{-1} (m).

8.4.7. 1,6,7,10-Tetramethylfluoranthene-8,9-dicarbonitrile (18)
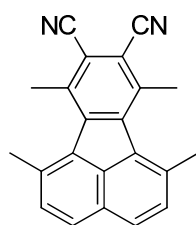
18   In a 100 mL Schlenk flask 3,8-dimethylacenaphthylene-1,2-dione (300 mg, 1.43 mmol, 1.0 eq.), pentan-3-one (0.81 mL, 7.62 mmol, 5.3 eq.) were suspended in methanol (16.5 mL). A solution of potassium hydroxide (660 mg, 12.00 mmol, 8.4 eq.) in methanol (3.3 mL) was added by syringe and the mixture was stirred for one hour at room temperature. The yellow solution was diluted with 30 mL dichloromethane and extracted three times with 10 % hydrochloric acid (50 mL). After drying with anhydrous sodium sulfate and quick removal of the solvent the crude product was transferred to a 50 mL Schlenk tube and vacuum dried. The vessel was purged with argon and a solution of dicyanoacetylene (**17**) (217 mg, 2.85 mmol, 2.0 eq.) in 1,2-dichloroethane (2.6 mL), additional 1,2-dichloroethane (5 mL) and three drops of acetic anhydride were added to the crude solid. The yellow solution

was stirred at 50 °C for 15 hours. The cooled reaction mixture was evaporated under reduced pressure, leaving a solid residue that was filtrated through a short plug of silica gel with dichloromethane as eluent. The product was obtained as a yellow solid 385 mg (88 %).

Mp: Gradually darkens above 267 °C; **^{1}H-NMR** (400 MHz, CDCl$_3$): δ = 7.86 (d, ½ AB, ^3J = 8.2 Hz, 2H), 7.47 (d, ½ AB, ^3J = 8.2 Hz, 2H), 2.92 (s, 6H), 2.84 ppm (s, 6H); **^{13}C{^{1}H}-NMR (101 MHz, CDCl$_3$):** δ = 143.75 (2C), 135.73 (2C), 135.44 (2C), 134.09 (1C), 132.39 (2CH), 132.01, 129.04 (2CH), 126.70, 116.34 (2CN), 115.37 (2C), 25.17 (2C), 22.66 ppm (2C); **MS** (EI, 120 °C): *m/z* 308.1326 (found), 308.1314 (calc'd), 308 (100 %, [M]$^{+\cdot}$), 293 (72 %, [M-CH$_3$]$^+$), 277 (17 %, [293-CH$_3$]$^+$); **IR**: ν = 2964 (w), 2926 (w), 2216 (s), 1608 (m), 1456 (s), 1438 (m), 1409 (s), 1262 (s), 1022 (s), 1197 (m), 1153 (m), 1022 (s), 844 (s), 790 (m), 627 cm^{-1} (s).

8.4.8. 8,9-Diiodo-1,6,7,10-tetramethylfluoranthene (20)
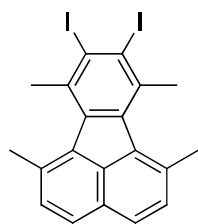
**20**   In a 50 mL Schlenk flask 3,8-dimethylacenaphthylene-1,2-dione (260 mg, 1.2 mmol, 1.0 eq.), pentan-3-one (1.22 mL, 7.6 mmol, 6.2 eq.) were suspended in methanol (16.5 mL). A solution of potassium hydroxide (660 mg, 12.0 mmol, 9.70 eq.) in methanol (3.3 mL) was added by syringe and the mixture was stirred for one hour at room temperature. The yellow solution was diluted with 100 mL dichloromethane and extracted three times with 10 % hydrochloric acid (50 mL). After drying with anhydrous sodium sulfate and quick removal of the solvent the crude product was transferred to a 50 mL Schlenk tube and vacuum dried. The vessel was purged with argon and acetic anhydride (5 mL) and diiodoacetylene (**19**) (687 mg, 2.5 mmol, 2.0 eq.) were added in one portion. The dark brown solution was stirred at 100 °C for 50 hours. The cooled reaction mixture was cooled to room temperature and all volatiles were removed under vacuum. The solid residue was purified by column chromatography on silica gel (dichloromethane). The product was obtained as a yellow solid 390 mg (61 %).

Mp: 136 °C; **^{1}H NMR** (700 MHz, CDCl$_3$): δ = 7.71 (d, ½ AB, 2H, ^3J = 8.3 Hz), 7.36 (d, ½ AB, ^3J = 8.3 Hz, 2H), 2.92 (s, 6H), 2.69 ppm (s, 6H); **^{13}C{^{1}H} NMR** (101 MHz, CDCl$_3$): δ = 140.54 (2C), 135.28 (2C), 134.16 (2C), 132.75 (1C), 131.86 (2CH), 126.92 (2CH), 126.48 (1C), 117.56 (2C), 96.95 (2C), 35.02 (2CH$_3$), 24.5 ppm (2CH$_3$); **IR**: ν = 2998 (w), 2915 (w), 1888 (w), 1717 (w), 1606 (w) 1534 (w), 1500 (w), 1438 (m), 1372 (m), 1303 (w), 1221 (w), 1186 (w), 1141 (w), 1021 (s), 959 (s), 821 (s) 776 (m), 673 (m), 621 cm^{-1} (s).

### 8.4.9. 1,6,7,10-Tetramethyl-8,9-bis(perfluorophenyl)fluoranthene (23)
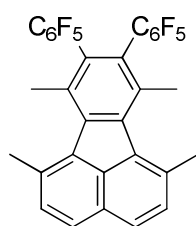
23　　　In a 50 mL Schlenk flask 3,8-dimethylacenaphthylene-1,2-dione (461 mg, 2.2 mmol, 1.0 eq.), pentan-3-one (1.22 mL, 7.6 mmol, 3.5 eq.) were suspended in methanol (12 mL). A solution of potassium hydroxide (1 g, 17.8 mmol, 8.1 eq.) in methanol (5 mL) was added by syringe and the mixture was stirred for one hour at room temperature. The yellow solution was diluted with 50 mL dichloromethane and extracted three times with 10 % hydrochloric acid (50 mL). After drying with anhydrous sodium sulfate and quick removal of the solvent the crude product was transferred to a 50 mL Schlenk tube and vacuum dried. The vessel was purged with argon and acetic anhydride (12 mL) and bis(pentafluorophenyl)acetylene (**26**) (1.1 g, 3.1 mmol, 1.4 eq.) were added in one portion. The dark brown solution was stirred at 110 °C for 6 days. The cooled reaction was evaporated and the dark solid residue that was purified by column chromatography on silica gel (pentane/dichloromethane 10:1). The product was obtained as a yellow-green solid 698 mg (54 %). Unreacted **26** (584 mg) can be recovered from the first (colourless) fraction.

Mp: 216 °C; **^{1}H-NMR** (400 MHz, CDCl$_3$): δ = 7.77 (d, ½ AB, ^3J = 8.2 Hz, 2H), 7.42 (d, ½ AB, ^3J = 8.2 Hz, 2H), 2.82 (s, 6H), 2.46 ppm (s, 6H); **^{19}F-NMR** (376 MHz, CDCl$_3$): AA'BB'C-type δ = -138.6–138.8 (m, *ortho*-4F), -152.9–153.1 (m, *para*-2F), -161.0–161.2 ppm (m, *meta*-4F); **^{13}C{^{1}H,^{19}F}-NMR (101 MHz, CDCl$_3$):** δ = 144.22 (4CF), 142.24 (2CF), 140.94 (4CF), 137.53 (2C),

133.75 (1C), 133.67 (2C), 133.43 (2C), 131.95 (2CH), 129.79 (2C), 127.33 (2CH), 126.74 (2C), 126.66 (1C), 114.34 (2C), 24.83 (2C), 21.85 ppm (2C); **MS** (EI, 130 °C): m/z 590.1103 (found), 509.1092 (calc'd), 509 (100 %, [M]$^{+\cdot}$), 575 (37 %, [M-CH$_3$]$^+$); **IR**: v = 3063 (w), 2949 (w), 1713 (s), 1520 (s), 1496 (s), 1434 (s), 1410 (s), 1376 (m), 1107 (m), 980 (s), 897 (s), 790 (s), 735 cm^{-1} (m).

8.4.10. 1,2-Bis(trifluoromethyl)corannulene (25)
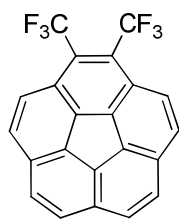
25 In a 100 mL round bottom flask, **12** (282 mg, 0.72 mmol, 1.0 eq.) was dissolved in tetrachloromethane (15 mL). *N*-bromosuccinimide (1.53 g, 8.64 mmol, 12.0 eq.) and 3% AIBN were added and the suspension was refluxed for 24 hours while irradiating with a 150W sunlight lamp. The reaction mixture was cooled and all volatiles were removed under reduced pressure. The solid residue was (partially) redissolved in dichloromethane (75 mL) and extracted four times with water (100 mL). After drying with anhydrous sodium sulfate and removal of the solvent the crude product was transferred to a 50 mL Schlenk tube and vacuum dried. A brown suspension formed upon addition of nickel powder (370 mg, 6.3 mmol, 8.8 eq.) and anhydrous DMF (29 mL), which was heated to 80 °C in the closed vessel for 8 hours and stirred overnight. The reaction was stopped by addition of water and the crude product was transferred to a separation funnel. Dichloromethane (75 mL) was added and the organic layer was washed with water (5 x 200 mL). After drying with anhydrous sodium sulfate, the product was finally purified by column chromatography on silica gel (pentane). The product was obtained from the first fraction as pale yellow needles, 59.4 mg (21 %). Crystals suitable for X-ray analysis were obtained by slow evaporation of a dichloromethane-pentane solution at room temperature.

Mp: 210-216 °C; **^{1}H NMR** (700 MHz, CDCl$_3$): δ = 8.05 (AB, ^3J = 9.0 Hz, 4H), 7.87 ppm (AB, ^3J = 8.6 Hz, 4H). The peaks at 8.18 and 8.17 of the first AB-type signal show weak ^{19}F interactions of J = 3.0 Hz; **^{19}F NMR** (376 MHz, CDCl$_3$): δ = -49.94 ppm (s, CF$_3$, 6F); **^{13}C{^{1}H} NMR** (176 MHz,

CDCl$_3$): δ = 136.75 (C$_{hub}$, 1C), 135.71 (C$_{hub}$, 2C), 134.42 (C$_{hub}$, 2C), 131.63 (C$_{flank}$, 2C), 131.42 (C$_{flank}$, 1C), 129.08 65 (C$_{rim}$, 2C), 128.98 65 (C$_{rim}$, 2C), 127.30 65 (C$_{rim}$, 2C), 127.00 65 (C$_{rim}$, 2C), 125.73 ppm (C$_{flank}$, 2C). <u>C</u>F$_3$ and the corresponding <u>C</u>-CF$_3$ cannot be observed; **MS** (EI, 70 °C): *m/z* 386.0545 (found), 386.0530 (calc'd), 386 (100 %, [M]$^{+\cdot}$), 317 (45 %, [M-CF$_3$]$^{+\cdot}$), 57 (41 %), 148 (26 %), 97 (17 %), 251 (14 %), 193 (5 %, [M]$^{2+}$); **IR**: ν = 3032 (w), 2958 (w), 2919 (w), 2849 (w), 1904 (w), 1791 (w), 1719 (w), 1632 (w), 1456 (w), 1433 (w), 1409 (w), 1350 (m), 1269 (m), 1237 (m), 1108 (s), 1040 (s), 959 (m), 894 (m), 832 (s), 794 (m), 731 (m), 715 (m), 676 (m), 610 (m) cm^{-1}.

### 8.4.11. 4,9-Dibromo-1,2-bis(trifluoromethyl)corannulene (26)

26
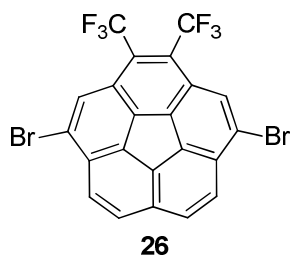
In a 100 mL round bottom flask, **12** (591 mg, 1.50 mmol, 1.0 eq.) was dissolved in tetrachloromethane (50 mL). *N*-bromosuccinimide (3.2 g, 18.00 mmol, 12.0 eq.) and 3% DBPO were added and the suspension was refluxed for 24 hours while irradiating with a 150W sunlight lamp. The reaction mixture was cooled and all volatiles were removed under reduced pressure. The solid residue was (partially) re-dissolved in dichloromethane (150 mL) and extracted four times with water (250 mL). After drying with anhydrous sodium sulfate and removal of the solvent the crude product was transferred to a 250 mL flask and dissolved in 71 mL 1,4-dioxane/water (12:5). Sodium hydroxide pellets (0.6 g, 15.0 mmol, 10 eq.) were added and the resulting suspension was refluxed for 20 minutes at 110 ºC. After cooling to room temperature, suspension was poured into water (100 mL), acidified with aqueous hydrochloric acid and the precipitate was filtered off under reduced pressure. The precipitate was dried under high vacuum and finally obtained as 0.64 g of a brown solid (78 %), insoluble in most organic solvents.

Mp: <300 °C; **^{1}H-NMR** (400 MHz, 1,1,2,2-Tetrachloroethane-d2): δ = 8.34 (s, 2H), 8.00 (d, ½ AB, ^3J = 8.9 Hz, 2H), 7.97 ppm (d, ½ AB, ^3J = 8.9 Hz, 2H); **^{19}F-NMR** (376 MHz, 1,1,2,2-Tetrachloroethane-d2): δ = -49.96 ppm (s, 6F, CF$_3$); **MS** (EI, 150 °C): *m/z* 541.8764 (found),

541.8740 (calc'd), 541 (100 %, [M]$^{+\cdot}$), 315 (25 %), 465 (24 %, [M-CF$_3$] $^{+\cdot}$), 157 (24 %), 334 (21 %), 167 (17 %); **IR**: ν = 2959 (w), 2925 (w), 2854 (w), 1728 (w), 1658 (w), 1617 (w), 1577 (w), 1493 (w), 1442 (w), 1404 (w), 1348 (w), 1296 (m), 1258 (s), 1222 (m), 1155 (s), 1058 (m), 1015 (m), 933 (w), 903 (w), 865 (m), 747 (m), 736 (w), 660 (w), 624 (w), 564 (m), 533 cm^{-1} (m).

8.4.12. 1,2,6-Tris(trifluoromethyl)corannulene (27)
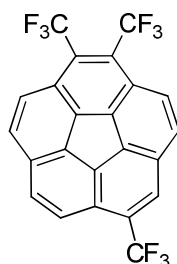

27   In a 100 mL round bottom flask, **13** (208 mg, 0.45 mmol, 1.0 eq.) was dissolved in tetrachloromethane (25 mL). *N*-bromosuccinimide (960 mg, 5.40 mmol, 12.0 eq.), 3% DBPO were added and the suspension was refluxed for 24 hours while irradiating with a 150W sunlight lamp. The reaction mixture was cooled and all volatiles were removed under reduced pressure. The solid residue was (partially) re-dissolved in dichloromethane (75 mL) and extracted four times with water (125 mL). After drying with anhydrous sodium sulfate and removal of the solvent the crude product was transferred to a 50 mL Schlenk tube and vacuum dried. A brown suspension formed upon addition of nickel powder (232 mg, 3.96 mmol, 8.8 eq.) and anhydrous DMF (22 mL), which was heated to 80 °C in the closed vessel for 8 hours and stirred overnight. The reaction was stopped by addition of water and the crude product was transferred to a separation funnel. Dichloromethane (100 mL) was added and the organic layer was washed with water (4 x 100 mL). After drying with anhydrous sodium sulfate, the product was purified by column chromatography on silica gel (pentane:dichloromethane 3:1). The product was obtained from the first fraction, as pale yellow solid 33.0 mg (16 %).

Mp: 183 °C (decomp.); **^{1}H NMR** (700 MHz, CDCl$_3$): δ = 8.21 (s, 1H), 8.20-8.17 (m, 2H), 8.07 (dd, ½ AB, *J* = 1.6, ^3J = 8.8 Hz, 1H), 7.94–7.89 ppm (m, 3H); ^{19}F interactions of *J* = 2.0 Hz can be observed for the multiplett at 8.20-8.17 ppm. **^{19}F NMR** (376 MHz, CDCl$_3$): δ = -50.11–

50.30 (m, 6F), -58.00 ppm (s, 3F). ^{13}C{^{1}H} NMR (175 MHz, CDCl$_3$): δ = 136.58 (C$_{hub}$, 1C), 136.03 (C$_{hub}$, 1C), 135.50 (C$_{hub}$, 1C), 135.09 (C$_{hub}$, 1C), 133.08 (C$_{hub}$, 1C), 131.61 (1C), 129.90 (1C), 129.76 (1C), 129.58 (1C), 129.39 (1C), 129.11 (1C), 128.92 (1C), 128.42 (C$_{rim}$, 1C), 127.94 (q, J = 6 Hz, C$_{rim}$, 1C), 127.79 (q, J = 6 Hz, C$_{rim}$, 1C), 127.26 (1C), 126.75 (1C), 126.59 (1C), 126.31 (q, J = 5.6 Hz, C$_{rim}$, 1C), 125.90 (1C), 124.30 (broad q, ^{1}J = 276 Hz, CF$_3$, 1C), 123.99 ppm (q, ^{1}J = 276 Hz, CF$_3$, 2C); **MS** (EI, 60 °C): m/z 454.04546 (found), 454.04041 (calc'd), 454 (100 %, [M]$^{+}$), 435 (25 %, [M-F]$^{+}$), 385 (23 %, [M-CF$_3$]$^{+}$), 425 (22%); **IR**: ν = 2954 (m), 2925 (m), 2855 (m), 1739 (w), 1645 (w), 1461 (m), 1727 (s), 1157 (s), 1122 (s), 1017 (m), 929 (w), 893 (w), 819 (m), 798 (s), 738 cm^{-1} (m).

8.4.13. 1,2,6,7-Tetrakis(trifluoromethyl)corannulene (28)
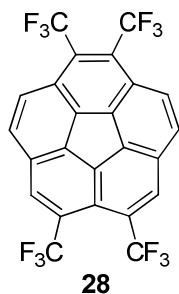
28 In a chemistation tube with septum, *sym*-**14** (23.0 mg, 0.04 mmol, 1.0 eq.) was dissolved in tetrachloromethane (10 mL). *N*-bromosuccinimide (85 mg, 0.48 mmol, 12.0 eq.), 3% AIBN were added and the suspension was refluxed for 48 hours while irradiating with a 150W sunlight lamp. The reaction mixture was cooled and all volatiles were removed under reduced pressure. The solid residue was re-dissolved in dichloromethane (50 mL) and extracted four times with water (75 mL). After drying with anhydrous sodium sulfate and removal of the solvent, the crude product was transferred to a chemistation tube and vacuum dried. A brown suspension formed upon addition of nickel powder (20.7 mg, 0.35 mmol, 8.8 eq.) and anhydrous DMF (20 mL), which was heated to 80 °C in the closed vessel for 8 hours and stirred overnight. The reaction was stopped by addition of water and the crude product was transferred to a separation funnel. Dichloromethane (100 mL) was added and the organic layer was washed with water (4 x 100 mL). After drying with anhydrous sodium sulfate, the product was purified by column chromatography on silica gel (hexane). The product was obtained from the first fraction, a pale yellow solid 2.5 mg (11 %).

¹H-NMR (400 MHz, CDCl₃): δ = 8.57 (s, 2H), 8.35–8.27 (m, ½ AB, 2H), 8.31 (d, ½ AB, ^3J = 9.2 Hz, 2H), 8.02 ppm (^3J = 9.2 Hz, 2H). The peaks of the downfield part of the AB signal show weak ¹⁹F couplings; **¹⁹F-NMR** (376 MHz, CDCl₃): δ = -50.46 (s, CF₃, 6F) -56.20 ppm (s, CF₃, 6F); **MS** (EI): *m/z* 522.0273 (found), 522.0278 (calc'd), 522 (100 %, [M]⁺), 502 (20 %, [M-F]⁺), 453 (25 %, [M-CF₃]⁺).

8.4.14. 1,2-Bis(pentafluorophenyl)corannulene (29)
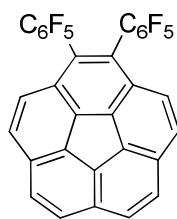
29   In a 100 mL round bottom flask, **23** (614.0 mg, 1.04 mmol, 1.0 eq.) was dissolved in tetrachloromethane (20 mL). *N*-bromosuccinimide (2.8 g, 15.60 mmol, 15.0 eq.), 3% DBPO were added and the suspension was refluxed for 28 hours while irradiating with a 150W sunlight lamp. The reaction mixture was cooled and all volatiles were removed under reduced pressure. The solid residue was (partially) re-dissolved in dichloromethane (100 mL) and extracted four times with water (125 mL). After drying with anhydrous sodium sulfate and removal of the solvent the crude product was transferred to a 50 mL Schlenk tube and vacuum dried. A brown suspension formed upon addition of nickel powder (537 mg, 9.15 mmol, 8.8 eq.) and anhydrous DMF (12 mL), which was heated to 80 °C in the closed vessel for 24 hours. The reaction was stopped by addition of water and the crude product was transferred to a separation funnel. Dichloromethane (100 mL) was added and the organic layer was washed with water (4 x 100 mL). After drying with anhydrous sodium sulfate, the product was purified by column chromatography on silica gel (pentane:dichloromethane 10:1). The product was obtained from the first fraction, as pale yellow solid 220 mg, (36 %). To remove unidentified remaining trace impurities, GPC separation with chloroform was performed.

Mp: 231 °C; **¹H-NMR** (700 MHz, CDCl₃): δ = 7.89 (d, ½ AB, ^3J = 8.8 Hz, 2H), 7.86 (d, ½ AB, ^3J = 8.9 Hz, 2H), 7.85 (d, ½ AB, ^3J = 8.7 Hz, 2H), 7.39 ppm (d, ½ AB, ^3J = 8.8 Hz, 2H); **¹⁹F-NMR** (376 MHz, CDCl₃): AA'BB'C-type δ = -137.65–137.90 (m, *ortho*-4F), -151.48–151.70 (m, *para*-2F), -

160.20–160.45 ppm (m, *meta*-4F); ^{13}C{^{1}H}-NMR (176 MHz, CDCl$_3$): δ = 145.54–143.35 (m, CF, 4C), 142.50–140.15 (m, CF, 2C), 138.69–136.56 (m, CF, 4C), 136.52 (C$_{hub}$, 1C), 135.50 (C$_{hub}$, 2C), 135.41 (C$_{hub}$, 2C), 131.50 (C$_{flank}$), 131.42 (C$_{flank}$), 128.76 (C$_{flank}$), 128.55 (C$_{rim}$, 2C), 128.25 (C$_{rim}$, 2C), 127.39 (C$_{rim}$, 2C), 125.88 (C$_{ipso}$, 2C), 124.96 (C$_{rim}$, 2C), 111.61 ppm (t, ^2J = 17.1 Hz, C$_{ipso}$, 2C); **MS** (EI, 100 °C): *m/z* 582.0450 (found), 582.0466 (calc'd), 582 (100 %, [M]$^{+\cdot}$), 562 (21 %, [M-HF]$^{+\cdot}$), 562 (21 %, [M-HF]$^{+\cdot}$), 562 (10 %, [M-2HF]$^{+\cdot}$), 291 (4 %, [M]$^{2+}$); **IR**: ν = 3039 (w), 1648 (m), 1520 (s), 1486 (s), 1300 (w), 1107 (m), 1079 (m), 983 (s), 952 (s), 904 (w), 818 (s), 735 (m), 700 (m), 563 cm^{-1} (m).

8.4.15. 4,9-Dibromo-1,2-bis(pentafluorophenyl)corannulene (30)
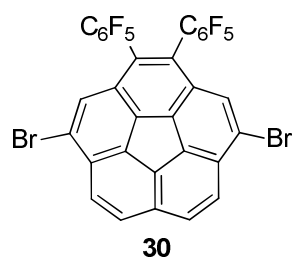
To 250 mL flask containing the brominated fluoranthene (477 mg, 0.45 mmol, 1 eq.), obtained as described for **29**, was added 1,4-dioxane (15 mL). Water (6.25 mL) and sodium hydroxide pellets (180 mg, 4.5 mmol, 10 eq.) were added and the resulting suspension was refluxed for 20 minutes at 110 ºC. After cooling to room temperature, the suspension was poured into water (100 mL), acidified with aqueous hydrochloric acid and the precipitate was filtered off under reduced pressure. The precipitate was dried under high vacuum. A light brown solid 171 mg (52 %), insoluble in most organic solvents, was obtained.

Mp: Gradually darkens above 321 °C; ^{1}**H-NMR** (400 MHz, CDCl$_3$): δ = 8.01–7.96 (m, 4H), 7.55 ppm (s, 2H); ^{19}**F-NMR** (376 MHz, CDCl$_3$) AA'BB'C-type: δ = -137.20–137.34 (m, *ortho*-4F), -150.08–150.22 (m, *para*-2F), -159.08–159.25 ppm (m, *meta*-4F); **MS** (EI, 165 °C): *m/z* 737.8670 (found), 737.08677 (calc'd), 740 (60 %, [M]$^{+\cdot}$), 660 (24 %, [M-Br]$^{+\cdot}$), (18 %, [M-2Br]$^{+\cdot}$); **IR**: ν = 2955 (w), 1717 (w), 1653 (m), 1524 (s), 1491 (s), 1112 (m), 1081 (w), 983 (s), 910 (m), 825 (w), 808 (w), 776 cm^{-1} (w).

8.4.16. 4,9-Dimethyl-1,2-bis(pentafluorophenyl)corannulene (31)
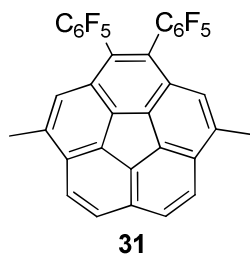
31 In a 50 mL Schlenk tube bromide **30** (75 mg, 0.1 mmol, 1.0 eq.), was suspended in abs. DME (8 mL). $NiCl_2$(dppp) (5.5 mg, 0.01 mmol, 9.70 eq.) and a solution of trimethylaluminium in toluene (2 mol/L, 0.5 mmol, 5 eq.) was added by syringe. The tube was sealed and the reaction mixture was heated to 75 °C for 24 hours. It was quenched by slow addition of ethanol under heavy stirring, while cooling with an ice bad. Dichloromethane was added and the mixture was extracted three times with 10 % hydrochloric acid (50 mL), dried with anhydrous sodium sulfate and evaporated. The product was purified by column chromatography on silica gel (pentane/dichloromethane 10:1) and GPC separation with chloroform to yield the product as a colourless powder, 18.5 mg (30 %).

Mp: Gradually darkens above 207 °C; **^{1}H-NMR** (700 MHz, $CDCl_3$): δ = 7.97 (d, ½ AB, ^3J = 8.8 Hz, 2H), 7.93 (d, ½ AB, ^3J = 8.8 Hz, 2H), 7.28 (s, 2H), 2.82 ppm (s, 3H); **^{19}F-NMR** (376 MHz, $CDCl_3$) AA'BB'C-type: δ = -137.41–138.39 (m, *ortho*-4F), -150.47–153.00 (m, *para*-2F), -159.97–161.29 ppm (m, *meta*-4F); **^{13}C{^{1}H}-NMR** (176 MHz, $CDCl_3$): δ = 145.54–143.79 (CF, 4C), 138.37 (C_{ipso}, 2C), 136.17 (C_{hub}, 1C), 135.54 (C_{hub}, 2C), 134.62 (C_{hub}, 2C), 131.80 (C_{flank}, 2C), 130.84 (C_{flank}, 1C), 138.96 (C_{flank}, 2C), 128.14 (C_{rim}, 2C), 125.48 (C_{ipso}, 2C), 125.35 (C_{rim}, 2C), 123.54 (C_{rim}, 2C), 111.96 (t, ^2J = 16.7 Hz, C_{ipso}, 2C), 19.11 ppm (CH_3, 2C). Two C-F signals cannot be assigned due to strong coupling and low S/N-ratio; **MS** (EI, 120 °C): *m/z* 610.0765 (found), 610.0779 (calc'd), 610 (100 %, [M]$^{+\cdot}$), 595 (19 %, [M-CH$_3$]$^+$), 443 (11 %, [M-C$_6$F$_5$H]$^{+\cdot}$), 305 (7 %, [M]$^{2+}$); **IR**: ν = 2971 (m), 2903 (m), 2848 (m), 2174 (s), 1653 (w), 1440 (s), 1369 (s), 1326 (s), 1026 (s), 979 (s), 813 (s), 722 (m), 683 cm^{-1} (w).

8.4.17. 1,6,7,10-Tetramethylfluoranthene-9-fused pentafluorophenylmaleimide (33a)
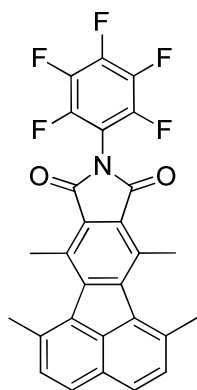
33a   In a 100 mL Schlenk flask 3,8-dimethylacenaphthylene-1,2-dione (500 mg, 2.38 mmol, 1.0 eq.), pentan-3-one (1.22 mL, 11.48 mmol, 4.8 eq.) were suspended in methanol (12 mL). A solution of potassium hydroxide (1 g, 17.82 mmol, 7.49 eq.) in methanol (5 mL) was added by syringe and the mixture was stirred for one hour at room temperature. The yellow solution was diluted with 50 mL dichloromethane and extracted three times with 10 % hydrochloric acid (50 mL). After drying with anhydrous sodium sulfate and quick removal of the solvent the crude product was transferred to a 50 mL Schlenk tube and vacuum dried. The vessel was purged with argon and nitrobenzene (11 mL) and 1-(perfluorophenyl)-1H-pyrrole-2,5-dione (691 mg 2.38 mmol, 1.0 eq.) were added in one portion. The dark red solution was stirred at 180 °C for 42 hours. The cooled reaction mixture was transferred to a small flask and the nitrobenzene was distilled off under reduced pressure, leaving a solid residue that was purified by column chromatography on silica gel (pentane/dichloromethane 3:1). The product was obtained as a yellow solid 494 mg (43 %).

Mp: 259 °C; **^{1}H NMR** (400 MHz, CDCl$_3$): δ = 7.85 (d, ½ AB, ^3J = 8.2 Hz, 2H), 7.48 (d, ½ AB, ^3J = 8.2 Hz, 2H), 3.06 (s, 6H), 2.88 ppm (s, 6H); **^{19}F NMR** (376 MHz, CDCl$_3$): AA'BB'C-type δ = -140.83–143.91 (m, *ortho*-2F), -150.87–153.18 (m, *para*-1F), -160.51–162.19 ppm (m, *meta*-2F); **^{13}C{^{1}H} NMR (101 MHz, CDCl$_3$):** δ = 166.01 (CO, 2C), 146.61 (2C), 135.41 (2C), 134.15 (1C), 132.73 (2C), 132.21 (2C), 131.16 (2C), 128.48 (2C), 128.23 (2C), 126.53 (1C), 25.16 (2C), 19.60 ppm (2C); **MS** (EI, 130 °C): *m/z* 493.1108 (found), 493.1101 (calc'd), 493 (100 %, [M]$^+$), 445 (23 %), 293 (20 %), 119 (17 %). **IR**: ν = 3476 (w), 2928 (w), 1775 (m), 1723 (s), 1606 (m)

1503 (s), 1465 (m), 1372 (s), 1348 (s), 1283 (s), 1193 (m), 1124 (s), 1093 (s), 976 (s), 842 (m), 794 (m) 708 (m), 625 (s) cm^{-1}.

8.4.18. Double cycloadduct with 1-(perfluorophenyl)-1H-pyrrole-2,5-dione (32)
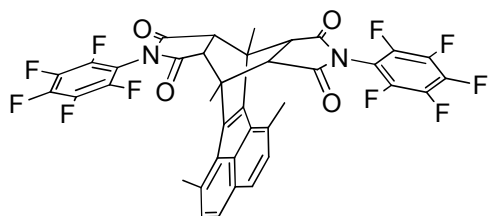
32

If the reaction is run with acetic anhydride or toluene instead of nitrobenzene for the second transformation, **32** is obtained as major product in 68 % yield.

Mp: 316 °C; **^{1}H NMR** (400 MHz, CDCl$_3$): δ = 7.62 (d, ½ AB, ^3J = 8.1 Hz, 2H), 7.23 (d, ½ AB, ^3J = 8.1 Hz, 2H), 3.27 (s, 4H), 2.80 (s, 6H), 2.66 ppm (s, 6H); **^{19}F NMR** (376 MHz, CDCl$_3$): ABCDE-type δ = -142.55 (dtd, J = 22.2, 6.7, 2.5 Hz, 1F), -142.68 (dtd, J = 22.2, 6.7, 2.2 Hz, 1F), -150.86 (tt, J = 21.5, 2.2, *para*-1F), -160.14 (tdd, J = 22.6, 6.3, 2.2, 1F), -160.98 ppm (tdd, J = 22.6, 6.3, 1.6, 1F); **^{13}C{^{1}H,^{19}F} NMR** (101 MHz, CDCl$_3$): δ = 172.31 (CO, 4C), 143.15 (4C), 139.65 (2C), 137.69 (4C), 136.37 (4C), 132.75 (1C), 132.24 (2C), 129.77 (1C), 128.88 (2C), 125.66 (2C), 106.53 (2C), 52.01 (4C), 42.75 (2C), 26.34 (2C), 25.18 ppm (2C); **MS** (EI, 100 °C): *m/z* 760.17702 (found), 760.14199 (calc'd), 495 (100 %, [M–C$_{10}$H$_4$F$_5$NO$_2$]$^{+\cdot}$), 480 (15 %,), 258 (34 %, [M–C$_{18}$H$_4$F$_{10}$N$_2$O$_4$]$^{+\cdot}$, 243 (26 %). **IR**: ν = 2902 (m), 1720 (s), 1610 (w), 1517 (s), 1358 (m), 1296 (m), 1190 (m), 1183 (m), 987 (m), 832 (w), 790 (m), 741 (m), 628 cm^{-1} (m).

### 8.4.19. 1,6,7,10-Tetramethylfluoranthene-9-fused heptafluorobutylmaleimide (33b)
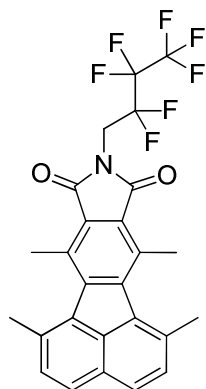
33b   In a 100 mL Schlenk flask 3,8-dimethylacenaphthylene-1,2-dione (800 mg, 3.80 mmol, 1.0 eq.), pentan-3-one (2.2 mL, 20.7 mmol, 5.5 eq.) were suspended with in dry methanol (44 mL). A solution of potassium hydroxide (1.76 g, 31.4 mmol, 8.3 eq.) in methanol (9 mL) was added by syringe and the mixture was stirred for one hour at room temperature. The yellow solution was diluted with 50 mL dichloromethane and extracted three times with 10 % hydrochloric acid (50 mL). After drying with anhydrous sodium sulfate and quick removal of the solvent, the crude product was transferred to a 50 mL Schlenk tube and vacuum dried. The vessel was purged with argon and nitrobenzene (13 mL) and 1-(2,2,3,3,4,4,4-heptafluorobutyl)-1H-pyrrole-2,5-dione (1.06 g, 3.8 mmol, 1.0 eq.) were added in one portion. The dark red solution was stirred at 180 °C for 72 hours. The cooled reaction mixture was transferred to a small flask and the nitrobenzene was removed under reduced pressure, leaving a solid residue that was purified by column chromatography on silica gel (pentane/dichloromethane 3:1). The product was obtained as a yellow solid 862 mg (45 %).

Mp: 231 °C; **^{1}H NMR** (400 MHz, CDCl$_3$): δ = 7.81 (d, ½ AB, ^3J = 8.2 Hz, 2H), 7.44 (d, ½ AB, ^3J = 8.2 Hz, 2H), 4.33 (t, ^3J = 15.6 Hz, 2H), 3.01 (s, 6H), 2.84 ppm (s, 6H); **^{19}F NMR** (376 MHz, CDCl$_3$): δ = -80.40 (t, ^3J = 9.4 Hz, 3F), -116.72 (dt, J = 15.0, 9.5 Hz, 2F), -127.50 (d, ^3J = 4.1 Hz, 2F); **^{13}C{^{1}H} NMR (101 MHz, CDCl$_3$):** δ = 167.94 (CO, 2C), 146.35 (2C), 135.23 (2C), 134.15 (1C), 132.89 (2C), 132.22 (2C), 130.65 (2C), 128.33 (2C), 128.24 (2C), 126.58 (1C), 25.22 (2C), 19.47 ppm (2C); **MS** (EI, 140 °C): m/z 509.12051 (found), 509.1226 (calc'd), 509 (100 %, [M]$^+$), 340 (50 %, [M-C$_3$F$_7$]$^+$), 239 (12 %). **IR**: ν = 2922 (w), 1760 (m), 1708 (m), 1462 (w), 1403

(m), 1348 (s), 1220 (s), 1177 (s), 979 (s), 948 (s), 931 (s), 912 (s), 859 (s), 794 (s), 737 (m), 692 cm^{-1} (m).

8.4.20. Corannulene-fused pentafluorophenylmaleimide (34a)
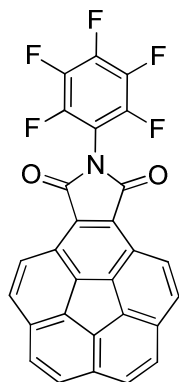
34a   In a 100 mL round bottom flask, **33a** (260 mg, 0.51 mmol, 1.0 eq.) was dissolved in tetrachloromethane (25 mL). *N*-bromosuccinimide (1.10 g, 6.13 mmol, 12.0 eq.) and 3% DBPO were added and the suspension was refluxed for 30 hours while irradiating with a 150W sunlight lamp. The reaction mixture was cooled and all volatiles were removed under reduced pressure. The solid residue was (partially) redissolved in dichloromethane (75 mL) and extracted four times with water (100 mL). After drying with anhydrous sodium sulfate and removal of the solvent the crude product was transferred to a 50 mL Schlenk tube and vacuum dried. A brown suspension formed upon addition of nickel powder (264 mg, 4.5 mmol, 8.8 eq.) and anhydrous DMF (20 mL) in an argon atmosphere, which was heated to 80 °C in the closed vessel for 8 hours and stirred overnight. The reaction was stopped by addition of water and the crude product was transferred to a separation funnel. Dichloromethane (75 mL) was added and the organic layer was washed with water (5 x 200 mL). After drying with anhydrous sodium sulfate, the product was finally purified by column chromatography on silica gel (pentane/dichloromethane 1:1). The product was obtained from the first yellow fraction, a yellow solid 65.7 mg (45 %). Crystals suitable for X-ray analysis were obtained by slow evaporation of a CDCl$_3$ solution at room temperature.

Mp: 285 °C; **^{1}H-NMR** (700 MHz, CDCl$_3$): δ = 8.44 (d, ½ AB, ^3J = 8.8 Hz, 2H), 7.98 (d, ½ AB, ^3J = 8.8 Hz, 2H), 7.89 (d, ½ AB, ^3J = 8.7 Hz, 2H), 7.84 ppm (d, ½ AB, ^3J = 8.7 Hz, 2H); **^{19}F-NMR** (376

MHz, CDCl$_3$): AA'BB'C-type δ = -142.17–142.35 (m, *ortho*-2F), -151.04–151.26 (m, *para*-1F), -160.64–160.82 ppm (m, *meta*-2F); **^{13}C{^{1}H}-NMR** (175 MHz, CDCl$_3$): δ = 165.88 (CO, 2C), 138.98 (C$_{hub}$ 2C), 135.93 (C$_{hub}$, 1C), 135.07 (C$_{hub}$, 2C), 132.31 (C$_{flank}$, 2C), 131.84 (C$_{flank}$, 2C), 131.10 (C$_{flank}$, 1C), 129.86 (C$_{rim}$, 2C), 139.19 (C$_{rim}$, 2C), 127.65 (C$_{rim}$, 2C), 125.48 (C$_{rim}$, 2C), 125.04 ppm (C$_{ipso}$, 2C); **MS** (EI, 150 °C): *m/z* 485.0464 (found), 485.0475 (calc'd), 485 (100 %, [M]$^{+\cdot}$), 441 (29 %), 423 (15 %), 248.1 (41 %, [M-C$_8$F$_5$NO$_2$]$^{+\cdot}$), 124.1 (17 %, [M-C$_8$F$_5$NO$_2$]$^{2+}$). **IR**: ν = 2919 (m), 292849 (m), 1775 (m), 1724 (s), 1507 (s), 1355 (s), 1293 (s), 1131 (m), 1086 (m), 987 (s), 1386 (w), 900 (m), 842 (m), 797 (s), 732 (s), 701 (s), 642 cm^{-1} (s).

### 8.4.21. Corannulene-fused heptafluorobutylmaleimide (34b)
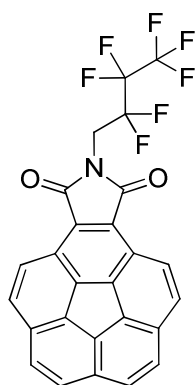
34b   In a 100 mL round bottom flask, **33b** (143 mg, 0.28 mmol, 1.0 eq.) was dissolved in tetrachloromethane (20 mL). *N*-bromosuccinimide (603 mg, 3.39 mmol, 12.0 eq.) and 3% DBPO were added and the suspension was refluxed for 32 hours while irradiating with a 150W sunlight lamp. The reaction mixture was cooled and all volatiles were removed under reduced pressure. The solid residue was (partially) re-dissolved in dichloromethane (75 mL) and extracted five times with water (150 mL). After drying with anhydrous sodium sulfate and removal of the solvent the crude product was transferred to a 50 mL Schlenk tube and vacuum dried. A brown suspension formed upon addition of nickel powder (146 mg, 2.46 mmol, 8.8 eq.) and anhydrous DMF (20 mL) in an argon atmosphere, which was heated to 80 °C in the closed vessel for 8 hours and stirred overnight. The reaction was stopped by addition of water and the crude product was transferred to a separation funnel. Dichloromethane (75 mL) was added and the organic layer was washed with water (5 x 200 mL). After drying with anhydrous sodium sulfate, the product was finally

purified by column chromatography on silica gel (pentane/dichloromethane 3:1). The product was obtained from the first yellow fraction, a yellow solid 43.4 mg (31 %).

Mp: 264 °C; **^{1}H-NMR** (700 MHz, CDCl$_3$): δ = 8.45 (d, ½ AB, ^3J = 8.8 Hz, 2H), 7.99 (d, ½ AB, ^3J = 8.8 Hz, 2H), 7.90 (d, ½ AB, ^3J = 8.6 Hz, 2H), 7.85 (d, ½ AB, ^3J = 8.6 Hz, 2H), 4.47 (t, ^3J = 15.7 Hz, 2H); **^{19}F-NMR** (376 MHz, CDCl$_3$): δ = -80.39 (t, ^3J = 9.4 Hz, 3F), -116.85 (dt, J = 15.5, 9.5 Hz, 2F), -127.43 (d, ^3J = 5.1 Hz, 2F); **^{13}C{^{1}H}-NMR** (175 MHz, CDCl$_3$): δ = 166.82 (CO, 2C), 137.93 (C$_{Hub}$ 2C), 134.93 (C$_{Hub}$, 1C), 135.14 (C$_{Hub}$, 2C), 131.22 (C$_{flank}$, 2C), 130.17 (C$_{flank}$, 2C), 131.11 (C$_{flank}$, 1C), 128.69 (CH$_{rim}$, 2C), 128.03 (CH$_{rim}$, 2C), 126.62 (CH$_{rim}$, 2C), 124.49 (CH$_{rim}$, 2C), 123.96 ppm (C$_{ipso}$, 2C); **MS** (EI, 130 °C): *m/z* 501.0584 (found), 501.0600 (calc'd), 501 (86 %, [M]$^{+\cdot}$), 332 (100 %, [M-C$_3$F$_4$]$^+$), 248 (23 %, [M-C$_6$H$_2$F$_7$NO$_2$]$^+$), 124 (48 %, [M-C$_6$H$_2$F$_7$NO$_2$]$^{2+}$). **IR**: ν = 2961 (m), 2921 (m), 2845 (m), 1741 (w), 1723 (w), 1518 (w), 1457 (w), 1375 (m), 1259 (m), 1090 (m), 1011 (s), 867 (w), 785 (s), 690 (w), 663 cm^{-1} (w)

8.4.22. Monofluorosumanene (39)
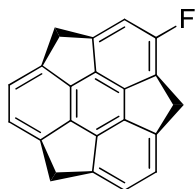
39　A flame-dried 10 mL Schlenk-tube was charged with **9** (19.6 mg, 0.74 mmol, 1 eq.) in abs. dichloromethane (6 mL) and cooled to -80 °C. Solid xenon(II)fluoride (20.0 mg, 1.18 mmol, 1.6 eq.) was added in one portion. The colourless solution was allowed to warm to room temperature, were it becomes black within one hour. After in total 2.5 h at room temperature, the mixture was diluted with more dichloromethane and evaporated onto silica gel. The dry silica gel was eluted with pentane:dichloromethane (10:1), to give 5 mg of crude product after evaporation of the solvent mixture. The residue was purified by HPLC using (Cosmosil Buckyprep, hexane/chloroform 7:3) to give the title compound as a colourless solid (1.6 mg, 8 %).

Mp: 248 °C; **^{1}H-NMR** (400 MHz, CD$_2$Cl$_2$): δ = 7.18–7.08 (m, 4H), 6.82 (d, $^3J_{H-F}$ = 11.6 Hz, 1H), 4.75–4.56 (m, 3H), 3.63 (d, ^2J = 19.7 Hz, 1H), 3.43 ppm (m, 2H); **^{19}F-NMR** (376 MHz, CDCl$_3$): δ

= -114.81 ppm (d, $^3J_{\text{F-H}}$ = 11.6 Hz, 1F); ^{13}C{^{1}H}-NMR (176 MHz, CDCl$_3$): δ = 158.31 (d, ^1J = 251 Hz, C$_F$, 1C), 152.90 (d, ^3J = 9 Hz, 1C), 150.02 (d, ^3J = 10 Hz, 1C), 149.31 (1C), 149.16 (1C), 149.03 (1C), 148.65 (1C), 148.60 (1C), 148.43 (1C), 148.31 (1C), 148.14 (d, J = 4 Hz, 1C), 144.62 (1C), 131.14 (d, ^2J = 21 Hz, 1C), 124.04 (C$_{\text{rim}}$, 1C), 123.54 (C$_{\text{rim}}$, 1C), 123.47 (C$_{\text{rim}}$, 1C), 123.12 (C$_{\text{rim}}$, 1C), 112.58 (d, ^2J = 28 Hz, 1C), 41.87 (CH$_2$, 1C), (CH$_2$, d, ^3J = 1 Hz, 1C), 39.32 ppm (CH$_2$, 1C); **MS** (EI °C): *m/z* 282.0843 (found), 282.0845 (calc'd), 282 (100 %, [M]$^{+\cdot}$), 141 (18 %, [M]$^{2+}$); **IR**: ν = 2916 (m), 2885 (m), 1715 (m), 1565 (m), 1395 (s), 1341 (m), 1190 (w), 1005 (m), 921 (m), 782 (s), 754 cm^{-1} (m).

8.4.23. 1-(Trifluoromethyl)sumanene (40)
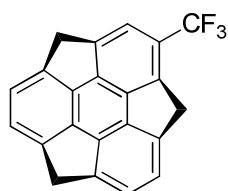
40   Sumanene **9** (33.0 mg, 0.12 mmol, 1.00 eq), methyltrioxorhenium (3.2 mg, 0.01 mmol, 0.10 eq), and 1-(trifluoromethyl)-1,2-benziodoxol-3(1H)-one (59.2 mg, 0.19 mmol, 1.5 eq) were charged into a flame-dried Schlenk tube and dissolved in 5 mL abs. DCE. Under an argon atmosphere the reaction mixture was stirred at 80 °C for 15 hours. During approximately 60 minutes the colour turned slowly to black. The solvent was evaporated and the crude product was purified by PTLC on silica gel using pentane:dichloromethane (3:1) as eluent. The product was isolated as a pale yellow solid from the fastest moving fraction, 6.5 mg (16 %).

Mp: 128 °C; ^{1}**H-NMR** (700 MHz, CDCl$_3$): δ 7.36 (s, 1H), 7.21–7.14 (m, 4H), 4.82 (d, ^2J = 19.7 Hz, 1H), 4.75 (d, ^2J = 19.2 Hz, 1H), 4.76 (d, ^2J = 19.4 Hz, 1H), 3.72 (d, ^2J = 19.9 Hz, 1H), 3.52 (d, ^2J = 19.5 Hz, 1H), 3.47 ppm (d, ^2J = 19.4 Hz, 1H); ^{19}**F-NMR** (376 MHz, CDCl$_3$): δ = -59.53 ppm (s, CF$_3$, 3F); ^{13}**C{^{1}H}-NMR** (176 MHz, CDCl$_3$): δ = 150.71 (1C), 149.55 (1C), 149.41 (1C), 149.34 (1C), 149.28 (1C), 149.27 (1C), 149.04 (1C), 148.56 (1C), 148.11 (1C), 147.87 (1C), 147.75 (1C), 146.93 (q, J = 2.8 Hz, 1C), 124.35 (q, ^2J = 32 Hz, 1C), 124.68 (C$_{\text{rim}}$, 1C), 124.36 (C$_{\text{rim}}$, 1C), 123.70 (C$_{\text{rim}}$, 1C), 123.60 (C$_{\text{rim}}$, 1C), 120.60 (C$_{\text{rim}}$, q, ^3J = 4 Hz, 1C), 42.06 (CH$_2$, 1C), 42.00 (CH$_2$, 1C), 41.96 ppm (CH$_2$, 1C). C̲F3 cannot be observed due to strong coupling and low S/N-ratio;

MS (EI °C): *m/z* 332.0810 (found), 332.0813 (calc'd), 332 (100 %, [M]$^+$), 263 (23 %, [M-CF$_3$]$^+$), 166 (8 %,[M]$^{2+}$), 132 (5 %, [M-CF$_3$]$^{2+}$); **IR**: ν = 2954 (m), 2926 (s), 2851 (m), 1717 (m), 1468 (w), 1389 (m), 1365 (m), 1281(m), 1159 (w), 1098 (s), 957 (w), 911 (w), 864 (w), 780 cm^{-1} (w).

8.4.24. Tris(dihydrospiro)[1,3]dithiane-sumanene (42)

42
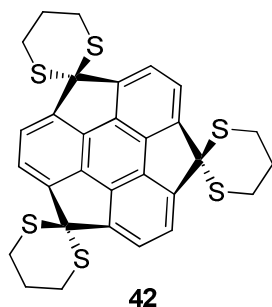
A flame-dried 30 mL flask was charged with sumanenetrione (**41**) (5.3 mg, 0.017 mmol, 1 eq.) and dichloromethane (8 mL). 1,3-propanedithiol (50 μL, 0.498 mmol, 29 eq.) and boron trifluoride diethyl etherate (100 μL, 0.789 mmol, 46 eq.) were added by syringe. The resulting solution was stirred at room temperature for 14 hours, whereupon water and 20 mL dichloromethane were added to the orange solution, the organic layer was washed with 10 % aqueous sodium hydroxide solution (30 mL) and twice with water. After drying with sodium sulfate, the crude was filtered and the solvent was evaporated, leaving a solid residue that was purified by PTLC with dichloromethane to give compound **42** as a colourless solid (5.6 mg, 64 %).

Mp: Darkens above 229 °C; **^{1}H NMR** (400 MHz, CDCl$_3$): δ = 7.37 (s, 6H), 3.28 (dd, *J* = 11.1, 4.5 Hz, 12H), 2.36–2.26 ppm (m, 6H); **^{13}C{^{1}H} NMR** (125 MHz, CDCl$_3$): δ = 156.74 (C$_{hub}$, 6C), 144.77 (C$_{flank,}$ 6C), 122.67 (C$_{rim}$, 6C), 61.07 (CS$_2$, 3C), 28.69 (CH$_2$, 6C), 24.67 ppm (CH$_2$, 3C); **MS** (EI): *m/z* 576.0208 (found), 576.0202 (calc'd), 576 (60 %, [M]$^+$), 529 (70 %, [M-C$_1$H$_3$S$_1$]$^+$), 455 (100 %), 381 (45 %), 351 (40 %), 323 (30 %); **IR**: ν = 2959 (m), 2920 (s), 2855 (m), 1719 (m), 1645 (m), 1465 (s), 1376 (m), 1256 (m), 1127 (w), 1033 (m), 808 (w), 724 cm^{-1} (w).

8.4.25. 1,1,4,4,7,7-Hexafluorosumanene (43)
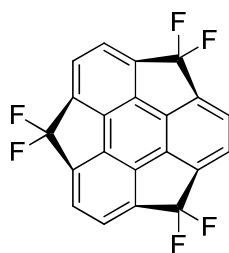
43

A carefully dried PP-tube was charged with *N*-iodosuccinimide (96 mg, 0.148 mmol, 29 eq.) and purged with argon. Dichloromethane (6 mL) was added by syringe and the mixture was cooled to -30 °C. Pyridine hydrofluoride (1.2 mL, 5.02 mmol, 341 eq.) was added in one portion, immediately followed by the drop wise addition of **41** (8.5 mg, 0.014 mmol, 1 eq.) in 9 mL dichloromethane. The pink slurry was stirred at -30 °C for 30 min, before it was taken out and stirred for 30 min at room temperature. To the purple mixture, water and dichloromethane (20 mL) were added and the organic phase was washed once with a sodium thiosulfate solution (30 mL) and twice with water (30 mL), dried over sodium sulfate, filtered, and evaporated. The residue was purified by PTLC (hexane/ethyl acetate 4:1) to give compound **43** as a colourless solid (4 mg, 73 %).

Mp: 266 °C; **^{1}H NMR** (400 MHz, CDCl$_3$): δ = 7.28 ppm (s, 6H); **^{19}F NMR** (376 MHz, CDCl$_3$): δ = -95.89 (d, ^2J = 272 Hz, 3F), -119.72 ppm (d, ^2J = 272 Hz, 3F); **^{13}C{^{1}H} NMR** (101 MHz, CDCl$_3$): δ = 124.26 (C$_{rim}$, 6C), 125.23 (t, ^1J = 261 Hz, C$_{C-F}$, 3C), 146.43 (t, ^2J = 28 Hz, C$_{flank}$, 6C), 147.51 ppm (d, ^3J = 8 Hz, C$_{hub}$, 6C); **MS** (EI): *m/z* 372.0367 (found), 372.0374 (calc'd), 372 (100 %, [M]$^+$), 353 (30 %, [M-F]$^+$), 333 (10 %, [353-HF]$^+$), 302 (5 %), 177 (9 %, [M-F]$^{2+}$); **IR**: ν = 2924 (m), 2858 (m), 1545 (m), 1519 (m), 1461 (m), 1391 (m), 1353 (w), 1222 (s), 1064 (m), 952 (m), 824 (s), 662 (w), 588 cm^{-1} (w).

If the reaction is carried out in a glass flask:

A flame-dried 50 mL flask was charged with *N*-iodosuccinimide (70 mg, 0.307 mmol, 27 eq.) and purged with argon. 4 mL dichloromethane were added by syringe and the mixture was cooled to -30 °C. Pyridine hydrofluoride (0.5 mL, 2.09 mmol, 183 eq.) was added in one portion, immediately followed by the drop wise addition of **42** (6.6 mg, 0.011 mmol, 1 eq.) in 7 mL dichloromethane. The pink slurry was stirred at -30 °C for 30 min, before it was taken

out and stirred for 30 min at room temperature. To the purple mixture, water and dichloromethane (20 mL) were added and the organic phase was washed once with a sodium thiosulfate solution (30 mL) and twice with water (30 mL), dried over sodium sulfate, filtered, and evaporated. The residue was purified by PTLC (hexane/ethyl acetate 4:1) to give compound **43** as a colourless solid (1 mg, 24 %), compound **44** as a yellow solid (0.9 mg, 23 %) and compound **45** as an orange solid (0.7 mg, 19 %).

8.4.26. 4,4,7,7-Tetrafluoro-sumanene-1-one (44)
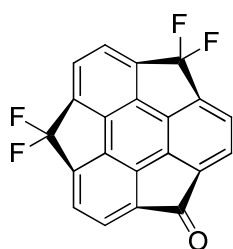
44   **Mp**: 235 °C; **^{1}H NMR** (400 MHz, CDCl$_3$): δ = 7.34 (s, 2H), 7.32 ppm (d, ½ AB, ^3J = 13 Hz, 4H); **^{19}F NMR** (376 MHz, CDCl$_3$): δ = -97.16 (d, ^2J = 273 Hz, 3F), -119.78 ppm (d, ^2J = 273 Hz, 3F); **^{13}C{^{1}H} NMR** (101 MHz, CDCl$_3$): δ = 188.19 (C$_{CO}$, 1C), 149.83 (d, ^5J = 2 Hz, C$_{flank}$, 2C), 149.08 (t, ^2J = 28 Hz, C$_{flank}$, 2C), 147.27 (t, ^2J = 29 Hz, C$_{flank}$, 2C), 146.49 (m, C$_{hub}$, 2C), 146.22 (m, C$_{hub}$, 2C), 142.77 (C$_{hub}$, 2C), 125.24 (t, ^1J = 261 Hz, C$_F$, 2C), 126.20 (C$_{rim}$, 2C), 124.75 (C$_{rim}$, 2C), 124.32 ppm (C$_{rim}$, 2C); **MS** (EI): m/z 350.0358 (found), 350.0355 (calc'd), 350 (100 %, [M]$^{+}$), 322 (30 %, [M-CO]$^{+}$), 302 (15 %, [322-HF]$^{+}$), 161 (12 %, [M-CO]$^{2+}$); **IR**: ν = 2927 (s), 2858 (s), 1727 (m), 1642 (w), 1461 (m), 1214 (s), 786 (m), 686 (m), 470 cm^{-1} (s).

8.4.27. 7,7-Difluoro-sumanene-1,4-dione (45)
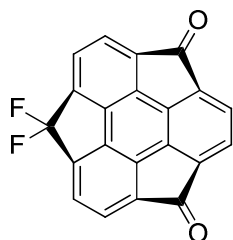
45   **Mp**: Darkens above 194 °C; **^{1}H NMR** (400 MHz, CDCl$_3$): δ = 7.38 (d, ½ AB, ^3J = 9.5 Hz, 4H), 7.36 – 7.35 ppm (m, 2H); **^{19}F NMR** (376 MHz, CDCl$_3$): δ = -98.60 (d, ^2J = 272 Hz,

3F), -119.99 ppm (d, ^2J = 272 Hz, 3F); ^{13}C{^{1}H} NMR (176 MHz, CDCl$_3$): δ = 188.13 (C$_{CO}$, 2C), 149.93 (d, ^5J = 1 Hz, C$_{flank}$, 2C), 149.52 (C$_{flank}$, 2C), 148.78 (t, ^2J = 28 Hz, C$_{flank}$, 2C), 146.23 (m, C$_{hub}$, 2C), 143.81 (C$_{hub}$, 2C), 142.53 (C$_{hub}$, 2C), 126.60 (C$_{rim}$, 2C), 126.13 (C$_{rim}$, 2C), 125.24 (t, ^1J = 256 Hz, C$_{C-F}$, 1C), 124.69 ppm (C$_{rim}$, 2C); **MS** (EI): *m/z* 328.0324 (found), 328.0336 (calc'd), 328 (100 %, [M]$^+$), 300 (18 %, [M-CO]$^+$), 272 (27 %, [M-2CO]$^+$), 253 (12 %, [272-HF]$^+$), 149 (17 %, [M-CO]$^{2+}$), 136 (9 %, [M-2CO]$^{2+}$); **IR**: ν = 2927 (s), 2854 (m), 1727 (s), 1564 (w), 1461 (m), 1384 (w), 1280 (m), 1218 (m), 1133 (m), 1083 (m), 944 (w), 832 (m), 774 (w), 724 (w), 554 cm^{-1} (w).

9. Abbrevations

AIBN	2,2'-azobis(2-methylpropionitrile)
br	broad
cat	catalytic amount
CR-TOF	charge-retraction time-of-flight
d	doublet
DBPO	dibenzoyl peroxide
DCE	1,2-dichloroethane
DCM	dichloromethane
DDQ	2,3-dichloro-5,6-dicyano-1,4-benzoquinone
dec	decomposition
DME	1,2-dimethoxyethan
DMF	*N,N*-dimethylformamide
EI	electron impact
eq	equivalent(s)
Fc	ferrocene, (bis(η^5-cyclopentadienyl)iron)
FVP	flash vacuum pyrolysis
HPLC	high performance liquid chromatography
IR	infrared spectroscopy
m	medium (IR), multiplett (NMR)
mp	melting point
MTO	methylrhenium trioxide
NBI	naphthalene bisimide
n. d.	not determined
NMR	nuclear magnetic resonance (spectroscopy)
PAH	polycyclic aromatic hydrocarbons
PBI	perylene bisimide

PP	polypropylene
ppm	parts per million
PTFE	poly(tetrafluoroethene)
q	quartet
rt	room temperature
s	strong (IR), singlet (NMR)
SWNT	single-walled carbon nanotubes
TEA	triethylamine
THF	tetrahydrofuran
TOF	time-of-flight
TRMC	time-resolved microwave conductivity
w	weak

10. References

[1]   a) H. W. Kroto, J. R. Heath, S. C. O'Brien, R. F. Curl, R. E. Smalley, *Nature* **1985**, *318*, 162-163; b) E. K. Osawa, *Kagaku* **1970**, *25*, 854-863.

[2]   J. R. Heath, S. C. O'Brien, Q. Zhang, Y. Liu, R. F. Curl, F. K. Tittel, R. E. Smalley, *J. Am. Chem. Soc.* **1985**, *107*, 7779-7780.

[3]   S. Iijima, *Nature* **1991**, *354*, 56-58.

[4]   a) M. S. Dresselhaus, G. Dresselhaus, J. C. Charlier, E. Hernández, *Phil. Trans. R. Lond. A* **2004**, *362*, 2065-2098; b) S. B. Sinnott, R. Andrews, *Crit. Rev. Solid State* **2001**, *26*, 145-249.

[5]   T. Dürkop, S. A. Getty, E. Cobas, M. S. Fuhrer, *Nano Lett.* **2003**, *4*, 35-39.

[6]   a) E. R. Darzi, T. J. Sisto, R. Jasti, *J. Org. Chem.* **2012**, *77*, 6624-6628; b) Y. Ishii, Y. Nakanishi, H. Omachi, S. Matsuura, K. Matsui, H. Shinohara, Y. Segawa, K. Itami, *Chem. Sci.* **2012**, *3*, 2340-2345.

[7]   K. S. Novoselov, A. K. Geim, S. V. Morozov, D. Jiang, Y. Zhang, S. V. Dubonos, I. V. Grigorieva, A. A. Firsov, *Science* **2004**, *306*, 666-669.

[8]   P. W. Sutter, J.-I. Flege, E. A. Sutter, *Nat. Mater.* **2008**, *7*, 406-411.

[9]   a) W. E. Barth, R. G. Lawton, *J. Am. Chem. Soc.* **1966**, *88*, 380-381; b) R. G. Lawton, W. E. Barth, *J. Am. Chem. Soc.* **1971**, *93*, 1730-1745.

[10]   J. C. Hanson, C. E. Nordman, *Acta Cryst. B* **1976**, *32*, 1147-1153.

[11]   L. T. Scott, M. M. Hashemi, D. T. Meyer, H. B. Warren, *J. Am. Chem. Soc.* **1991**, *113*, 7082-7084.

[12]   L. T. Scott, P.-C. Cheng, M. M. Hashemi, M. S. Bratcher, D. T. Meyer, H. B. Warren, *J. Am. Chem. Soc.* **1997**, *119*, 10963-10968.

[13]   V. M. Tsefrikas, L. T. Scott, *Chem. Rev.* **2006**, *106*, 4868-4884.

[14]   a) S. Hagen, M. S. Bratcher, M. S. Erickson, G. Zimmermann, L. T. Scott, *Angew. Chem. Int. Ed. Engl.* **1997**, *36*, 406-408; b) G. Mehta, G. Panda, *Chem. Commun.* **1997**, 2081-2082.

[15]   G. Mehta, G. Panda, P. V. V. Srirama Sarma, *Tetrahedron Lett.* **1998**, *39*, 5835-5836.

[16]   L. T. Scott, M. M. Boorum, B. J. McMahon, S. Hagen, J. Mack, J. Blank, H. Wegner, A. de Meijere, *Science* **2002**, *295*, 1500-1503.

[17]   T. J. Seiders, K. K. Baldridge, J. S. Siegel, *J. Am. Chem. Soc.* **1996**, *118*, 2754-2755.

[18]   T. J. Seiders, E. L. Elliott, G. H. Grube, J. S. Siegel, *J. Am. Chem. Soc.* **1999**, *121*, 7804-7813.

[19]   a) A. Sygula, P. W. Rabideau, *J. Am. Chem. Soc.* **1999**, *121*, 7800-7803; b) A. Sygula, P. W. Rabideau, *J. Am. Chem. Soc.* **2000**, *122*, 6323-6324; c) A. Sygula, G. Xu, Z. Marcinow, P. W. Rabideau, *Tetrahedron* **2001**, *57*, 3637-3644.

[20]   A. M. Butterfield, B. Gilomen, J. S. Siegel, *Org. Process Res. Dev.* **2012**, *16*, 664-676.

[21]   a) Y.-T. Wu, J. S. Siegel, *Chem. Rev.* **2006**, *106*, 4843-4867; b) A. Sygula, *Eur. J. Org. Chem.* **2011**, *2011*, 1611-1625.

[22]   a) A. Ayalon, M. Rabinovitz, P.-C. Cheng, L. T. Scott, *Angew. Chem. Int. Ed. Engl.* **1992**, *31*, 1636-1637; b) A. Ayalon, A. Sygula, P.-C. Cheng, M. Rabinovitz, P. W. Rabideau, L. T. Scott, *Science* **1994**, *265*, 1065-1067; c) M. Baumgarten, L. Gherghel, M. Wagner, A. Weitz, M. Rabinovitz, P.-C. Cheng, L. T. Scott, *J. Am. Chem. Soc.* **1995**, *117*, 6254-6257; d) P. W. Rabideau, Z. Marcinow, R. Sygula, A. Sygula, *Tetrahedron Lett.* **1993**, *34*, 6351-6354; e) G. Zilber, V. Rozenshtein, P.-C. Cheng, L. T. Scott, M. Rabinovitz, H. Levanon, *J. Am. Chem. Soc.* **1995**, *117*, 10720-10725.

[23]   a) I. Aprahamian, D. V. Preda, M. Bancu, A. P. Belanger, T. Sheradsky, L. T. Scott, M. Rabinovitz, *J. Org. Chem.* **2005**, *71*, 290-298; b) D. Eisenberg, E. A. Jackson, J. M. Quimby, L. T. Scott, R. Shenhar, *Angew. Chem. Int. Ed.* **2010**, *49*, 7538-7542; c) D. Eisenberg, J. M. Quimby, D. Ho, R. Lavi, L. Benisvy, L. T. Scott, R. Shenhar, *Eur. J. Org. Chem.* **2012**, *2012*, 6321-6327.

[24]   D. Eisenberg, J. M. Quimby, E. A. Jackson, L. T. Scott, R. Shenhar, *Chem. Commun.* **2010**, *46*, 9010-9012.

[25]   I. Aprahamian, D. Eisenberg, R. E. Hoffman, T. Sternfeld, Y. Matsuo, E. A. Jackson, E. Nakamura, L. T. Scott, T. Sheradsky, M. Rabinovitz, *J. Am. Chem. Soc.* **2005**, *127*, 9581-9587.

[26]   a) A. V. Zabula, S. N. Spisak, A. S. Filatov, V. M. Grigoryants, M. A. Petrukhina, *Chem. Eur. J.* **2012**, *18*, 6476-6484; b) A. V. Zabula, S. N. Spisak, A. S. Filatov, M. A. Petrukhina, *Organometallics* **2012**, *31*, 5541-5545.

[27]   S. N. Spisak, A. V. Zabula, A. S. Filatov, A. Y. Rogachev, M. A. Petrukhina, *Angew. Chem. Int. Ed.* **2011**, *50*, 8090-8094.

[28]   A. V. Zabula, A. S. Filatov, S. N. Spisak, A. Y. Rogachev, M. A. Petrukhina, *Science* **2011**, *333*, 1008-1011.

[29]   a) T. J. Seiders, K. K. Baldridge, J. M. O'Connor, J. S. Siegel, *J. Am. Chem. Soc.* **1997**, *119*, 4781-4782; b) P. A. Vecchi, C. M. Alvarez, A. Ellern, R. J. Angelici, A. Sygula, R. Sygula, P. W. Rabideau, *Angew. Chem. Int. Ed.* **2004**, *43*, 4497-4500; c) P. A. Vecchi, C. M. Alvarez, A. Ellern, R. J. Angelici, A. Sygula, R. Sygula, P. W. Rabideau, *Organometallics* **2005**, *24*, 4543-4552; d) B. Zhu, A. Ellern, A. Sygula, R. Sygula, R. J. Angelici, *Organometallics* **2007**, *26*, 1721-1728.

[30]   E. L. Elliott, G. A. Hernandez, A. Linden, J. S. Siegel, *Org. Biomol. Chem.* **2005**, *3*, 407-413.

[31]   H. B. Lee, P. R. Sharp, *Organometallics* **2005**, *24*, 4875-4877.

[32]   R. Maag, B. H. Northrop, A. Butterfield, A. Linden, O. Zerbe, Y. M. Lee, K.-W. Chi, P. J. Stang, J. S. Siegel, *Org. Biomol. Chem.* **2009**, *7*, 4881-4885.

[33]   a) H. A. Wegner, L. T. Scott, A. de Meijere, *J. Org. Chem.* **2003**, *68*, 883-887; b) Y.-T. Wu, T. Hayama, K. K. Baldridge, A. Linden, J. S. Siegel, *J. Am. Chem. Soc.* **2006**, *128*, 6870-6884; c) B. D. Steinberg, E. A. Jackson, A. S. Filatov, A. Wakamiya, M. A. Petrukhina, L. T. Scott, *J. Am. Chem. Soc.* **2009**, *131*, 10537-10545.

[34]   A. S. Filatov, L. T. Scott, M. A. Petrukhina, *Cryst. Growth Des.* **2010**, *10*, 4607-4621.

[35]   Y.-T. Wu, D. Bandera, R. Maag, A. Linden, K. K. Baldridge, J. S. Siegel, *J. Am. Chem. Soc.* **2008**, *130*, 10729-10739.

[36]   J. Mack, P. Vogel, D. Jones, N. Kaval, A. Sutton, *Org. Biomol. Chem.* **2007**, *5*, 2448-2452.

[37]   G. H. Grube, E. L. Elliott, R. J. Steffens, C. S. Jones, K. K. Baldridge, J. S. Siegel, *Org. Lett.* **2003**, *5*, 713-716.

[38]   L. T. Scott, E. A. Jackson, Q. Zhang, B. D. Steinberg, M. Bancu, B. Li, *J. Am. Chem. Soc.* **2011**, *134*, 107-110.

[39]   M. A. Petrukhina, K. W. Andreini, J. Mack, L. T. Scott, *J. Org. Chem.* **2005**, *70*, 5713-5716.

[40]   L. T. Scott, M. M. Hashemi, M. S. Bratcher, *J. Am. Chem. Soc.* **1992**, *114*, 1920-1921.

[41]   T. J. Seiders, K. K. Baldridge, G. H. Grube, J. S. Siegel, *J. Am. Chem. Soc.* **2001**, *123*, 517-525.

[42]   T. Hayama, K. K. Baldridge, Y.-T. Wu, A. Linden, J. S. Siegel, *J. Am. Chem. Soc.* **2008**, *130*, 1583-1591.

[43]   H. Sakurai, T. Daiko, T. Hirao, *Science* **2003**, *301*, 1878.

[44]   U. D. Priyakumar, G. N. Sastry, *J. Chem. Phys. A* **2001**, *105*, 4488-4494.

[45]   G. Mehta, S. R. Shahk, K. Ravikumarc, *J. Chem. Soc., Chem. Commun.* **1993**, 1006-1008.

[46]   a) T. Amaya, H. Sakane, T. Muneishi, T. Hirao, *Chem. Commun.* **2008**, 765-767; b) T. Amaya, H. Sakane, T. Nakata, T. Hirao, *Pure Appl. Chem.* **2010**, *82*, 969-978.

[47]   a) H. Sakurai, T. Daiko, H. Sakane, T. Amaya, T. Hirao, *J. Am. Chem. Soc.* **2005**, *127*, 11580-11581; b) S. Mebs, M. Weber, P. Luger, B. M. Schmidt, H. Sakurai, S. Higashibayashi, S. Onogi, D. Lentz, *Org. Biomol. Chem.* **2012**, *10*, 2218-2222.

[48]   T. Amaya, S. Seki, T. Moriuchi, K. Nakamoto, T. Nakata, H. Sakane, A. Saeki, S. Tagawa, T. Hirao, *J. Am. Chem. Soc.* **2008**, *131*, 408-409.

[49]   T. Amaya, T. Nakata, T. Hirao, *J. Am. Chem. Soc.* **2009**, *131*, 10810-10811.

[50]   T. Amaya, K. Mori, H.-L. Wu, S. Ishida, J.-i. Nakamura, K. Murata, T. Hirao, *Chem. Commun.* **2007**, 1902-1904.

[51]   a) R. Tsuruoka, S. Higashibayashi, T. Ishikawa, S. Toyota, H. Sakurai, *Chem. Lett.* **2010**, *39*, 646-647; b) T. Amaya, M. Hifumi, M. Okada, Y. Shimizu, T. Moriuchi, K. Segawa, Y. Ando, T. Hirao, *J. Org. Chem.* **2011**, *76*, 8049-8052; c) E. Cauët, D. Jacquemin, *Chem. Phys. Lett.* **2012**, *519–520*, 49-53.

[52]   a) S. Higashibayashi, H. Sakurai, *J. Am. Chem. Soc.* **2008**, *130*, 8592-8593; b) S. Higashibayashi, R. Tsuruoka, Y. Soujanya, U. Purushotham, G. N. Sastry, S. Seki, T. Ishikawa, S. Toyota, H. Sakurai, *Bull. Chem. Soc. Jpn.* **2012**, *85*, 450-467.

[53]   Q. Tan, S. Higashibayashi, S. Karanjit, H. Sakurai, *Nat. Commun.* **2012**, *3*, 891.

[54]   a) K. Müller, C. Faeh, F. Diederich, *Science* **2007**, *317*, 1881-1886; b) W. K. Hagmann, *J. Med. Chem.* **2008**, *51*, 4359-4369; c) S. Purser, P. R. Moore, S. Swallow, V. Gouverneur, *Chem. Soc. Rev.* **2008**, *37*, 320-330.

[55]   G. Sandford, *Phil. Trans. R. Lond. A* **2000**, *358*, 455-471.

[56]   a) J.-M. Vincent, *Chem. Commun.* **2012**, *48*, 11382-11391; b) F. Babudri, G. M. Farinola, F. Naso, R. Ragni, *Chem. Commun.* **2007**, 1003-1022.

[57] R. Schmidt, J. H. Oh, Y.-S. Sun, M. Deppisch, A.-M. Krause, K. Radacki, H. Braunschweig, M. Könemann, P. Erk, Z. Bao, F. Würthner, *J. Am. Chem. Soc.* **2009**, *131*, 6215-6228.

[58] a) J. E. Anthony, A. Facchetti, M. Heeney, S. R. Marder, X. Zhan, *Adv. Mat.* **2010**, *22*, 3876-3892; b) S. V. Bhosale, S. V. Bhosale, S. K. Bhargava, *Org. Biomol. Chem.* **2012**, *10*, 6455-6468; c) T. Osawa, T. Kajitani, D. Hashizume, H. Ohsumi, S. Sasaki, M. Takata, Y. Koizumi, A. Saeki, S. Seki, T. Fukushima, T. Aida, *Angew. Chem. Int. Ed.* **2012**, *51*, 7990-7993.

[59] a) R. T. Weitz, K. Amsharov, U. Zschieschang, E. B. Villas, D. K. Goswami, M. Burghard, H. Dosch, M. Jansen, K. Kern, H. Klauk, *J. Am. Chem. Soc.* **2008**, *130*, 4637-4645; b) J. Chang, Q. Ye, K.-W. Huang, J. Zhang, Z.-K. Chen, J. Wu, C. Chi, *Org. Lett.* **2012**, *14*, 2964-2967.

[60] P. Deng, Y. Yan, S.-D. Wang, Q. Zhang, *Chem. Commun.* **2012**, *48*, 2591-2593.

[61] R. Schmidt, M. M. Ling, J. H. Oh, M. Winkler, M. Könemann, Z. Bao, F. Würthner, *Adv. Mat.* **2007**, *19*, 3692-3695.

[62] M. Gsänger, J. H. Oh, M. Könemann, H. W. Höffken, A.-M. Krause, Z. Bao, F. Würthner, *Angew. Chem. Int. Ed.* **2010**, *49*, 740-743.

[63] D. O'Hagan, *Chem. Soc. Rev.* **2008**, *37*, 308-319.

[64] a) D. Chopra, T. N. G. Row, *CrystEngComm* **2011**, *13*, 2175-2186; b) F. Cozzi, R. Annunziata, M. Benaglia, K. K. Baldridge, G. Aguirre, J. Estrada, Y. Sritana-Anant, J. S. Siegel, *Phys. Chem. Chem. Phys.* **2008**, *10*, 2686-2694; c) G. W. Coates, A. R. Dunn, L. M. Henling, D. A. Dougherty, R. H. Grubbs, *Angew. Chem. Int. Ed.* **1997**, *36*, 248-251; d) F. Cozzi, F. Ponzini, R. Annunziata, M. Cinquini, J. S. Siegel, *Angew. Chem. Int. Ed.* **1995**, *34*, 1019-1020; e) R. Berger, G. Resnati, P. Metrangolo, E. Weber, J. Hulliger, *Chem. Soc. Rev.* **2011**, *40*, 3496-3508.

[65] H.-J. Schneider, *Chem. Sci.* **2012**, *3*, 1381-1394.

[66] C. R. Patrick, G. S. Prosser, *Nature* **1960**, *187*, 1021-1021.

[67] F. Ponzini, R. Zagha, K. Hardcastle, J. S. Siegel, *Angew. Chem. Int. Ed.* **2000**, *39*, 2323-2325.

[68] B. M. Schmidt, Master Thesis, Freie Universität Berlin, 2009.

[69] B. Topolinski, Master Thesis, Freie Universität Berlin, 2011.

[70]   A. K. Meyer, Master Thesis, Freie Universität Berlin, 2011.

[71]   P. Roesch, Bachelor Thesis, Freie Universität Berlin, 2011.

[72]   S. Grabowsky, M. Weber, Y.-S. Cheng, D. Lentz, B. M. Schmidt, M. Hesse, P. Luger, *Z. Naturforsch., B: J. Chem. Sci.* **2010**, *65b*, 452-460.

[73]   M. Nishio, *CrystEngComm* **2004**, *6*, 130-158.

[74]   M. Nishio, Y. Umezawa, K. Honda, S. Tsuboyama, H. Suezawae, *CrystEngComm* **2009**, *11*, 1757-1788.

[75]   W. B. Jennings, B. M. Farrell, J. F. Malone, *Acc. Chem. Res*. **2001**, *34*, 885-894.

[76]   a) A. S. Filatov, E. A. Jackson, L. T. Scott, M. A. Petrukhina, *Angew. Chem. Int. Ed.* **2009**, *48*, 8473-8476; b) A. S. Filatov, A. K. Greene, E. A. Jackson, L. T. Scott, M. A. Petrukhina, *J. Organomet. Chem.* **2011**, *696*, 2877-2881.

[77]   a) F. Mo, J. M. Yan, D. Qiu, F. Li, Y. Zhang, *Angew. Chem. Int. Ed*. **2010**, *122*, 2072-2076; b) D. Qiu, F. Mo, Z. Zheng, Y. Zhang, J. Wang, *Org. Lett*. **2010**, *12*, 5474-5477.

[78]   B. Topolinski, B. M. Schmidt, M. Kathan, S. I. Troyanov, D. Lentz, *Chem. Commun.* **2012**, *48*, 6298-6300.

[79]   B. B. Shrestha, S. Karanjit, S. Higashibayashi, H. Sakurai, 92nd Annual Meeting of The Chemical Society of Japan, 2012.

[80]   A. A. Popov, I. E. Kareev, N. B. Shustova, E. B. Stukalin, S. F. Lebedkin, K. Seppelt, S. H. Strauss , O. V. Boltalina, L. Dunsch, *J. Am. Chem. Soc.* **2007**, *129*, 11551–11568.

[81]   E. Mejia, A. Togni, *ACS Catal.* **2012**, *2*, 521-527.

[82]   A. Sygula, S. D. Karlen, R. Sygula, P. W. Rabideau, *Org. Lett.* **2002**, *4*, 3135-3137.

[83]   N. Rahanyan, A. Linden, K. K. Baldridge, J. S. Siegel, *Org. Biomol. Chem.* **2009**, *7*, 2082-2092.

[84]   C. Moureu, J. C. Bongrand, *Bull. Soc. Chem.* **1909**, V, 846.

[85]   P. J. Stang, F. Diederich, *Modern Acetylenic Chemistry*, VCH, Weinheim, **1995**.

[86]   H. Vaughn, J. A. Nieuwland, *J. Am. Chem. Soc* **1932**, *54*, 787-790.

[87]   A. Jäger, Research Internship Report, Freie Universität Berlin, 2011.

[88]   J. M. Birchall, F. L. Bowden, R. N. Haszeldine, A. B. P. Lever, *Inorg. Phys. Theor.* **1967**, 747-753.

[89]   B. Topolinski, Research Internship Report, Freie Universität Berlin, 2010.

[90]   M. Yamada, Research Internship Report, Freie Universität Berlin, 2011.

[91]   M. Kathan, Bachelor Thesis, Freie Universität Berlin, 2011.

[92]   A. Schwarzer, E. Weber, *Cryst. Growth Des.* **2008**, *8*, 2862-2874.

[93]   K. Bynum, R. Prip, R. Callahan, R. Rothchild, *J. Fluorine Chem.* **1998**, *90*, 39-46.

[94]   a) D. W. Jones, W. S. McDonald, *J. Chem. Soc., Chem. Commun.* **1980**, 417-418; b) M. Krivec, M. Gazvoda, K. Kranjc, S. Polanc, M. Kočevar, *J. Org. Chem.* **2012**, 77, 2857-2864.

[95]   S. Higashibayashi, H. Sakurai, *Chem. Lett.* **2011**, *40*, 122-128.

[96]   a) W. B. Motherwell, J. A. Wilkinson, *Synlett* **1991**, *1991*, 191-192; b) T. Fuchigami, T. Fujita, *J. Org. Chem.* **1994**, *59*, 7190-7192; c) C. Ye, B. Twamley, J. n. M. Shreeve, *Org. Lett.* **2005**, *7*, 3961-3964; for a recent review see d) V. Hugenberg, G. Haufe, *J. Fluorine Chem.* **2012**, *143*, 238-262.

[97]   a) S. C. Sondej, J. A. Katzenellenbogen, *J. Org. Chem.* **1986**, *51*, 3508-3513; b) Y. Ie, M. Nitani, Y. Aso, *Chem. Lett.* **2007**, *36*, 1326-1327; c) V. Hugenberg, R. Fröhlich, G. Haufe, *Org. Biomol. Chem.* **2010**, *8*, 5682-5691.

[98]   a) R. D. Chambers, G. Sandford, M. Atherton, *J. Chem. Soc., Chem. Commun.* **1995**, 177; b) R. D. Chambers, G. Sandford, M. E. Sparrowhawk, M. J. Atherton, *J. Chem. Soc., Perkin Trans. 1* **1996**, 1941-1944.

[99]   Y. Morita, S. Nakao, S. Haesuwannakij, S. Higashibayashi, H. Sakurai, *Chem. Commun.* **2012**, *48*, 9050-9052.

[100]   K. Fuchibe, T. Akiyama, *J. Am. Chem. Soc.* **2006**, *128*, 1434-1435.

[101]   Gaussian 03, Revision D.01, M. J. Frisch, G. W. Trucks, H. B. Schlegel, G. E. Scuseria, M. A. Robb, J. R. Cheeseman, J. A. Montgomery, Jr., T. Vreven, K. N. Kudin, J. C. Burant, J. M. Millam, S. S. Iyengar, J. Tomasi, V. Barone, B. Mennucci, M. Cossi, G. Scalmani, N. Rega, G. A. Petersson, H. Nakatsuji, M. Hada, M. Ehara, K. Toyota, R. Fukuda, J. Hasegawa, M. Ishida, T. Nakajima, Y. Honda, O. Kitao, H. Nakai, M. Klene, X. Li, J. E. Knox, H. P. Hratchian, J. B. Cross, V. Bakken, C. Adamo, J. Jaramillo, R. Gomperts, R. E. Stratmann, O. Yazyev, A. J. Austin, R. Cammi, C. Pomelli, J. W. Ochterski, P. Y. Ayala, K. Morokuma, G. A. Voth, P. Salvador, J. J. Dannenberg, V. G. Zakrzewski, S. Dapprich, A. D. Daniels, M. C. Strain, O. Farkas, D. K. Malick, A. D. Rabuck, K. Raghavachari, J. B. Foresman, J. V. Ortiz, Q. Cui, A. G. Baboul, S. Clifford, J. Cioslowski, B. B. Stefanov, G. Liu, A. Liashenko, P. Piskorz, I. Komaromi, R. L. Martin,

D. J. Fox, T. Keith, M. A. Al-Laham, C. Y. Peng, A. Nanayakkara, M. Challacombe, P. M. W. Gill, B. Johnson, W. Chen, M. W. Wong, C. Gonzalez, J. A. Pople, Gaussian, Inc., Wallingford CT, 2004.

[102] A. C. Blackburn, A. J. Dobson, R. E. Gerkin, *Acta Cryst.* **1996***, C52,* 1482-1486.

[103] CCDC Deposition Number705499, Private Communication to the Database, 2008.

[104] Y. Ie, M. Nitani, Y. Aso, *Chem. Lett.* **2007**, *36*, 1326-1327.

[105] GaussView, Version 5, Roy Dennington, Todd Keith, John Millam, Semichem Inc., Shawnee Mission KS, 2009.

[106] A. Saeki, Y. Koizumi, T. Aida, S. Seki, *Acc. Chem. Res.* **2012**, *45*, 1193-1202.

[107] Jason U. Wallace, PhD. Thesis, University of Rochester, 2009.

[108] B. M. Schmidt, S. Seki, B. Topolinski, K. Ohkubo, S. Fukuzumi, H. Sakurai, D. Lentz, *Angew. Chem. Int. Ed*. **2012**, *124*, 11548-11551.

[109] a) F. C. Grozema, L. D. A. Siebbeles, J. M. Warman, S. Seki, S. Tagawa, U. Scherf, *Adv. Mater.* **2002**, *14*, 228-231; b) S. Seki, S. Tagawa, *Polym. J.* **2007**, *39*, 277-293; c) Y. Kunimi, S. Seki, S. Tagawa, *Solid State Commun*. **2000**, *114*, 469-472.

[110] a) P. G. Le Comber, W. E. Spear, *Phys. Rev. Lett.* **1970**, *25*, 509-511; b) G. Juska, K. Arlauskas, M. Viliunas, *Phys. Rev. Lett.* **2000**, *84*, 4946-4949.

[111] A. Saeki, Y. Yamamoto, Y. Koizumi, T. Fukushima, T. Aida, S. Seki, *J. Phys. Chem. Lett.* **2011**, *2*, 2549–2554.

[112] A. Saeki, S. Seki, T. Takenobu, Y. Iwasa, *Adv. Mater.* **2008**, *20*, 920-23.

[113] C. Bruno, R. Benassi, A. Passalacqua, F. Paolucci, C. Fontanesi, M. Marcaccio, E. A. Jackson, L. T. Scott, *J. Phys. Chem. B* **2009,** *113,* 1954-1962.

[114] Y. Li, C. Li, W. Yue, W. Jiang, R. Kopecek, J. Qu, Z. Wang, *Org. Lett.* **2010**, *12*, 2374-2377.

[115] I. V. Kuvychko, S. N. Spisak, Y.-S. Chen, A. A. Popov, M. A. Petrukhina, S. H. Strauss, O. V. Boltalina, *Angew. Chem. Int. Ed.* **2012**, *51*, 4939-4942.

[116] D. O'Hagan, *Chem. Soc. Rev.* **2008**, *37*, 308-319.

[117] M. Kühnel, PhD Thesis, Freie Universität Berlin, 2011.

[118] A. A. Popov, I. E. Kareev, N. B. Shustova, E. B. Stukalin, S. F. Lebedkin, K. Seppelt, S. H. Strauss, O. V. Boltalina, L. Dunsch, *J. Am. Chem. Soc.* **2007**, *129*, 11551-11568.

[119] R. Koller, K. Stanek, P. Eisenberger, I. Kieltsch, A. Togni, *Org. Synth.* **2011**, *88*, 168-180.

[120] T. Umemoto, R. P. Singh, Y. Xu, N. Saito, *J. Am. Chem. Soc.* **2010**, *132*, 18199-18205.

[121] SADABS: Area-Detector Absorption Correction; Siemens Industrial Automation, INC.: Madison, WI, 1996.

[122] A. Thorn, G. M. Sheldrick, *Acta Cryst. Sect. A* **2008**, *64*, C221.

[123] L. Farrugia, *J. Appl. Crystallogr.* **1997**, *30*, 565.

[124] Persistence of Vision Pty. Ltd. http://povray.org/.

[125] CrystalClear: Crystal Structure Analysis Package, Rigaku and Rigaku/MSC, The Woodlands, TX 77381, USA, 2007.

[126] A. Arvai, C. Nielsen, ADSC Quantum-210 ADX Program, Area Detector System Corporation; Poway, CA, USA, 1983.

[127] T. Otwinowski, W. Minor in Methods in Enzymology, Vol. 276 (Eds.: C. W. Carter Jr., R. M. Sweet), Academic Press, New York, 1997, pp. 307.

[128] L. Palatinus, G. Chapuis, *J. Appl. Cryst.* **2007**, *40*, 786-790.